

**Phenotypic plasticity
from a predator perspective:
empirical and theoretical
investigations**

**Dissertation
der Fakultät für Biologie
der Ludwig-Maximilians-Universität
München**

vorgelegt von

MICHAEL KOPP

11.2.2003

Erstgutachter: Prof. Dr. Wilfried Gabriel

Zweitgutachter: Prof. Dr. Sebastian Diehl

Datum der mündlichen Prüfung: 16. April 2003

Zusammenfassung	3
Abstract	5
General Introduction: A predator perspective on phenotypic plasticity	7
Part 1. Trophic size polyphenism in <i>Lembadion bullinum</i>: costs and benefits of an inducible offense	9
1.1 Introduction	9
1.2 Material and methods	11
1.3 Results	16
1.4 Discussion	24
Part 2. Reciprocal phenotypic plasticity in a predator prey system: inducible offenses against inducible defenses?	30
2.1 Introduction	30
2.2 Material and methods	31
2.3 Results	36
2.4 Discussion	39
Part 3. Modeling a coevolving predator-prey system with reciprocal phenotypic plasticity	44
3.1 Introduction	44
3.2 The model	47
3.3 Results	61
3.4 Discussion	127
Conclusions	133
Acknowledgements	134
Danksagungen	135
Literature cited	136
Curriculum vitae	147
Lebenslauf	148

Zusammenfassung

Phänotypische Plastizität ist in Räuber-Beute Beziehungen weit verbreitet. Beuteorganismen setzen induzierbare Verteidigungen ein, um ihre Überlebenschancen in Zeiten mit hohem Prädationsrisiko zu verbessern. Räuber können ihrerseits induzierbare Angriffsmechanismen (trophische Polyphänismen) besitzen und ihren Phänotyp an die vorherrschende Beute anpassen. Bisher haben induzierbare Verteidigungen deutlich mehr Aufmerksamkeit erhalten als induzierbare Angriffsmechanismen. In dieser Arbeit zeige ich drei Gebiete auf, in denen eine „Räuberperspektive“ dazu beitragen kann, unser Verständnis von phänotypischer Plastizität in Räuber-Beute Systemen zu vergrößern.

Im ersten Teil beschreibe ich einen induzierbaren Angriffsmechanismus bei dem räuberischen Ciliaten *Lembadion bullinum*: Die mittlere Zellgröße einer genetisch einheitlichen Lembadienpopulation nimmt mit der Größe der vorherrschenden Beuteart zu. Dieser Größenpolyphänismus kann als das Ergebnis eines Kompromisses zwischen den Kosten und Nutzen des induzierbaren Angriffsmechanismus (trade-off) erklärt werden. Große Lembadien sind überlegen, wenn es darum geht, große Beute zu überwältigen. Demgegenüber erreichen kleinen Lembadien bei Anwesenheit von kleiner Beute höhere Zellteilungsraten. Daher sollten induzierbare Angriffsmechanismen dann entstehen, wenn Räuber in einer veränderlichen Umwelt leben, in der wichtige Merkmale ihrer Beute räumlich oder zeitlich variieren.

Im zweiten Teil untersuche ich das Zusammenspiel zwischen dem induzierbaren Angriffsmechanismus von *Lembadion* und einer induzierbaren Verteidigung. *Lembadion* gibt ein Kairomon (einen chemischen Botenstoff) ab, der Verteidigungen bei mehreren Beutearten induziert. Unter anderem löst er bei dem herbivoren Ciliaten *Euplotes octocarinatus* die Bildung seitlicher „Flügel“ aus. Wie ich zeige, kann *Lembadion* die Wirkung dieser Verteidigung verringern, indem er seinen Angriffsmechanismus aktiviert. Dies ist eines der ersten bekannten Beispiele für reziproke phänotypische Plastizität in einem Räuber-Beute System. Die Gegenreaktion von *Lembadion* beeinträchtigt die Fit-

ness der Beute, es konnte aber nicht nachgewiesen werden, dass sie die Fitness von *Lembadion* erhöht. Dennoch diskutiere ich die Hypothese, dass die phänotypische Plastizität in beiden Arten das Ergebnis von (diffuser) Coevolution zwischen Räuber und Beute ist.

Im dritten Teil verfolge ich die obige Idee weiter und entwickle ein mathematisches Modell eines Räuber-Beute Systems, in dem Coevolution und reziproke phänotypische Plastizität vorkommen und in dem der induzierbare Angriffsmechanismus des Räubers eine unzweifelhaft wirksame Gegenanpassung gegen die induzierbare Verteidigung der Beute ist. Aus dem Modell ergeben sich drei wesentliche Schlussfolgerungen: Erstens kann die induzierbare Verteidigung der Beute die Populationsdynamik stabilisieren. Der Einfluss der Gegenanpassung des Räubers ist weniger eindeutig und hängt vom Verhältnis der Kosten und Nutzen des Angriffsmechanismus ab. Zweitens kann die phänotypische Plastizität nur dann aufrechterhalten werden, wenn sowohl die Verteidigung als auch der Angriffsmechanismus hinreichend effektiv sind. Drittens deuten vorläufige Ergebnisse darauf hin, dass ein induzierbarer Angriffsmechanismus gegenüber einem konstitutiven (d.h. permanent ausgebildeten) genau dann von Vorteil ist, wenn die Populationen im Modell Räuber-Beute-Zyklen vollführen. Daraus ergibt sich die Hypothese, dass phänotypische Plastizität als Anpassung an zeitliche Heterogenität entstehen kann, die auf der internen Dynamik von Räuber-Beute Systemen beruht.

Abstract

Phenotypic plasticity is common in predator-prey interactions. Prey use inducible defenses to increase their chances of survival in periods of high predation risk. Predators, in turn, display inducible offenses (trophic polyphenisms) and adjust their phenotypes to the prevailing type of prey. In the past, inducible defenses have received considerably more attention than inducible offenses. Here, I point out three areas where taking a predator perspective can increase our understanding of phenotypic plasticity in predator-prey systems.

In Part 1, I describe an inducible offense in the predatory ciliate *Lembadion bullinum*: Mean cell size in a genetically uniform *Lembadion* population increases with the size of the dominant prey species. This size polyphenism can be explained as the result of a trade-off: Large *Lembadion* are superior in feeding on large prey, whereas small *Lembadion* achieve higher division rates when small prey is available. Consequently, inducible predator offenses may evolve as adaptations to environments where important prey characteristics vary over space or time.

In Part 2, I investigate the interplay of *Lembadion*'s inducible offense with an inducible prey defense. *Lembadion* releases a kairomone (i.e. an infochemical) that induces defenses in several prey species. For example, in the herbivorous ciliate *Euplotes octocarinatus*, it triggers the production of protective lateral "wings". I show that *Lembadion* can reduce the effect of this defense by activating its inducible offense. This is one of the first known examples of reciprocal phenotypic plasticity in a predator-prey system. While the counter-reaction of *Lembadion* decreases the fitness of the prey, it could not be shown to significantly increase the fitness of *Lembadion* itself. Nevertheless, I discuss the hypothesis that phenotypic plasticity in both species is a result of (diffuse) coevolution.

In Part 3, I further pursue the idea of coevolution and develop a mathematical model of a coevolving predator-prey pair which displays reciprocal phenotypic plasticity. In this model, the inducible offense is a truly effective counter-adaptation to the prey's de-

fense. The model yields three main conclusions: First, the inducible prey defense can stabilize predator-prey population dynamics. The effect of the inducible counter-offense is less clear and depends on the relative magnitude of its costs and benefits. Second, the maintenance of phenotypic plasticity requires that both the defense and the offense are sufficiently strong. Third, preliminary results suggest that an inducible offense is favored over a constitutive (permanently expressed) one if and only if the model populations perform predator-prey cycles. This leads to the hypothesis that phenotypic plasticity may evolve as an adaptation to temporal heterogeneity created by the internal dynamics of predator-prey systems.

General Introduction:

A predator perspective on phenotypic plasticity

Organisms living in variable environments can optimize their fitness by showing adaptive phenotypic plasticity (Stearns 1989, Pigliucci 2001). Spectacular examples have been described in the context of predator-prey interactions. This is not surprising, as foraging and predator avoidance have a large impact on fitness, and the presence of food or predators may vary greatly over space and time. Therefore, phenotypic plasticity is common in both predators and prey.

In prey, protective traits that are expressed only in the presence of predators are known as inducible defenses. These have been described in all main groups of animals as well as in plants, and have become a major study object during recent years (reviewed by Tollrian and Harvell 1999a). Inducible defenses may involve changes in a prey's morphology, behavior, life-history, or chemistry. The evolution of inducible defenses is favored under the following conditions (Tollrian and Harvell 1999a, p. 5): (1) Predation risk is variable, (2) the presence of predators is indicated by a reliable cue, and (3) there is a functional trade-off between the benefits and costs of the defense.

In analogy, offensive traits of predators have been called inducible offenses (Padilla 2001) if they are expressed only in the presence of certain types of prey. The ability to express an inducible offense is frequently referred to as diet-induced or trophic polyphenism. Following Padilla (2001), I will use the term polyphenism for discrete as well as continuous phenotypic variation, as the difference is not essential for the discussion of inducible offenses. Here, I will only consider morphological offenses. Examples have been reported from a variety of taxa, including fishes (variation of jaw morphology: e.g. Meyer 1987, Mittelbach et al. 1999), amphibians (typical and cannibalistic larval morphs: e.g. Collins and Cheek 1983), insects (variation of jaw and head morphology:

e.g. Bernays 1986, Greene 1989), crabs (Smith and Palmer 1994), cladocerans (size of feeding basket in *Leptodora*: Abrusán 2003), snails (different radula types: Padilla 2001), rotifers (trimorphisms in *Asplanchna*: e.g., Gilbert 1980), and protozoa (induction of “giants” or “macrostomes”, i.e. large-mouthed morphs: e.g. Williams 1961, Giese 1973).

Compared to inducible defenses, inducible offenses have received considerably less attention. Therefore, the aim of this study is to shed more light on the predator side of phenotypic plasticity. In particular, I will focus on the following general hypotheses:

1. *Like inducible defenses, inducible offenses can be discussed in a cost-benefit framework.*
2. *Inducible defenses and inducible offenses may interact in a reciprocal fashion.*
3. *This reciprocal phenotypic plasticity might be a result of predator-prey coevolution.*

Accordingly, the present work is subdivided into three parts. In Part 1, I describe an inducible offense in the predatory ciliate *Lembadion bullinum*, and I analyze the costs and benefits experienced by induced predators. This part is a slightly modified version of a publication by Kopp and Tollrian (2003). In Part 2, I present one of the first examples of reciprocal phenotypic plasticity in a predator-prey system: *Lembadion* activates its offense in response to the inducible defense of one of its prey. Furthermore, I investigate whether this counter-reaction is adaptive. In Part 3, I develop a mathematical model in order to analyze the ecological and evolutionary dynamics of a predator-prey system with reciprocal phenotypic plasticity.

Part 1. Trophic size polyphenism in *Lembadion bullinum*: costs and benefits of an inducible offense

1.1 Introduction

In analogy to the conditions favoring inducible defenses (see general introduction), the evolution of inducible offenses should be promoted by (1) fluctuations in the quality or quantity of available prey, (2) reliable cues indicating the presence of certain prey types, and (3) a functional trade-off between the benefits and costs of the offense. However, few studies have tested these predictions so far. In particular, the costs of inducible offenses have rarely been studied (e.g., Gilbert and Stemberger 1985, Hewett 1988, Meyer 1989, Goldman and Dennett 1990, Trowbridge 1991, Robinson et al. 1996, Hampton and Starkweather 1998). Here, I describe an inducible offense in the predatory ciliate *Lembadion bullinum* and experimentally demonstrate the cost-benefit trade-off governing the fitness of the various phenotypes.

Lembadion (Fig. 1) is a primarily benthic inhabitant of lakes, ponds and slow streams (Foissner et al. 1994). It is a raptorial feeding predator of large protists and has its gape size limited by the dimensions of a huge, but inflexible peristome (cell mouth). *Lembadion* is well known to elicit inducible defenses in several prey species (see Part 2). In addition, Kuhlmann (1993) described that *Lembadion* can form “giant cannibals”, which are induced in dense cultures when alternative food (in this case, *Colpidium campylum*) becomes scarce. Under such conditions, a few cells switch to cannibalism and delay their division until they are more than twice as large as the “normal” cells which they subsequently prey upon. This transformation is reversible: When *Colpidium* is offered again, the giants undergo several rapid divisions and regain the “normal” size.

The aim of the present study was two-fold: First, the polyphenism of *Lembadion* should be characterized further. In particular, it is unknown so far whether giant induction requires starvation and cannibalism, or whether enlarged morphs can also be induced by the consumption of large non-conspecific prey, as is the case in other phenotypically plastic ciliates (e.g., Giese 1973). Therefore, I performed induction experiments, where I tried to induce different morphs by raising *Lembadion* with prey of different size. Second, I investigated the benefits and costs for large morphs. Giants apparently are adapted to feeding on large prey. On the other hand, the quick reversal of giant formation suggests that large cells become disadvantaged once small prey is available. To test this hypothesis, I performed feeding experiments with various combinations of prey and predator size, and I estimated population growth rate of small and large *Lembadion* morphs in the presence of small prey.

Fig. 1: Two individuals of the ciliate *Lembadion bullinum* (ventral view, anterior end to the right). These predators have a huge but inflexible cell mouth (the long “gap” in the lower half of each cell), which enables them to ingest prey of almost their own size. The length of the lower individual is approximately 140 μm .



1.2 Material and methods

1.2.1 Study organisms

An initially clonal strain of *Lembadion* was kindly provided by K. Wiackowsky (University of Krakow, Poland). *Lembadion* usually reproduce by binary fission at a maximum rate of about one division per day. Conjugation (sexual recombination) was infrequently observed in stock cultures, but never during experiments. Thus, while my *Lembadion* were not strictly clonal, genetic diversity was arguably very low.

The prey organisms *Colpidium campylum*, *Euplotes octocarinatus* and *Euplotes aediculatus* were kindly provided by H.-W. Kuhlmann (University of Münster, Germany). *Colpidium kleini* were obtained from K. Wiackowsky.

1.2.2 Stock cultures

Stock cultures of the different ciliate species were kept in 100 ml evaporation dishes or 1 l Fernbach flasks at 20°C in the dark. *Lembadion* were raised in artificial SMB medium (1.5 mM NaCl, 0.05 mM KCl, 0.4 mM CaCl₂, 0.05 mM MgCl₂, 0.05 MgSO₄, 2.0 mM phosphate buffer, pH 6.8; (Miyake 1981)) with *Euplotes octocarinatus*, *Euplotes aediculatus* or *Colpidium campylum* as food. *Euplotes* were kept in SMB and fed the unicellular green alga *Chlorogonium elongatum*. *Chlorogonium* was raised in SMC medium (= SMB + 1.25 mM NH₄NO₃, 15 mM FeCl₃, 0.8 mM MnCl₂, slightly modified after Miyake 1981) at 20°C under constant light and aeration. *Colpidium campylum* and *Colpidium kleini* were cultured in a medium consisting of SMC + 300 mg yeast extract + 1 “protozoan pellet” (Carolina Biological Supply, Burlington, NC, USA) per l. This medium was inoculated with *Aerobacter aerogenes* and incubated on a shaker for 24 h. The resulting bacterial suspension was then inoculated with *Colpidium* and incubated for another 2 or 3 days. Finally, *Colpidium* were harvested by gentle centrifugation (200 g, using “pear-shaped” centrifuge tubes with cylindrical bottom) and re-suspended in fresh SMB.

1.2.3 General methods

Experiments were generally conducted in 6-well tissue culture plates (with 10 ml wells) at 20°C in the dark. Replicates of *Lembadion* were taken from independent stock cultures. A newly inoculated stock culture was assumed to be independent from its parent culture after one week. In experiments 2, 3, and 4, the following standardization procedure was applied to obtain cells with a well-defined nutritional state: An appropriate number of well-fed *Lembadion* with clearly visible food vacuoles were selected from a stock culture, transferred to fresh medium and starved for 24 h.

Measurements of cell dimensions were performed on fixed samples using a computer-based image analysis system (AnalySIS, Soft Imaging Systems, Münster, Germany) connected to a Leitz Orthoplan microscope at 160-fold magnification. Volume of *Lembadion* was estimated as $\pi/6 \cdot \text{length} \cdot \text{width}^2$, i.e. cells were assumed to be prolonged spheroids. Fixation was achieved by addition of glutaraldehyde at a final concentration of 2 % (Sherr et al. 1989).

For the feeding experiments (experiment 3 and 4), prey were live-stained with DAPI (see Lessard et al. 1996, Pfister and Arndt 1998). This yields a brightly fluorescing nucleus, which can be easily detected inside the predator's food vacuoles. To obtain stained *Euplotes* or *Colpidium*, the cells were incubated with 1 µg / ml DAPI for 2 h. After the exposure, *Euplotes* were filtrated over a 15 µm gauze, whereas *Colpidium* were centrifuged 3 times and subsequently re-suspended in fresh SMB. To allow the prey to recover from this procedure, experiments were started not earlier than 1 h after the removal of the stain.

In replicated experimental treatments, measurements of individual cell properties, such as length, width, or number of food vacuoles, were generally done on samples of 10 to 30 cells per replicate. The means from these samples were used for statistical tests, in order to avoid pseudoreplication. However, numerical results will be presented as means \pm standard deviations of the individual data, frequently pooled over all the replicates of a treatment. Statistics were calculated with STATISTICA for Windows 5.1 (StatSoft, Inc., Tulsa, OK, USA).

1.2.4 Experiment 1: Size of *Lembadion* raised with different prey

In experiment 1, I investigated the morphological reaction of *Lembadion* to four differently sized prey species: *Colpidium campylum*, *Colpidium kleini*, *Euplotes octocarinatus*, and *Euplotes aediculatus*. In the following, the *Lembadion* morphs induced with these prey will be referred to as the C-, K-, O-, and A-form, respectively.

Each of the four prey species (treatments) was used as food for four *Lembadion* cultures (replicates). Prior to the experiment, the *Lembadion* had been raised on *Euplotes octocarinatus*. After at least 10 days of cultivation – this time span had been suggested by preliminary experiments – 3 samples were taken from each replicate at intervals of two days. From each sample, length and width of 30 cells were measured. Mean prey dimensions were determined from appropriate samples. The mean of prey length \times width was computed as an index of prey size or “bulkiness”.

1.2.5 Experiment 2: Peristome size of *Lembadion* raised with different prey

Experiment 2 was designed to determine the influence of prey size on the anatomy of *Lembadion*'s peristome (cell mouth). I measured peristome length and width both absolutely and relative to cell length and width.

In this experiment, I applied three prey treatments. Similarly to experiment 1, *Lembadion* were raised for at least 10 days with either *Colpidium campylum* (C-form, 3 replicates), *Euplotes octocarinatus* (O-form, 12 replicates) or *Euplotes aediculatus* (A-form, 9 replicates). Before fixation, the cells were starved for 24 h as described in the general methods section. Sample size per replicate varied between 15 and 30 because the peristome can only be measured in cells with a proper orientation on the slide.

1.2.6 Experiment 3: Feeding rate of small and large *Lembadion* with large prey

The results of the previous experiments indicated that large prey induce large-sized *Lembadion* morphs, which possess a large peristome. In the following, I investigated the benefits and costs experienced by these large morphs. The benefits were studied in ex-

periment 3, by estimating the feeding rate of small and large *Lembadion* feeding on large prey.

In experiment 3a, the C-form (small) and the A-form (large) were fed *Euplotes aediculatus*. In experiment 3b, the C-form (small) and the O-form (intermediate) were fed *Euplotes octocarinatus*. In both experiments, treatments with each predator morph were replicated three times. Per replicate, around 100 standardized *Lembadion* of the respective morph were offered approximately 4000 stained prey in 1 ml of medium. After 1 h cells were fixed by addition of glutaraldehyde and the number of fluorescing food vacuoles per cell was determined immediately under an epifluorescence microscope at 160-fold magnification. In addition, length and width of 10 cells per replicate were measured for calculation of volume-specific feeding rates (i.e. absolute feeding rates divided by mean predator volume).

1.2.7 Experiment 4: Feeding rate of small and large *Lembadion* with small prey

As a test for potential costs paid by large morphs, experiment 4 was designed to study the influence of cell size on *Lembadion*'s success in feeding on small prey. In addition, I also aimed to study possible interaction effects with prey density. Therefore, I compared the feeding rates of the C- and the A-form at various densities of *Colpidium campylum*.

Accordingly, the experiment had a 2×4 factorial design: Each of the two predator morphs was offered four prey densities, two low ones and two high ones (6.25, 12.5, 500, and 1250 per ml). Each of the resulting eight treatments was replicated 11 times.

Preliminary experiments had shown that *Lembadion* needs some time to "habituate" to a new type of prey. Therefore, the usual standardization procedure was extended as follows: 48 h before the experiment, 200 well-fed cells were selected from each of 11 stock cultures of both morphs and transferred to 10 ml of fresh medium containing approximately 2000 *Colpidium campylum* per ml (6-well tissue culture plates). For the last 24 hours before the experiment, the cells were starved as usual. Each of the resulting 2×11 cultures of standardized predators (which had reached a final number of at least 400 cells) was then split into four aliquots and used for one block of replicates spanning the four prey densities.

Prey were live-stained as described in section 1.2.3. The experiments were carried out in 50 ml glass vessels. The vessels were placed horizontally into a slowly rotating “plankton wheel” (~35 rounds per h) to ensure homogenous mixing without turbulence. After 1 h, the *Lembadion* were filtered through a 15 μm gauze, fixed with glutaraldehyde, and the number of fluorescing food vacuoles per cell was determined immediately. Additionally, length and width of 30 cells from the 6.25 prey per ml treatment of each block (see above) were measured for calculation of volume-specific feeding rates (i.e. absolute feeding rates divided by mean predator volume). The data were analyzed with non-parametric two-way ANOVAs (Scheirer-Ray-Hare extension of Kruskal-Wallis test, Sokal and Rohlf 1995, p. 446).

1.2.8 Experiment 5: Maximal population growth rate of small and large *Lembadion* with small prey

In experiment 5, I investigated how cell size influences the maximal population growth rate that *Lembadion* can attain with small prey. This was achieved by culturing both the C-form and the A-form with excess *Colpidium campylum* as food.

The results of experiment 1 showed that *Lembadion* changes its cell size in response to a new type of prey. Therefore, it is not possible to measure steady state growth rates of the A-form with *Colpidium campylum* as food. To correct for prey-induced changes in mean cell volume, I calculated population growth rates not only for cell number but also for total biovolume (i.e. for cell number times mean cell volume). These volume-corrected population growth rates are the best approximation for steady-state growth rates available. The volume-correction applied here should not be confused with the calculation of volume-specific feeding rates in experiments 3 and 4.

I did five replicates for the A-form and six for the C-form. Each replicate was started with 100 well-fed *Lembadion* selected from independent stock cultures, which were placed into 10 ml of medium containing approximately 5000 *Colpidium campylum* per ml (day 0). After 24 h, 100 cells were transferred to fresh medium with the same amount of prey to continue the experiment (day 1). The rest were counted, fixed and measured (length and width) in order to determine the daily population growth rate r

and volume-corrected growth rate r_{vol} . This procedure was repeated for 8 days (days 1 to 8). In the period between day 0 and day 1, the *Lembadion* were supposed to habituate to the experimental conditions. Therefore, the data from day 1 were excluded from the analysis.

1.3 Results

1.3.1 Experiment 1: Size of *Lembadion* raised with different prey

The size of *Lembadion* remained constant over the three sampling dates and increased continuously with prey dimensions. The four prey species induced four distinguishable size morphs of *Lembadion*, which I refer to as the C-, K-, O-, and A-form (Fig. 2). Biometrical data for these morphs and their respective prey are given in Table 1.

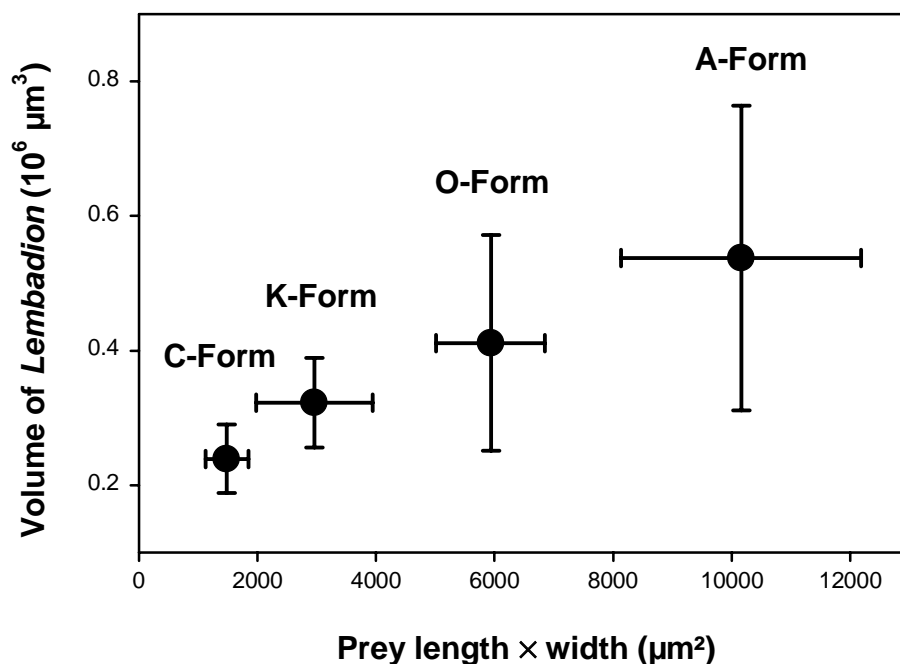


Fig. 2: Results from experiment 1.

Mean volume of four *Lembadion* morphs as a function of mean prey “bulkiness” (= length × width), showing the close correlation between predator and prey size. Prey were *Colpidium campylum* for the C-form, *Colpidium kleini* for the K-form, *Euplotes octocarinatus* for the O-form and *Euplotes aediculatus* for the A-form. Data were pooled over 4 replicates and 3 sampling dates for each prey species. Error bars represent standard deviations. For further biometrical data, see table 1.

Table 1: Results from experiment 1: Length and width of four *Lembadion* morphs and the prey they were induced with. Data are means \pm SD. n is the total number of measured cells (30 cells per sample \times 3 samples per replicate \times 4 replicates).

<i>Lembadion</i>				Prey			
	length (μm)	width (μm)	n		length (μm)	width (μm)	n
C-form	100.9 \pm 6.48	66.9 \pm 5.70	360	<i>C. campylum</i>	59.1 \pm 7.71	25.0 \pm 4.69	70
K-form	112.5 \pm 6.71	73.6 \pm 6.23	360	<i>C. kleini</i>	77.7 \pm 14.85	37.4 \pm 6.57	190
O-form	125.5 \pm 12.07	77.4 \pm 11.81	360	<i>E. octocarinatus</i>	90.1 \pm 6.27	65.6 \pm 6.83	90
A-form	143.1 \pm 11.87	82.5 \pm 14.77	360	<i>E. aediculatus</i>	124.4 \pm 10.70	81.0 \pm 10.22	260

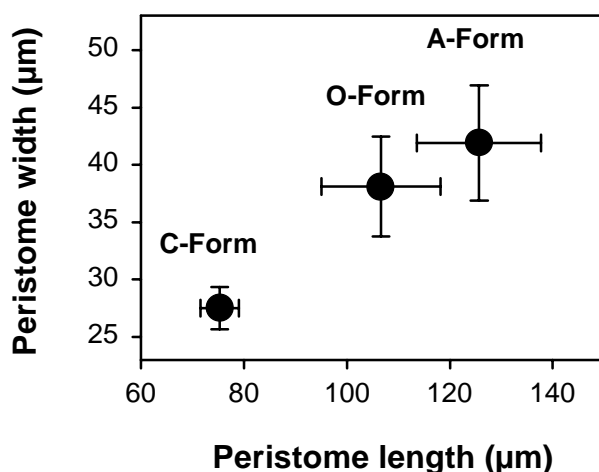
Repeated measures ANOVAs showed that prey species had a significant impact on mean length, width and volume of *Lembadion*, whereas there was no significant influence of time (Table 2). Therefore, the data from the three sampling dates could be pooled to yield one mean value per replicate for each parameter. Using these values, there was a very close correlation between mean prey bulkiness (length \times width), and mean length ($R^2 = 0.96$, $p < 0.0001$, $n=16$), width ($R^2 = 0.92$, $p < 0.0001$), and volume ($R^2 = 0.96$, $p < 0.001$) of the corresponding predator morph.

1.3.2 Experiment 2: Peristome size of *Lembadion* raised with different prey

The dimensions of the peristome differed between the *Lembadion* cells from all 3 prey treatments (Fig. 3), with both length and width being largest in the A-form and smallest in the C-form (Table 3). Cell lengths and widths were similar to those recorded in experiment 1. Relative peristome length (i.e. peristome length divided by cell length) was slightly higher in the O- and A-form than in the C-form (C-form: 0.74 ± 0.031 , O-Form: 0.80 ± 0.045 , A-form: 0.82 ± 0.036 ; see Table 3), whereas relative peristome width did not differ significantly between the three morphs (C-form: 0.52 ± 0.046 , O-form: 0.56 ± 0.073 , A-form: 0.55 ± 0.059 ; see Table 3). Thus, the peristome changes almost isometrically with cell size.

Table 2: Results of repeated measures ANOVAs for experiment 1: The effect of prey species and time on mean length, width and volume of *Lembadion*.

Mean cell length						
	d.f. Effect	MS Effect	d.f. Error	MS Error	<i>F</i>	<i>p</i>
Prey species	3	3866.89	12	8.51	454.60	< 0.001
Time	2	20.93	24	6.15	3.40	0.0501
Interaction	6	6.50	24	6.15	1.06	0.415
Mean cell width						
	d.f. Effect	MS Effect	d.f. Error	MS Error	<i>F</i>	<i>p</i>
Prey species	3	498.12	12	10.85	45.89	< 0.001
Time	2	3.18	24	8.61	0.37	0.695
Interaction	6	13.99	24	8.61	1.62	0.184
Mean cell volume						
	d.f. Effect	MS Effect	d.f. Error	MS Error	<i>F</i>	<i>p</i>
Prey species	3	$1.87 \cdot 10^{11}$	12	$2.14 \cdot 10^9$	87.57	< 0.001
Time	2	$1.66 \cdot 10^8$	24	$1.77 \cdot 10^9$	0.09	0.911
Interaction	6	$1.30 \cdot 10^9$	24	$1.77 \cdot 10^9$	0.73	0.628

**Fig. 3:** Results from experiment 2.

Mean length and width of the peristome (cell mouth) in three *Lembadion* morphs (pooled over all replicates). Large prey induce predators with large peristomes and, therefore, a large gape-size. The C-form was raised with *Colpidium campylum* (small prey), the O-form with *Euplotes octocarinatus* (intermediate sized prey) and the A-form with *Euplotes aediculatus* (large prey). Error bars represent standard deviations.

Table 3: Results of overall Kruskal-Wallis H-tests and *post-hoc* Mann-Whitney U-tests with Bonferroni correction (i.e. differences are significant for $p < 0.0167$) for experiment 2: The effect of prey species on absolute and relative length and width of the peristome (cell mouth) of *Lembadion*. Relative peristome length = peristome length / cell length (analogous for width). No *post-hoc* tests were conducted for relative peristome width, as the overall H-test did not indicate any significant differences. The C-form was raised with *Colpidium campylum* (small prey), the O-form with *Euplotes octocarinatus* (intermediate sized prey) and the A-form with *E. aediculatus* (large prey).

Peristome length $H = 18.9, p = 0.0001$			Relative peristome length $H = 7.95, p = 0.0188$		
	<i>U</i>	<i>p</i>		<i>U</i>	<i>p</i>
C- vs. O-form	0	0.0044	C- vs. O-form	0	0.0044
C- vs. A-form	0	0.0091	C- vs. A-form	0	0.0091
O- vs. A-form	0	< 0.0001	O- vs. A-form	44	0.5079
Peristome width $H = 14.75, p = 0.0006$			Relative peristome width $H = 1.96, p = 0.3746$		
	<i>U</i>	<i>p</i>		<i>U</i>	<i>p</i>
C- vs. O-form	0	0.0044	C- vs. O-form	-	-
C- vs. A-form	0	0.0091	C- vs. A-form	-	-
O- vs. A-form	11	0.0013	O- vs. A-form	-	-

1.3.3 Experiment 3: Feeding rate of small and large *Lembadion* with large prey

In both experiments, *Lembadion* raised with one of the *Euplotes* species achieved significantly higher feeding rates than the smaller *Lembadion* raised with *Colpidium campylum*. In particular, the C-form was almost completely unable to feed on *Euplotes aediculatus*.

In experiment 3a (*Euplotes aediculatus* as food), the C-form reached a mean feeding rate of 0.006 ± 0.010 ingested prey per predator per hour, whereas the A-form ingested 0.60 ± 0.075 prey items per predator per hour (*t*-test, $p < 0.001$). Data are means \pm stan-

standard error (= standard deviation of the means from the 3 replicates). In experiment 3b (*Euplotes octocarinatus* as prey) mean feeding rates were 0.30 ± 0.120 in the C-form and 1.37 ± 0.172 in the A-form (t -test, $p < 0.001$). Calculating volume-specific feeding rates (number of prey consumed per h and per $10^6 \mu\text{m}^3$ predator volume) yielded qualitatively similar results (experiment 3a: C-form 0.047 ± 0.081 , A-form 1.24 ± 0.309 , $p = 0.003$; experiment 3b: C-form 1.98 ± 0.722 , A-form 4.46 ± 0.829 , $p = 0.018$).

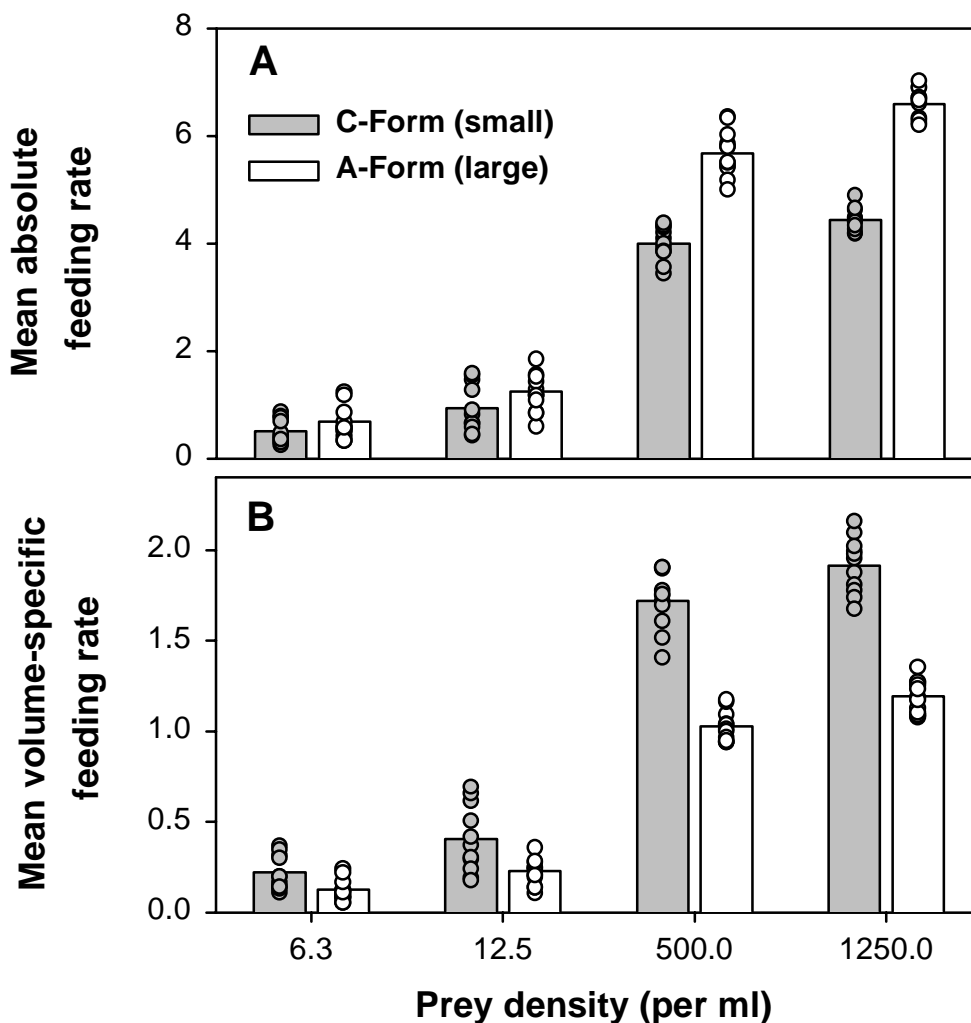


Fig. 4: Results from experiment 4.

Mean absolute (A) and volume-specific (B) feeding rate of two *Lembdion* morphs feeding on stained *Colpidium campyllum* (i.e. small prey) for 1 h as a function of prey density. Absolute feeding rate is number of prey consumed per predator per hour. Volume-specific feeding rate is number of prey consumed per $10^6 \mu\text{m}^3$ predator volume per hour. Dots are means from the 11 replicates, whereas bars show the grand mean for all replicates. Although the large A-form always consumed significantly more prey than the small C-form, it consumed less prey per unit volume. This is evidence that the A-form suffers fitness costs which become apparent in the presence of small prey. See text for statistical analysis.

Experiment 4: Feeding rate of small and large *Lembdion* with small prey

Both predator type and prey density had a significant effect on absolute as well as volume-specific feeding rates, with no significant interactions between the two factors (absolute feeding rates: predator type $H = 6.95$, $p = 0.008$; prey density $H = 70.35$, $p < 0.0001$; interaction $H = 1.96$, $p = 0.58$; volume-specific feeding rates: predator type $H = 9.48$, $p = 0.002$; prey density $H = 99.20$, $p < 0.0001$; interaction $H = 0.97$, $p = 0.81$; see Fig. 4). At all prey densities, absolute feeding rates were higher in the A-form. Volume-specific feeding rates, however, were higher in the C-form. This is because mean feeding rates of the two morphs differed only by a factor of 1.38 (averaged over the four prey densities), whereas their mean volume differed by a factor of 2.38 (mean volume of the A-form: $554 \pm 126 \cdot 10^3 \mu\text{m}^3$; mean volume of the C-form: $233 \pm 47 \cdot 10^3 \mu\text{m}^3$). Both measures of feeding rate increased with prey density and nearly leveled off at 1250 prey per ml.

1.3.4 Experiment 5: Maximal population growth rate of small and large *Lembdion* with small prey

Population growth rates for both cell number (r) and total biovolume (volume-corrected growth rates r_{vol}) were significantly higher in the C-form than in the A-form (Table 4, significant effects of predator morph). These differences remained constant over the course of the experiment (non-significant interactions between time and predator morph, reflecting the parallel graphs in Fig. 5 A). Although growth rates varied significantly over time (significant time effects), there was no consistent (increasing or decreasing) trend, but merely fluctuations around some constant base level.

In the course of the experiment, the volume of the C-form remained more or less constant, whereas the volume of the A-form decreased considerably but did not reach the level of the C-form (Fig 5 B). This is reflected by a significant effect of the interaction between time and predator morph on mean predator volume (Table 4).

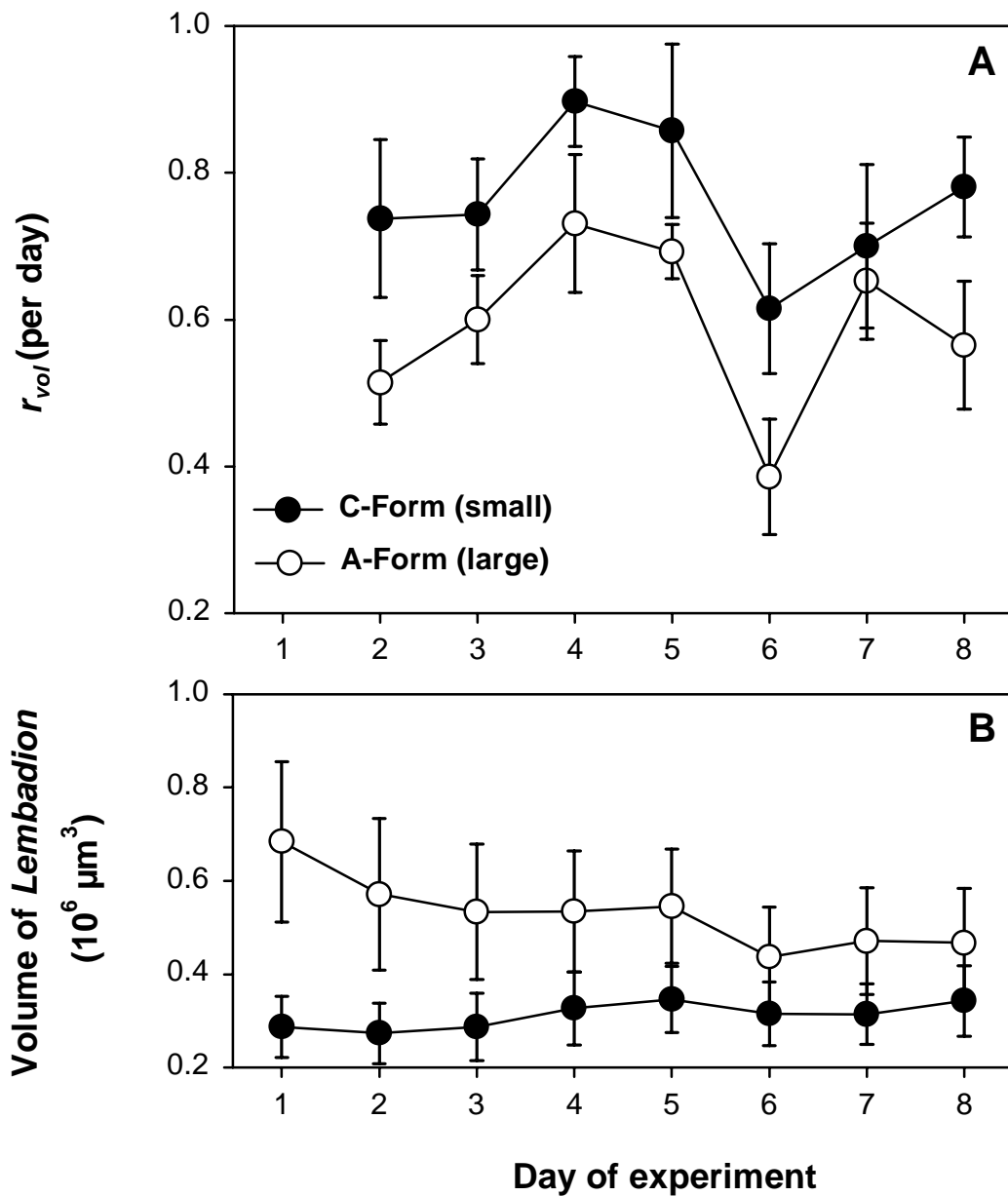


Fig. 5: Results from experiment 5.

A) Daily volume-corrected growth rates r_{vol} (means \pm SD) for the C-form (solid dots) and the A-form (empty dots) when fed with excess *Colpidium campylum* for a period of 8 days; **B)** mean volume of the two morphs over time (means \pm SD of pooled individual data from all replicates); The A-form consistently grows slower than the C-form. This difference does not change over time, although the volume of the A-form steadily decreases. Our results indicate a volume-independent cost for large morphs. For statistical analysis, see Table 4.

Table 4: Results of repeated measures ANOVAs for experiment 5: the effect of *Lembadion* morph and time on population growth rate r , volume-corrected population growth rate r_{vol} and mean cell volume. Data for mean cell volume have been log-transformed before the analysis.

Population growth rate r						
	d.f. Effect	MS Effect	d.f. Error	MS Error	F	p
<i>Lembadion</i> morph	1	0.16	9	0.01	28.56	0.0005
Time	6	0.03	54	0.00	6.75	< 0.001
Interaction	6	0.01	54	0.00	1.38	0.240
Volume-corrected population growth rate r_{vol}						
	d.f. Effect	MS Effect	d.f. Error	MS Error	F	p
<i>Lembadion</i> morph	1	0.55	9	0.01	105.31	< 0.001
Time	6	0.11	54	0.01	15.28	< 0.001
Interaction	6	0.01	54	0.01	1.46	0.209
Mean cell volume						
	d.f. Effect	MS Effect	d.f. Error	MS Error	F	p
<i>Lembadion</i> morph	1	6.05	9	0.01	1011.87	< 0.001
Time	7	0.04	63	0.00	13.97	< 0.001
Interaction	7	0.11	63	0.00	38.30	< 0.001

1.4 Discussion

1.4.1 An inducible offense

My results show that *Lembadion bullinum* displays a prey-induced size polyphenism, that is it is able to express an inducible offense. Moreover, the polyphenism is continuous. In other words, *Lembadion* is able to gradually adjust its size to the size of its prey: the larger the prey, the larger the predator (Fig. 2). This adjustment involves an isometric change in the dimensions of the peristome (cell mouth) and, thus, of gape-size (Fig. 3). By raising *Lembadion* with four differently sized prey species I obtained four distinguishable morphs or phenotypes, which I termed the C-, K-, O- and A-form, respectively. The size distributions of these morphs overlap widely. Thus, the morphs are not qualitatively different, but merely differ in the average expression of a phenotypically plastic trait, that is size. Mean size of a morph is stable as long as the size of the dominant prey does not change (Table 2). Indeed, cultures of the various morphs can be maintained for months (personal observation). Continuous polyphenisms similar to that of *Lembadion* have been reported from *Onychodromus indica* (Kamra and Sapra 1994), *Stylonychia mytilus* (Giese and Alden 1938), *Blepharisma americanum* (Giese 1973), and *Didinium nasutum* (Hewett 1980).

The “giant cannibals” described by Kuhlmann (1993, see introduction, section 1.1) can be interpreted as part of *Lembadion*’s continuous polyphenism. I regularly found giants in my stock cultures, too. Generally, they were smaller than the A-form (personal observation), which is in accordance with their feeding on smaller prey (starved C-form conspecifics are smaller than *Euplotes aediculatus*). Thus, they fit neatly into the continuum shown in Fig. 2, and do not appear to be qualitatively different from other morphs. I conclude that “giants” are simply the morph adjusted to feeding on small conspecifics. Trophic polyphenisms are frequently coupled with cannibalism, in protozoa (reviewed in Giese 1973, Waddell 1992, Ricci and Banchetti 1993) and elsewhere (Gilbert 1980, Collins and Cheek 1983).

In the following, I will discuss the inducible offense of *Lembadion* within the framework of costs, cues, and environmental variability. Thereby, I assume that the smallest

Lembadion morph, the C-form, is “normal” or “non-induced”, whereas all other morphs are “induced” to varying degrees.

1.4.2 Benefits and costs

The induced large cell size of *Lembadion* must be expected to have benefits as well as costs. Without benefits, it would not be adaptive. Without costs, it should be expressed permanently. This trade-off between benefits and costs has been investigated in experiments 3 to 5.

The benefit for large morphs is the ability to consume large prey, which leads to an expansion of the utilized food range. The large A-form can feed on *Euplotes aediculatus*, which for the small C-form is virtually inaccessible (experiment 3a). Similarly, the intermediate O-form is much more successful than the C-form in capturing *Euplotes octocarinatus* (experiment 3b). These results are most easily explained as an effect of gape size (experiment 2, Fig. 3). Similar “gape size offenses” have been reported from other protozoa (Giese and Alden 1938, Williams 1961, Giese 1973, Hewett 1980, Wicklow 1988, Gomez-Saladin and Small 1993, Ricci and Banchetti 1993, Kamra and Sapra 1994) and the rotifer *Asplanchna* (Gilbert 1980).

Costs paid by large morphs should become apparent in the presence of small prey, since, under these conditions, large *Lembadion* regularly transform to small morphs. Furthermore, preliminary experiments indicate that with a mixture of two prey species, *Lembadion* always adjusts its size to the smaller one (personal observation). My discussion will focus on demographic costs, that is I assume that *Lembadion*'s fitness can be measured in terms of population growth rate r . This assumption seems justified because protozoa generally live in variable environments (Taylor and Berger 1980, Fenchel 1982) that select for “ r -strategists” specialized on rapid growth and fast exploitation of food resources. While r was determined directly in experiment 5, it should be also closely linked to the volume-specific feeding rates measured in experiment 4.

Experiment 4 was designed to investigate the influence of cell size on *Lembadion*'s success in capturing small *Colpidium campylum*. At all prey densities, the A-form achieved higher absolute feeding rates than the C-form, but lower volume-specific ones (Fig. 4).

In other words, the effect of their larger gape-size did not fully compensate for their increased cell volume. Volume-specific feeding rates should be roughly proportional to population growth rate r , since gross growth efficiency (yield) in protozoa is generally found to be independent of volume (Finlay and Fenchel 1996). In contrast to absolute feeding rates, volume-specific feeding rates reflect that large cells generally need more food than small cells, due to their higher demands of energy for growth and reproduction. Certainly, any extrapolation from short-term feeding experiments to long-term fitness consequences must be applied with care. In particular, my estimate of cell volume is quite rough and it is unknown how volume influences metabolic rates. Nevertheless, lacking more specific information, volume-specific feeding rates can serve as a useful first approximation to fitness (e.g. Goldman and Dennett 1990, Finlay and Fenchel 1996). Therefore, the results from experiment 4 indicate that the A-form experiences costs in the presence of small prey.

The mechanism leading to these costs probably differs depending on prey density. At low prey densities, the predators did not become satiated, and their (absolute) feeding rates are proportional to “success rate” (i.e. the gradient at the origin of a typical type II functional response curve, Jeschke et al. 2002), which is a measure of their efficiency in attacking and capturing prey. Volume-specific success rate might be decreased in large cells because they have an unfavorable ratio of peristome area to volume. Costs via decreased foraging efficiency with alternative prey have also been reported for some other inducible offenses (Ehlinger and Wilson 1988, Hewett 1988, Meyer 1989, Ehlinger 1990, Goldman and Dennett 1990, Trowbridge 1991, Thompson 1992, Hampton and Starkweather 1998)

At high prey densities, almost all predators are “digestion-limited” (Jeschke et al. 2002), that is their feeding rate is limited by the time needed to digest a single prey item and the number of prey items that can be digested simultaneously (“gut capacity”). Since the duration of the trials was too short for prey to become digested (prey items inside food vacuoles looked still almost intact; personal observation), feeding rates in the high prey density treatments of experiment 4 are basically a measure of gut capacity. Because the “gut” of a ciliate simply is its cytoplasm, my results show that, for some unknown reason, food vacuoles are packed more loosely into large *Lembadion* cells. Under the assumption that digestion time for one food vacuole is not smaller in large morphs than it

is in small ones, this will lead to consistently lowered volume-specific feeding rates in large morphs also over longer time scales (i.e. when feeding rate is determined by an equilibrium of ingestion and digestion).

Finally, experiment 5 yielded direct evidence that large morphs suffer demographic fitness costs. When both the C- and the A-form were cultured with excess *Colpidium campylum*, the A-form attained significantly lower population growth rates r . This result also holds true for volume-corrected population growth rates r_{vol} , which take into account that the mean size of the A-form decreased over the course of the experiment. The mechanism behind these costs may be found in the looser packing of food vacuoles indicated by experiment 4. Again, however, this extrapolation can only be tentative. In any case, the mechanism does not seem to be directly linked to cell volume, but rather to some aspect of physiology: Although, over the course of the experiment, the difference in cell volume between the two morphs decreased roughly by a factor of 3 (Table 4 and Fig. 5 B), the difference in r_{vol} remained constant (non-significant interaction between predator type and time, see Tables 2, 3 and Fig. 5 A). This indicates that readjusting the cell physiology to a new prey species requires more time than the mere change in cell size. Costs in terms of lowered population growth rate have also been reported for large morphs of *Didinium nasutum* (Hewett 1988), and theoretically predicted for the “campanulate” morph of *Asplanchna silvestrii* (Gilbert and Stemberger 1985).

In summary, expressing its inducible offense by increasing in cell size is advantageous for *Lembadion* when only large prey is present. Due to their increased gape-size, large morphs can exploit resources that are inaccessible to small morphs. With small prey, in contrast, large morphs suffer costs, as they attain lower volume-specific feeding rates (though higher absolute ones) and a lower maximal population growth rate. These costs can be characterized as environmental costs (Tollrian and Harvell 1999b) because they only act in a specific environment (i.e. when the large morph faces small prey). However it cannot be ruled out, that there are additional allocation costs (Tollrian and Harvell 1999b) for the production and operation of large cells.

1.4.3 Cues

The induction of offenses requires cues that indicate various types of prey. It is not clear how *Lembadion* “measures” prey size. To my knowledge, this question has not yet fully been answered for any other protozoan predator with a continuous size polyphenism, either. Since *Lembadion* reacts to a physical property of prey (i.e. size), this reaction need not be species-specific. Therefore, the identification of prey via chemical cues (see e.g. Buhse 1967, Lennartz and Bovee 1980, Lennartz 1986, Gomez-Saladin and Small 1993, Smith-Somerville et al. 2000) appears rather unlikely. Much more parsimonious would be the use of mechanical cues. This hypothesis is in accordance with Kuhlmann’s (1993) finding that the induction of giants relies on direct cell-to-cell contacts. In *Oxytricha bifaria*, giant formation is triggered by the energy of collisions with potential prey (Ricci et al. 1991). Yet, Kuhlmann did not find evidence for a similar mechanism in *Lembadion*. Thus, it seems most plausible to us that *Lembadion* “measures” prey size using a mechanical cue that is directly linked to the feeding process.

Once a change in prey size has been determined, transformation is initiated and predator size readjusted. Although I did not explicitly measure the rate (speed) of transformation, conclusions from my results combined with the findings of Kuhlmann (1993) give rise to some interesting speculations, which might warrant further investigation. The formation of large morphs appears to be a one-step process. According to Kuhlmann, giant cannibals appear spontaneously in starving cultures and gain their final size within one generation (though only a few cells are lucky enough to swallow a large prey item in the first place). In contrast, the transformation from large to small morphs is effectuated via multiple cell divisions and, thus, takes several generations. In experiment 5, transformation of the A-form fed *Colpidium campylum* was not fully completed after 8 days (about 7.6 generations). This appears very slow, and may in part be explained by the *ad libitum* food conditions applied in this experiment, as in many protozoans, including *Lembadion* (personal observation), cell size is positively correlated with food concentration (see references given in Zalkinder 1979). In experiment 1, all transformations seem to have been completed within 10 days. Kuhlmann reports that most “giants”, when fed *Colpidium campylum*, regain the size of “normal” cells (C-form) within 2 or 3 days, but for some of them, the transformation may last 5 to 10 days. Taken together, these findings suggest that the formation of large morphs might be faster than

that of small ones. The rate of transformation might also depend on environmental conditions such as food concentration. A slow, “prudent” reduction of cell size might be adaptive, as the risk from having the wrong morphology is greater for small cells (starvation) than for large ones (non-lethal demographic costs).

1.4.4 Environmental variability

Like other examples of phenotypic plasticity (Stearns 1989, Tollrian and Harvell 1999a), inducible offenses can be discussed as adaptations to a variable environment, in particular with fluctuating food supply. While the microenvironment of *Lembadion* has not yet been the subject of any detailed field study, protozoa are generally found to live a “feast and famine” existence (Fenchel 1982), to which they have evolved numerous adaptations (apart from trophic polyphenisms e.g., high starvation resistance (Fenchel 1982, Lynn et al. 1987), swarmer phenotypes (Nelsen and Debault 1978, Salt 1979) or encystation (see De Puytorac 1984)). An essential adaptation to fluctuating food supply is the ability to rapidly and efficiently exploit ephemeral food patches. This might be the reason why the highly efficient and rapidly growing small morphs are preferred once small prey is available in sufficient concentration. In the absence of small prey, transformation to a large morph enables *Lembadion* to switch to alternative food sources. A special case of this strategy is the use of cannibalism as a “life-boat” mechanism (van den Bosch et al. 1988). Conspecifics are likely to be abundant after a rich food patch has been depleted. In summary, its continuous polyphenism allows *Lembadion* to fine-tune its morphology to the prevailing environmental conditions. The evolution of inducible predator offenses can be expected in situations where important prey characteristics vary with time or space and might be more common than generally expected.

Part 2. Reciprocal phenotypic plasticity in a predator prey system: inducible offenses against inducible defenses?

2.1 Introduction

Studies on phenotypic plasticity in species interactions have almost exclusively focused on one-sided events. In predator-prey relationships, researchers have described numerous examples of inducible defenses in prey and fewer cases of inducible offenses (diet-induced trophic polyphenisms) in predators (see citations in the general introduction). However, the interplay between inducible defenses and offenses remains largely unstudied. Notable exceptions come from plant-herbivore systems, where plants can induce chemical defenses in response to herbivory (reviewed in Karban and Baldwin 1997), and herbivores may counter these defenses by activating detoxification mechanisms (Snyder and Glendinning 1996, Bernays and Chapman 2000) or expressing alternative digestive enzymes (Bolter and Jongsma 1995, Jongsma and Bolter 1997, see Karban and Agrawal 2002 for a general review of offensive traits in herbivores). Also, behavioral ecologists have started to investigate patch-selection games between predator and prey (Alonzo 2002, Lima 2002 and references therein). Finally, in some intraspecific interactions, environmentally induced cannibalistic morphs elicit morphological (Wicklow 1988) or behavioral (Chivers et al. 1997 with further references) defenses in their conspecific prey. In a recent review, Agrawal (2001) argues that such “reciprocal phenotypic changes in ecological time” (“ecological arms races”) might be more common than generally expected. He points out that phenotypic plasticity, as opposed to or in addition to fixed adaptations, is a likely outcome of coevolution. Adler and Grünbaum (1999) as well as Lima (2002) argue that the study of reciprocal phenotypic plas-

ticity promises new insights into the ecology and evolution of predator-prey interactions.

The system *Lembadion bullinum* – *Euplotes octocarinatus* provides an excellent opportunity for the study of reciprocal phenotypic plasticity. Both species are known to display morphological plasticity in predation-related traits. In Part 1, I have shown that *Lembadion* can express an inducible offense – an increase in cell size and gape size – when confronted with large prey. In addition, *Lembadion* elicits inducible defenses in several prey species (Kuhlmann and Heckmann 1985, for review see Wicklow 1997, and Kuhlmann et al. 1999). In the herbivorous ciliate *Euplotes octocarinatus*, a kairomone (info-chemical) released from *Lembadion*'s cell surface (Peters-Regehr et al. 1997) induces the production of protective lateral “wings” (Kuhlmann and Heckmann 1985), which cause the normally ovoid prey cells to adopt an almost circular shape. These wings inhibit ingestion by *Lembadion* and are also effectively employed against other gape-limited predators (Kuhlmann and Heckmann 1994).

Here, I will test the hypothesis that the inducible offense of *Lembadion* can act as a counter-adaptation to the inducible defense of *Euplotes octocarinatus*. I have performed an induction experiment, where I induced a larger predator size by offering defended prey, and I have tested whether these induced predators can overcome the prey's defense. I will discuss whether phenotypic plasticity in both species can be viewed as a result of predator-prey coevolution.

2.2 Material and methods

For stock cultures, cultivation and general methods, see Part 1, section 1.2.

2.2.1 Cultivation of defended prey

Defended *Euplotes octocarinatus* were induced by co-culturing them with the predatory turbellarian *Stenostomum sphagnetorum* (raised with *Chlorogonium*) under conditions of abundant food. *Stenostomum* induces the same morphological reaction in *Euplotes* as

does *Lembadion* (Kuhlmann and Heckmann 1985) but can be much more easily separated from the ciliates after exposure.

2.2.2 Size experiment with induced versus non-induced prey

The aim of the first experiment was to study the morphological reaction of *Lembadion* to the inducible defense of *Euplotes octocarinatus*. Six replicated cultures of *Lembadion* were fed daily with defended prey, whereas six control cultures received undefended prey. After two weeks, 20 well-fed cells (containing visible food vacuoles) from each culture were subjected to starvation for 24 h (for better standardization) and subsequently fixed and measured. Measurements included cell length, cell width, and length and width of the cell mouth (peristome).

Undefended prey employed in this experiment averaged $82.1 \pm 6.61 \mu\text{m}$ in length and $50.0 \pm 5.21 \mu\text{m}$ in width ($n = 60$), whereas defended prey were $102.4 \pm 10.52 \mu\text{m}$ long and $78.2 \pm 9.81 \mu\text{m}$ wide ($n = 60$; t -test on means of three replicates with 20 measurements each: d.f. = 4, $p < 0.001$ for both length and width).

In Part 1, I have termed *Lembadion* raised on undefended *Euplotes octocarinatus* the O-form, and I have shown that these predators display an intermediate expression of the inducible offense (i.e. they are of intermediate size). However, as they represent the smallest (least induced) morph in this part, I will now refer to them as the “normal” or “non-induced” morph, and to *Lembadion* raised on defended *Euplotes octocarinatus* as the “induced” morph. While this terminology is slightly inaccurate, it greatly simplifies discussion.

2.2.3 Feeding experiments

Two short-term feeding experiments were designed to test whether a potential counter-reaction of *Lembadion* is effective in overcoming the induced defense of *Euplotes octocarinatus*. In short, I measured the feeding rate of *Lembadion* raised with defended and non-defended *Euplotes octocarinatus*, respectively. The duration of the feeding trials was chosen such that the predators did not become satiated (i.e. the vast majority did not

consume more than one prey item, although, given enough time, they can easily ingest several; personal observation). Therefore, feeding rate can be interpreted as a measure of the predator's efficiency in hunting a particular prey, which is an important component of fitness.

Since raising *Lembadion* with induced *Euplotes octocarinatus* (as in the size experiment) is very laborious, I instead used non-induced *Euplotes aediculatus* as a substitute food to obtain induced predators, because non-induced *Euplotes aediculatus* are similar in size to induced *Euplotes octocarinatus*. This procedure is justified, as *Lembadion* most likely reacts only to prey size, not to particular prey species (see Part 1, section 1.4.3). Furthermore, preliminary experiments had shown that the morphological reactions of *Lembadion* to these two types of prey are similar (size of *Lembadion* receiving *Euplotes aediculatus* as food: length $143.0 \pm 11.87 \mu\text{m}$, width $82.5 \pm 14.77 \mu\text{m}$ ($n = 360$); with defended *Euplotes octocarinatus* as food: length $140.5 \pm 11.16 \mu\text{m}$, width $84.8 \pm 14.05 \mu\text{m}$ ($n = 360$); multivariate F -test (ANOVA) on means of four replicates: $p > 0.13$). Therefore, *Lembadion* raised on non-induced *Euplotes aediculatus* (the A-form in the terminology of Part 1) will also be called "induced".

Lembadion were obtained from independent stock cultures for each replicate. Well-fed cells with visible food vacuoles were selected 24 h before the experiments and starved in food free medium until exposure to the prey. Subsamples of both predators and prey were measured before the experiments.

In contrast to the procedure described in section 1.2.3, the concentration of fixative used in the feeding experiments was only 0.25 %, which caused the cells to appear shorter and wider than with the usual 2 %. Therefore, the size data from the feeding experiments should not be compared directly to those from the previous experiment. For the future, I strongly recommend the 2 % concentration.

2.2.4 Feeding experiment 1

The first feeding experiment had a 2×2 factorial design with two types of prey (induced vs. non-induced), two types of predator (induced vs. non-induced), and 8 replicates per treatment. In each trial, 100 *Euplotes* were offered to 100 *Lembadion* in an

individual well of a 12-well tissue culture plate containing 1 ml of medium. After 20 min, feeding was stopped by addition of glutaraldehyde, and the remaining *Euplotes* were counted. I calculated both the absolute feeding rate (number of prey consumed per predator per hour) and the volume-specific feeding rate (absolute feeding rate divided by mean predator volume).

Undefended *Euplotes octocarinatus* employed in the experiment had a mean length of $80.2 \pm 9.78 \mu\text{m}$ and a mean width of $54.0 \pm 7.82 \mu\text{m}$ ($n = 250$), whereas the mean length of defended *Euplotes octocarinatus* was $98.4 \pm 9.31 \mu\text{m}$ and their mean width $79.2 \pm 9.97 \mu\text{m}$ ($n = 200$).

2.2.5 Feeding experiment 2

In the second feeding experiment, I used only defended prey and offered them to either induced or non-induced *Lembadion*. In addition to comparing the mean feeding rates of the two predator morphs, this experiment had the aim of assessing how individual feeding rates of single predators are influenced by predator size (cell length and width). This was achieved by the use of fluorescently labeled prey, which also allowed the use of much higher prey densities than in the previous experiment.

In an attempt to further standardize initial conditions, both predator morphs were fed approximately 1300 non-induced *Euplotes octocarinatus* per ml during the last 48 h leading up to the starvation period preceding the trials. This caused a reduction in the size of the induced morph, but the difference to the normal morph remained highly significant (see results). Fluorescent live-staining of prey was accomplished as described in section 1.2.3.

Each treatment was replicated 11 times. I stained 11 cultures of independently raised and induced *Euplotes octocarinatus*, divided them into two aliquots each and used each pair of aliquots for one pair of replicates (induced and non-induced predator). In each trial, approximately 4000 *Euplotes octocarinatus* were offered to around 100 *Lembadion* in 1 ml of medium using 6-well tissue culture plates. For each predator, I recorded length, width, and the number of fluorescing food vacuoles. The induced prey

employed in the experiment averaged $98.5 \pm 9.74 \mu\text{m}$ in length and $78.9 \pm 7.70 \mu\text{m}$ in width ($n = 1100$).

To analyze the relationship between cell dimensions and individual feeding rate I used multiple logistic regression. For each treatment, data from all replicates were pooled together. Length and width were entered as independent variables. The logistic regression model then predicts the probability that a cell of given dimensions will consume one or more prey items during the experiment. Pooling the classes with one or more consumed prey is a negligible simplification, since less than 4 % of the predators consumed more than one prey.

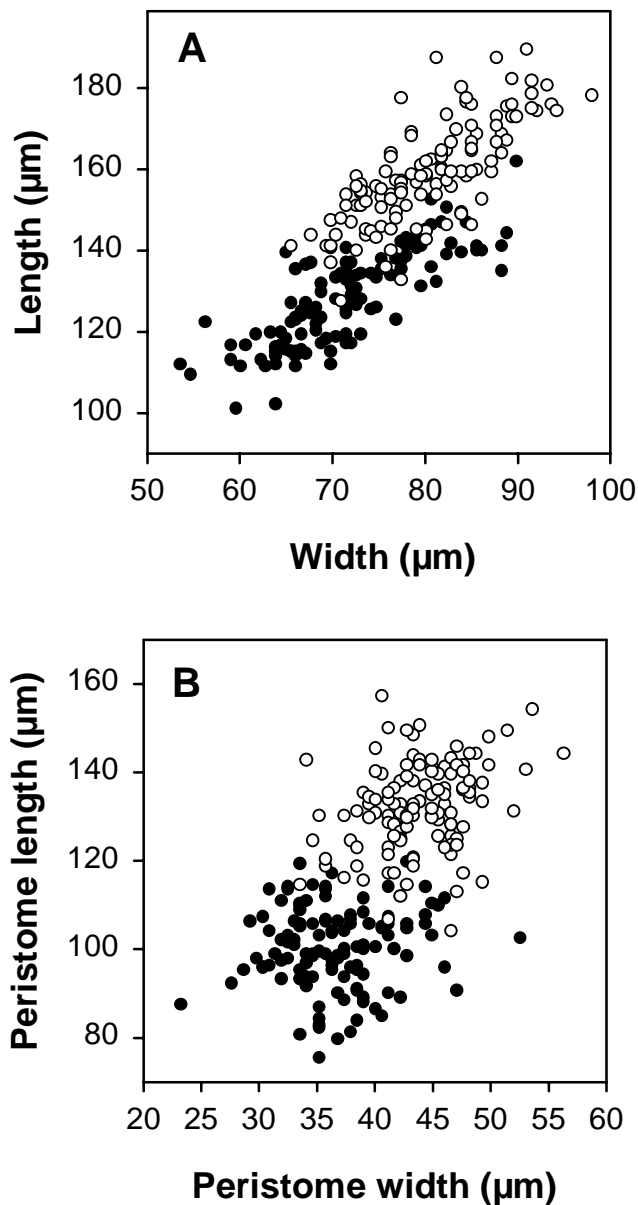


Fig. 6: The morphological reaction of *Lembadion bullinum* to the inducible defense of its prey *Euplotes octocarinatus*.

The inducible defense of *Euplotes octocarinatus* induces an increase in the cell size of *Lembadion* (i.e. *Lembadion* expresses an inducible offense). The figures show morphometric data of two *Lembadion* morphs: **A**) cell dimensions and **B**) dimensions of the cell mouth (peristome). The non-induced *Lembadion* morph (filled circles) was raised on undefended prey, whereas the induced morph (open circles) was raised on defended prey.

2.3 Results

2.3.1 Size experiment with induced versus non-induced prey

Feeding on defended prey induced *Lembadion* to undergo a transformation towards increased cell sizes: *Lembadion* raised on defended *Euplotes octocarinatus* were significantly larger and had a larger peristome than control cells raised on undefended prey (Fig. 6, Table 5). In both morphs, cell length was positively correlated with peristome length (non-induced morph: $R^2 = 0.81$, induced morph: $R^2 = 0.88$, both $p < 0.001$), and cell width was positively correlated with peristome width (non-induced morph: $R^2 = 0.47$, induced morph: $R^2 = 0.39$, both $p < 0.001$).

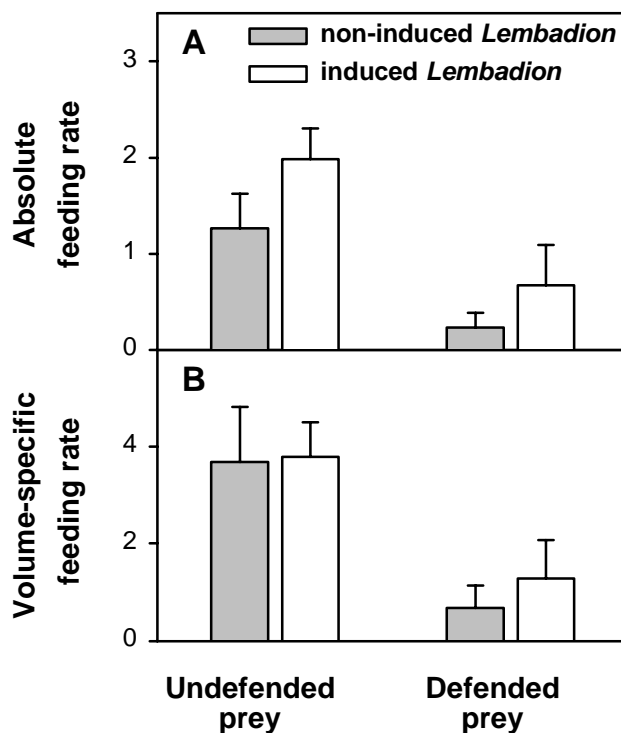


Fig. 7: Effect of *Lembadion*'s counter-reaction to the inducible prey defense – feeding rates of normal and induced *Lembadion bullinum* preying upon defended and undefended *Euplotes octocarinatus* in feeding experiment 1 (means \pm SD of eight replicates):

A) absolute feeding rates (ingested prey per predator per hour) and **B)** volume-specific feeding rates (ingested prey per $10^6 \mu\text{m}^3$ predator volume per hour). The offense of *Lembadion* increased absolute feeding rate, but had no significant influence on volume-specific feeding rate. In contrast, the defense of *Euplotes* decreased both absolute and volume-specific feeding rate. See Table 5 for statistical analysis.

2.3.2 Feeding experiment 1

Both the defense of the prey and the offense of the predator had a significant effect on absolute feeding rate of *Lembadion*, with no significant interaction between the two factors (Fig. 7 A, Table 6). Undefended *Euplotes octocarinatus* were more vulnerable to predation than defended ones, and induced *Lembadion* consumed more prey than did

non-induced ones. However, the offense of *Lembadion* only partially offset the defense of *Euplotes octocarinatus*: The number of defended prey captured by the induced morph was lower than the number of undefended prey captured by the non-induced morph. Volume-specific feeding rate was influenced significantly only by the defense of the prey, not by the offense of the predator (Fig. 7 B, Table 6; i.e. the effect of the offense on absolute feeding rate was not large enough to overcompensate for the increase in predator volume). Non-induced *Lembadion* were on average $120.0 \pm 9.78 \mu\text{m}$ long and $73.4 \pm 7.52 \mu\text{m}$ wide ($n = 240$). The corresponding values for induced predators were 139.6 ± 10.91 for length and $84.1 \pm 8.66 \mu\text{m}$ for width ($n = 240$).

2.3.3 Feeding experiment 2

In contrast to the previous experiment, feeding experiment 2 showed hardly any difference between absolute feeding rates of the two morphs: Non-induced *Lembadion* reached 0.21 ± 0.080 ingested prey per predator per hour, whereas induced predators achieved a value of 0.23 ± 0.120 (paired t -tests on the replicate means, d.f. = 10, $p > 0.45$). Similarly, there was no significant difference for volume-specific feeding rates (non-induced morph 4.51 ± 1.774 ingested prey per $10^6 \mu\text{m}^3$ predator volume per hour, induced morph 4.21 ± 1.821 ; paired t -test, d.f. = 10, $p > 0.45$).

Table 5: Morphometric data for the normal and induced morph of *Lembadion*. The normal morph was raised with undefended *E. octocarinatus* as prey, and the induced morph was raised with defended *E. octocarinatus*. Data are means \pm standard deviations from the pooled data sets in μm ($n = 120$). t -Tests were done on the mean values from six replicates.

	Normal morph	Induced morph	t_{10}	p
Length	128.5 ± 11.77	159.1 ± 12.59	10.70	< 0.001
Width	71.7 ± 7.63	80.3 ± 6.64	4.87	0.001
Peristome length	100.6 ± 9.52	132.1 ± 10.12	16.27	< 0.001
Peristome width	36.8 ± 4.59	43.9 ± 4.09	5.95	< 0.001

For both morphs, individual feeding rate was positively affected by cell width and negatively affected by cell length (Table 7). The size difference between the two morphs was less than in the previous experiments (probably due to the pre-feeding of both morphs with non-induced *Euplotes octocarinatus*, see material and methods), but still highly significant. The non-induced cells averaged $129.6 \pm 8.54 \mu\text{m}$ in length and $78.1 \pm 7.66 \mu\text{m}$ in width, whereas the induced ones reached a mean length of $140.1 \pm 11.22 \mu\text{m}$ and a mean width of $83.5 \pm 8.76 \mu\text{m}$.

Table 6: Results of ANOVA on the effects of predator and prey type on absolute and volume-specific feeding rate in feeding experiment 1. Post-hoc comparisons for the absolute feeding rates using the Student-Neumann-Keuls test indicate significant pairwise differences between all treatments.

Absolute feeding rate				
	d.f. Effect	MS Effect	<i>F</i>	<i>p</i>
Prey defense	1	5.556	102.048	< 0.001
Predator offense	1	1.242	22.805	< 0.001
Interaction	1	0.007	0.135	0.716
Error	28	0.054		
Volume-specific feeding rate				
	d.f. Effect	MS Effect	<i>F</i>	<i>p</i>
Prey defense	1	31.678	95.206	< 0.001
Predator offense	1	0.134	0.402	0.531
Interaction	1	0.946	2.842	0.103
Error	28	0.333		

2.4 Discussion

Among the current challenges in the study of phenotypic plasticity, Agrawal (2001) has identified the search for “reciprocal phenotypic changes in ecological time”. Here, I present evidence for this kind of reciprocity in the predator-prey system *Lembadion bullinum* – *Euplotes octocarinatus*: *Lembadion* reacts to the inducible defense of *Euplotes* by expressing an inducible offense, that is a plastic increase in cell size and gape size (Fig. 6). This counter-reaction is the best evidence so far in a predator-prey system for reciprocal phenotypic plasticity in predation-related morphological traits. Wicklow (1997) probably observed a similar “ecological arms race” involving *Lembadion magnum*, a close relative of *Lembadion bullinum*. In a vernal succession pool, he described a temporal correlation between the occurrence of an enlarged morph of *Lembadion magnum* and inducibly defended *Sterkiella* spec. I suggest that more examples of this kind can be found in systems where phenotypic plasticity is wide-spread, such as the microbial or metazoan plankton.

Table 7: Results of multiple logistic regression on the effect of predator length and width on absolute feeding rate in feeding experiment 2.

		<i>B</i>	SE of <i>B</i>	Wald statistic (1 d.f.)	<i>p</i>
Normal Morph (<i>n</i> = 910)	Length	-0.080	0.014	31.069	< 0.001
	Width	0.197	0.019	106.208	< 0.001
	Intercept	-6.748	1.441	21.939	< 0.001
Induced morph (<i>n</i> = 1051)	Length	- 0.052	0.010	27.178	< 0.001
	Width	0.118	0.014	74.663	< 0.001
	Intercept	-4.095	1.013	16.344	< 0.001

Despite the clear morphological effect, the counter-reaction of *Lembadion* proved rather ineffective against the defense of *Euplotes octocarinatus*. In feeding experiment 1, the inducible offense of the predator increased absolute feeding rate for both defended and undefended prey, but this increase was not strong enough to fully compensate for the effect of the prey's defense. In feeding experiment 2, the offense had no significant effect on feeding rate with defended prey at all. In neither experiment was the increase in feeding rate due to the offense large enough to more than compensate for the increase in mean predator volume – that is, the offense had no significant influence on volume-specific feeding rate. The effect of the prey's defense was only investigated in feeding experiment 1, where it significantly decreased absolute and volume-specific feeding rates of both predator morphs.

In the following, I will use absolute feeding rate as a measure of prey fitness and volume-specific feeding rate as a measure of predator fitness. Of course, these are only approximations. For the prey, I measure fitness by survival and neglect demographic costs of the defense, which, according to Kusch and Kuhlmann (1994), are not very large (~ 10 % increase in generation time). For the predator, I assume that large cells need more food than small ones for survival and reproduction and that therefore, volume-specific feeding rate is roughly proportional to population growth rate (see Part 1, section 1.2.4).

With these considerations in mind, my results give rise to the following conclusions: When employed against defended or undefended *Euplotes octocarinatus* the inducible offense of *Lembadion* may decrease the fitness of the prey (see below for a discussion of the discrepancies between feeding experiment 1 and 2), but I could not find a significant increase in the fitness of *Lembadion* itself. Conversely, the defense of *Euplotes octocarinatus* decreased the fitness of the predator and simultaneously increased the fitness of the prey. Most importantly, the protective effect of the defense was weakened, but not totally neutralized by the offense of *Lembadion*. That is, despite the counter-reaction of the predator the defense remained clearly adaptive.

A mechanistic explanation for why the offense of *Lembadion* is relatively ineffective against the defense of *Euplotes octocarinatus* is offered by the biometrical results from the size experiment and from feeding experiment 2. The key findings are: (1) Induction

leads to approximately isometric changes in predator cell size (see also Part 1). In particular, an increase in width (to match defended prey) cannot be achieved without a correlated increase in length. (2) Within morphs, length is negatively correlated with absolute feeding rate (Table 7). Under the assumption that this effect also works between morphs, absolute feeding rate will increase due to induction only if the increase in width between the two morphs is sufficiently large compared to the increase in length. Similarly, volume-specific feeding rate will increase only if the increase in absolute feeding rate is sufficiently large compared to the increase in volume. These trade-offs limit *Lembadion*'s ability to effectively counter the defense of *Euplotes octocarinatus*.

In both morphs, the absolute feeding rate of *Lembadion* increased with cell width but decreased with length. The effect of width supports the notion of gape-limitation, as cell width is positively correlated with peristome width. However, the negative effect of length was unexpected, and I can only speculate about the mechanistic basis of this result. Perhaps, long cells are handicapped in some step of the predation process. For example, they may be less agile when attacking prey. The negative effect of length on feeding rate indicates the action of a factor independent of gape-size, which clearly warrants further investigation.

The offense of *Lembadion* had a significant effect on absolute feeding rate only in feeding experiment 1, but not in feeding experiment 2. This discrepancy may be explained by the experimental conditions: In feeding experiment 2, prey were live-stained with DAPI, and prey density was 40-fold higher than in feeding experiment 1. However, mean numbers of prey captured per predator and time were even lower in feeding experiment 2 than in feeding experiment 1. This means that the success rate (number of prey captured per available prey) in both morphs was considerably decreased in feeding experiment two. This could be due to either reduced "palatability" of the stained prey, or a "swarming effect" (predator confusion, see Bertram 1978, Jeschke and Tollrian in prep.) caused by the unnaturally high prey density. In summary, the obvious effect of the experimental conditions on success rate has apparently also influenced the difference in feeding rate between the two morphs. As the conditions in feeding experiment 1 were certainly more realistic, it seems safe to conclude that the offense does have an influence on absolute feeding rate and therefore, prey fitness, *at least under some conditions*.

Predator-prey coevolution?

Agrawal (2001) and Wicklow (1997) have suggested that reciprocal phenotypic plasticity is a result of predator-prey coevolution. Before this hypothesis can be discussed in the light of my results, it must be carefully reformulated to match the conditions of the system *Lembadion bullinum* – *Euplotes octocarinatus*.

First of all, it is important to note that the interaction between *Lembadion* and *Euplotes octocarinatus* is not an exclusive one. Both the defense of *Euplotes octocarinatus* and the offense of *Lembadion* are effectively employed against a variety of other predators or prey, respectively (Part 1, Kuhlmann 1993, Kuhlmann and Heckmann 1994). However, there is an important difference regarding the induction mechanisms. The defense of *Euplotes octocarinatus* is induced by a kairomone, the L-factor, which is released from the cell surface of *Lembadion* (Peters-Regehr et al. 1997) and is different from the kairomones from other predators, such as *Amoeba* (Kusch 1993a, 1999) or *Stenostomum* (Kusch 1993b). In contrast, the offense of *Lembadion* seems to be triggered by a non-specific mechanical recognition of prey size (though the precise mechanism is unknown, see Part 1, section 1.4.3). This non-specific response indicates that phenotypic plasticity in *Lembadion* evolved as a general adaptation to an environment with variable prey size.

Arguably, however, part of this variability in prey size might stem from inducible prey defenses. *Lembadion* faces an extraordinary amount of inducible prey. Wicklow (1997) lists eleven species from six genera, and there are probably more examples waiting to be discovered by protozoologists. All of these prey species employ defenses that rely on an increase in size, and all of them react specifically to chemical cues from *Lembadion* (though not necessarily to the L-factor). The evolution of these specific responses implies that *Lembadion* is (or has been) an important predator of these species. Therefore, it is at least plausible to assume that the combined effect of their defenses is sufficiently strong to reduce the fitness of *Lembadion*, and the resulting selection pressure might have contributed to the evolution of *Lembadion*'s plasticity by diffuse coevolution (Janzen 1980). In other words, the inducible offense might have evolved partly as a counter-adaptation to inducible prey defenses (in addition to being an adaptation to variation in the size between different prey species).

In this formulation, the coevolution hypothesis is not supported by the present data. As indicated by the feeding experiments, *Lembadion* cannot gain fitness by employing its inducible offense against the inducible defense of *Euplotes octocarinatus*. Therefore, the counter-reaction of *Lembadion* that is shown in Fig. 6 does not seem to be adaptive (though it is not maladaptive, either).

Nevertheless, it is too early for the coevolution hypothesis to be rejected finally. First, no data are available concerning the effect of the offense against the inducible defenses of other prey species. Second, in a truly coevolutionary situation, the counter-reaction of *Lembadion* might in fact have been adaptive *in the past*. In the meantime, however, *Euplotes octocarinatus* could have improved its defense, for example by investing primarily in cell width, which poses the greatest problems for *Lembadion* (see above). In other words, *Euplotes octocarinatus* might be currently one step ahead of *Lembadion* in a coevolutionary arms race (Krebs and Dawkins 1979). Such arms races, however, cannot be detected by simple feeding experiments.

In summary, although the present experiments do not yield positive evidence for the coevolution hypothesis, more data are needed for a definite assessment. Future work might shed more light on the selection pressures exerted on *Lembadion* and on the relative contribution by inducible defenses. Therefore, it would be desirable to test the benefits that the inducible offense provides against other inducibly defended prey and to analyze prey size variability and its sources in the field.

Part 3. Modeling a coevolving predator-prey system with reciprocal phenotypic plasticity

3.1 Introduction

In Part 2, I have studied reciprocal phenotypic plasticity in the predator-prey system *Lembadion bullinum* – *Euplotes octocarinatus*, and I have discussed the hypothesis that the inducible offense of *Lembadion* is a coevolutionary counter-adaptation to inducible prey defenses. I showed that *Lembadion* expresses its offense in response to the defense of *E. octocarinatus* but does not gain a measurable fitness benefit from this reaction. Thus, although I could indeed document reciprocal phenotypic plasticity, I was not able to make a strong case for the coevolution hypothesis.

Nevertheless, the interplay between phenotypic plasticity and predator-prey coevolution is of general interest to evolutionary ecology and, therefore, deserves further study. In particular, two sets of questions arise:

1. What is the effect of (reciprocal) phenotypic plasticity on the ecological and evolutionary dynamics of a coevolving predator-prey system? As a limiting case, this includes the question for the consequences of phenotypic plasticity on the population dynamics in a predator-prey system without evolution.
2. Under what conditions does reciprocal phenotypic plasticity evolve? In particular, when does an inducible prey defense lead to the evolution of an inducible counter-offense?

Here, I will present an effort to answer these questions by means of mathematical modeling. My focus will be on the first question, but I will shortly discuss the second one as well.

My approach is also an attempt to bridge the gap between models of predator-prey coevolution and models of phenotypic plasticity. In the past, these two lines of theoretical research have been largely separated. Models of predator-prey coevolution (reviewed by Abrams 2000) typically do not involve phenotypically plastic traits. Instead, they usually focus on the possibility for evolutionary “arms races” or “Red Queen dynamics” (e.g. Saloniemi 1993, Dieckmann et al. 1995, Abrams and Matsuda 1997a, Gavrillets 1997), the effect of coevolution on the stability of predator-prey interactions (Doebeli 1997), or the direction of change in prey or predator traits in response to changes in the biotic or abiotic environment (Abrams 1986, 1990, 1997, 1999). Similarly, all documented cases of non-behavioral predator-prey coevolution I am aware of (reviewed by Vermeij 1994, Abrams 2000) focus on fixed traits (e.g. resistance / toxicity in garter snakes and toxic newts: Brodie and Brodie 1990, 1999; limb morphology in the evolution of large mammalian predators and their prey: Bakker 1983; claw strength / shell-thickness in crabs and gastropods from Lake Tanganyika: West et al. 1991). On the other hand, models of phenotypic plasticity largely concentrate on single species – which, of course, precludes the study of coevolution. In the 1980s and 1990s, a strong effort has been made to develop a theoretical basis for the evolution of phenotypic plasticity (reviewed by Scheiner 1993, Via et al. 1995, Roff 1997, de Jong and Bijma 2002), and the issue continues to attract the attention of mathematical biologists (e.g. Gabriel 1999, de Jong and Gavrillets 2000, Tufto 2000, van Dooren 2001, de and Behera 2002, Sultan and Spencer 2002). A considerable body of literature is devoted to quantitative genetic models of plasticity evolution (e.g. Via and Lande 1985, Gomulkiewicz and Kirkpatrick 1992, Gavrillets and Scheiner 1993). Other models have been designed to understand the benefits of inducible as opposed to permanently expressed (constitutive) traits (Lively 1986a, Lynch and Gabriel 1987, Gabriel and Thomas 1988, Clark and Harvell 1992, Gabriel and Lynch 1992, Moran 1992, Adler and Karban 1994, Padilla and Adolph 1996, Gabriel 1999, Lively 1999, Vos et al. 2002). The latter question is frequently asked in the study of inducible defenses – with the well-known answer being that inducible defenses are favored if there is variation in predation risk, a reliable cue indicating actual predation risk, and a trade-off between costs and benefits of the defense (Tollrian and Harvell 1999a). Researchers also have begun to investigate the ecological effects of phenotypic plasticity (sometimes referred to as trait-mediated indirect effects), for example the consequences of inducible defenses on predator-prey dynamics

or competitive interactions (Ives and Dobson 1987, Edelman-Keshet and Rausher 1989, Frank 1993, Lundberg et al. 1994, Ruxton and Lima 1997, Underwood 1999, Underwood and Rausher 2002; see also empirical works by e.g. Peacor and Werner 1997, reviewed by Lima 1998, Relyea 2000, Bernot and Turner 2001).

In contrast, relatively few models have studied phenotypic plasticity from a coevolutionary perspective, and most of these models deal with behavioral interactions. In particular, a series of papers has investigated patch-selection games between predator and prey (Alonzo 2002, Lima 2002 and references therein), whereupon Lima (2002) argued for the need to “put predators back into behavioral predator-prey interactions”. Several authors (e.g. van Baalen and Sabelis 1993, Brown et al. 1999, van Baalen and Sabelis 1999) have analyzed how the mutual evolutionarily stable patch selection strategies influence the stability of predator-prey population dynamics. Adler and Grünbaum (1999) have modeled the optimal patch selection behavior of predators foraging on inducibly defended prey. To my knowledge, a recent model by Gardner and Agrawal (2002) is the only approach that combines phenotypic plasticity with an explicitly dynamic representation of coevolution. Based on their results, these authors suggest that inducibility of chemical plant defenses slows down the evolution of counter-offenses in herbivores.

Here, I will present a model that is designed to analyze the ecological and evolutionary dynamics of a coevolving predator-prey system with reciprocal phenotypic plasticity. Although this approach has been inspired by the interaction between *Lembadion bullinum* and *Euplotes octocarinatus*, the model is not designed to mimic any particular empirical system. In contrast to the system *Lembadion* – *Euplotes octocarinatus*, my model is restricted to an exclusive two-species interaction, and the offense is a true adaptation against the defense (i.e. its benefits can exceed the costs).

My analysis will focus on the following questions:

1. What are the effects of (a) an inducible defense and (b) an inducible counter-offense on predator-prey population dynamics?
2. What are the effects of (a) an inducible defense and (b) an inducible counter-offense on predator-prey coevolutionary dynamics? In particular, what are the conditions for the coexistence of induced and non-induced phenotypes (morphs) in both species?

In addition, I will provide an outlook discussing the evolution of phenotypic plasticity in dynamic predator-prey systems.

3.2 The model

3.2.1 Overview

I will develop my model by combining an ecological predator-prey model, which describes the between-generation population dynamics, with a quantitative genetic model, which describes phenotypic plasticity and evolution. The ecological model is based on the classical Nicholson-Bailey model (Nicholson 1933, Nicholson and Bailey 1935), and the genetic model is based on the environmental threshold model (Hazel et al. 1990, Hazel and Smock 1993), which is a variant of the threshold model of quantitative genetics (Falconer and Mackay 1996, pp. 299-310, Roff 1996).

This approach yields a discrete-time predator-prey model with no external sources of spatial or temporal heterogeneity. The prey have an inducible defense and the predators may or may not have an inducible counter-offense. Individuals may be either induced or non-induced, but intermediate phenotypes are not possible. This all-or-nothing type of reaction norm has been described for both inducible defenses (e.g. Lively 1986b) and inducible offenses (e.g. Collins and Cheek 1983). The plastic traits are subject to a trade-off, and costs for the induced phenotypes are paid in terms of reduced fecundity. The cue for defense induction is predator density, and the cue for offense induction is the proportion of defended prey. Individuals express the induced phenotypes if the cue exceeds a threshold. These induction thresholds are normally distributed in the populations and are subject to selection (i.e. they are modeled as quantitative genetic characters). Intermediate mean induction thresholds enable coexistence of the induced and non-induced phenotypes, whereas evolution towards extremely low or high induction thresholds leads to exclusive expression of a single phenotype.

There are two versions of the model: In model 1, the prey have an inducible defense, but there is only one type of predator. In model 2, the predators possess an inducible coun-

counter-offense to the prey's defense. In addition, I will briefly analyze a variant of model 2 (model 2a) where the inducible offense of the predator is complemented by a constitutive offense based on a major locus allele (that is on a one-locus-two-allele model).

As with all models, I was facing a trade-off between simplicity and realism. For example, in the Nicholson-Bailey model, prey growth is potentially unlimited and predators never become satiated. I accepted these and other unrealistic assumptions in order to keep the model as simple as possible.

3.2.2 The Nicholson-Bailey model

I start from the classical discrete-time population model by Nicholson and Bailey (Nicholson 1933, Nicholson and Bailey 1935):

$$\begin{aligned} N_{t+1} &= \lambda N_t \exp(-aP_t) \\ P_{t+1} &= bN_t(1 - \exp(-aP_t)) \end{aligned} \tag{1}$$

Here, N is prey density, P predator density, λ the fecundity of the prey, a the success rate (Jeschke et al. 2002) of the predator (a measure of predation efficiency), b the number of new predators produced per consumed prey, and t is an index of time in units of one generation (see Table 8 for an overview of my terminology). The time indices will be added only in the context of explicit dynamics. As is well-known, the above model produces dynamics that are always unstable and inevitably lead to the extinction of the model populations.

Table 8: Mathematical terminology

Variables	
N	prey density
P	predator density
μ	mean of prey induction threshold
ν	mean of predator induction threshold
d	prey defense ($d = 0$: non-induced, $d = 1$: induced)
o	predator offense ($o = 0$: non-induced, $o = 1$: induced)
q	frequency of offense allele C^+ (model 2a)
Parameters	
a_0, a_1	success rate of predators foraging on undefended and defended prey, respectively (model 1)
a_{ij}	success rate of predator with offense $o = j$ foraging on prey with defense $d = i$ (model 2)
b	predator conversion efficiency
c_d	costs of prey defense
c_o	costs of predator offense
λ	prey fecundity
h_n^2	heritability of the prey's induction threshold
h_p^2	heritability of the predators' induction threshold
σ_n^2	variance of the prey's induction threshold
σ_p^2	variance of the predators' induction threshold

Table 8 (continued): Mathematical terminology

Derived quantities	
\hat{a}_1	value of a_1 such that $w_{n0} = w_{n1}$ at equilibrium
$(a_1)_b$	maximal value of a_1 allowing for the existence of multiple ecological equilibria (model 1)
$(a_1)_s$	maximal value of a_1 allowing for the existence of a stable ecological equilibrium (model 1)
$(a_{10})_s$	maximal value of a_{10} allowing for the existence of a stable ecological equilibrium (model 2)
\bar{d}	proportion of induced prey, induction frequency of prey (population-level reaction norm)
\bar{o}	proportion of induced predators, induction frequency of predator (population-level reaction norm)
\hat{P}	predator density such that $w_{n0} = w_{n1}$
w_{n0}, w_{n1}	fitness of non-induced and induced prey, respectively
w_{p0}, w_{p1}	fitness of non-induced and induced predators, respectively
\bar{w}_n, \bar{w}_p	mean fitness of prey and predator, respectively
Indices etc.	
0, 1	non-induced, induced
n	prey
p	predator
t	time
*	equilibrium
\bar{u}	mean of quantity u

In the following, I will frequently use a formulation involving fitness terms:

$$\begin{aligned} N_{t+1} &= N_t \bar{w}_n \\ P_{t+1} &= P_t \bar{w}_p \end{aligned} \tag{2}$$

where $\bar{w}_n = N_{t+1}/N_t$ is the mean fitness of the prey and $\bar{w}_p = P_{t+1}/P_t$ is the mean fitness of the predator. The basic structure (2) will be preserved in all modifications of eq. (1).

3.2.3 Model 1: Plasticity in the prey

I assume that the prey is dimorphic with two alternative phenotypes d : undefended / non-induced ($d = 0$) or defended / induced ($d = 1$). The main effect of the defense is to decrease the predator's success rate a . However, the defense is also costly to the prey and decreases fecundity by a constant proportion c_d . Thus, the fitness of the undefended and defended prey is

$$\begin{aligned} w_{n0} &= \lambda \exp(-a_0 P) \\ w_{n1} &= (1 - c_d) \lambda \exp(-a_1 P) \end{aligned} \tag{3}$$

respectively, with a_0 denoting the success rate of predators foraging on undefended prey, and a_1 the success rate of predators foraging on defended prey ($a_0 > a_1$). Let \bar{d} be the proportion of defended prey (the prey's induction frequency). The mean fitness of the prey is

$$\bar{w}_n = w_{n0}(1 - \bar{d}) + w_{n1}\bar{d} \tag{4}$$

and the (mean) fitness of the predator is

$$\bar{w}_p = P^{-1} b N_t \left((1 - \bar{d})(1 - \exp(-a_0 P)) + \bar{d}(1 - \exp(-a_1 P)) \right). \tag{5}$$

The phenotype of each individual is determined once at the beginning of the generation and cannot be changed thereafter (i.e. plasticity is irreversible). The defense is expressed if predator density exceeds an threshold x , that is

$$d = \begin{cases} 0, & P < x \\ 1, & P \geq x \end{cases} \quad (6)$$

The individual induction thresholds x are assumed to be normally distributed in the prey population (i.e. they are realizations of a random variable X) with mean μ and variance σ_n^2 . For a given predator density P , a proportion

$$\bar{d} = F(P, \mu) = \int_{-\infty}^P f(x, \mu) dx \quad (7)$$

of the total prey population expresses the defense, whereas the remaining proportion $(1 - \bar{d})$ remains undefended (f denotes the probability density function of the normal distribution, and F the cumulative frequency distribution). Note that an individual with a low induction threshold x has a high tendency to express the defense. Accordingly, a low mean induction threshold μ in the population leads to a high induction frequency. Due to the normality assumption, both x and μ may be negative.

To introduce evolution of the induction threshold, I assume that a positive fraction of σ_n^2 (i.e. the heritability h_n^2) is due to additive genetic variance. (The purely ecological model is regained by setting $h_n^2 = 0$). Differences in the fitness of induced and non-induced prey cause shifts in the mean induction threshold μ , which now is function of time and will be referred to as μ_t .

Hazel and Smock (1993) showed that the selection differential in the environmental threshold model is

$$S_n = \frac{\sigma_n^2}{w_n} f(P_t, \mu_t) (w_{n0} - w_{n1}). \quad (8)$$

Consequently, the mean prey induction threshold in the next generation is

$$\mu_{t+1} = \mu_t + h_n^2 S_n. \quad (9)$$

I assume that σ_n^2 and h_n^2 are constants, that is the heritability of the induction thresholds is not influenced by selection. Although this assumption is certainly a simplification, the work of Roff (1994) suggests that the maintenance of genetic variation is less of a problem in threshold characters than it is in continuous traits.

Model 1 can be summarized by

$$\begin{aligned} N_{t+1} &= N_t \bar{w}_n \\ P_{t+1} &= P_t \bar{w}_p \\ \mu_{t+1} &= \mu_t + h_n^2 S_n \end{aligned} \quad (10)$$

3.2.4 Model 2: Plasticity in both prey and predator

3.2.4.1 Two types of predators

I will now introduce an inducible counter-offense of the predator which can offset, to a certain degree, the effect of the prey's defense. The counter-offense relies on a quantitative threshold trait similar to that in the prey and is triggered by the proportion of defended prey \bar{d} . In addition, it reduces predator fecundity by a proportion c_o .

In addition to the two prey phenotypes, there are now two predator phenotypes o : without offense / non-induced ($o = 0$) and with offense / induced ($o = 1$). The proportion of predators with offense (i.e. the predators' induction frequency) will be denoted by \bar{o} .

As there are now four possible combinations of prey and predator phenotypes, four success rate parameters are needed. Therefore, let a_{ij} be the success rate of predators with phenotype $o = j$ foraging on prey with phenotype $d = i$ ($i, j = 0, 1$). My basic assumptions are

- $a_{10} < a_{00}$: The prey's defense is effective against a non-induced predator.
- $a_{11} > a_{10}$: The predator's offense is effective in reducing the effect of the prey's defense.

Additional assumptions are:

- $a_{11} \leq a_{01}$: When the predator is induced, the defense is not harmful for the prey.
- $a_{01} \geq a_{00}$: The offense does not lower success rate when the prey is undefended.

The latter assumptions preclude scenarios where induction can both increase or decrease success rate, depending on the phenotype of the other species. In the following, I will nearly always assume that

- $a_{01} = a_{00}$: The offense has no effect when the prey is undefended.

Below, I will deduce further restrictions on the relationship between the a_{ij} , which assure that the predator experiences a real trade-off.

First, however, it is necessary to calculate the fitness of all four – prey or predator – phenotypes. For that purpose, one must determine how much prey of each phenotype is consumed by induced and non-induced predators, respectively. This can be done by setting up a set of differential equations that describe the within-generation dynamics generated by predation. The following approach is a general way to deduce the exponential terms in Nicholson-Bailey type models (Mangel and Roitberg 1992), and is equivalent to the more common interpretation of these terms as the zero term of a Poisson distribution.

It is convenient to introduce a set of auxiliary variables: Let N_0 be the density of non-induced prey, N_1 the density of induced prey, P_0 the density of non-induced predators, P_1 the density of induced predators, C_0 the amount (“density”) of prey consumed by non-induced predators, and C_1 the amount of prey consumed by induced predators. The within-generation dynamics of these variables can be described by

$$\begin{aligned}
\frac{dN_0}{dt} &= -(a_{00}P_0 + a_{01}P_1)N_0 \\
\frac{dN_1}{dt} &= -(a_{10}P_0 + a_{11}P_1)N_1 \\
\frac{dC_0}{dt} &= (a_{00}N_0 + a_{10}N_1)P_0 \\
\frac{dC_1}{dt} &= (a_{01}N_0 + a_{11}N_1)P_1 \\
\frac{dP_0}{dt} &= \frac{dP_1}{dt} = 0
\end{aligned} \tag{11}$$

with the initial conditions being

$$\begin{aligned}
N_0 &= (1 - \bar{d})N_t, & N_1 &= \bar{d}N_t, \\
P_0 &= (1 - \bar{o})P_t, & P_1 &= \bar{o}P_t, \\
C_0 &= C_1 = 0
\end{aligned} \tag{12}$$

(Note that an index t refers to the value of the respective variable at the beginning of generation t , whereas t in the left-hand side of a differential equation is meant to be continuous.) With ‘ \sim ’ denoting the value of a variable at the end of the generation, one gets

$$\begin{aligned}
\tilde{N}_0 &= (1 - \bar{d})N_t \exp(-a_{00}P_0 - a_{01}P_1) \\
\tilde{N}_1 &= \bar{d}N_t \exp(-a_{10}P_0 - a_{11}P_1) \\
\tilde{C}_0 &= \frac{a_{00}P_0}{a_{00}P_0 + a_{01}P_1} (1 - \bar{d})N_t (1 - \exp(-a_{00}P_0 - a_{01}P_1)) \\
&\quad + \frac{a_{10}P_0}{a_{10}P_0 + a_{11}P_1} \bar{d}N_t (1 - \exp(-a_{10}P_0 - a_{11}P_1)) \\
\tilde{C}_1 &= \frac{a_{01}P_1}{a_{00}P_0 + a_{01}P_1} (1 - \bar{d})N_t (1 - \exp(-a_{00}P_0 - a_{01}P_1)) \\
&\quad + \frac{a_{11}P_1}{a_{10}P_0 + a_{11}P_1} \bar{d}N_t (1 - \exp(-a_{10}P_0 - a_{11}P_1))
\end{aligned} \tag{13}$$

The latter two equations state that the total amount of captured prey is “shared” by the two predator morphs according their relative densities, weighted by the respective success rate parameters. The fitness of the various phenotypes is then

$$\begin{aligned}
 w_{n0} &= \lambda \frac{\tilde{N}_0}{N_0} = \lambda \exp(-a_{00}P_0 - a_{01}P_1) \\
 w_{n1} &= \lambda(1 - c_d) \frac{\tilde{N}_1}{N_1} = \lambda(1 - c_d) \exp(-a_{10}P_0 - a_{11}P_1) \\
 w_{p0} &= \frac{b}{P_0} \tilde{C}_0 \\
 w_{p1} &= \frac{b}{P_1} (1 - c_0) \tilde{C}_1
 \end{aligned} \tag{14}$$

and the mean fitness is

$$\begin{aligned}
 \bar{w}_n &= w_{n0}(1 - \bar{d}) + w_{n1}\bar{d} \\
 \bar{w}_p &= w_{p0}(1 - \bar{o}) + w_{p1}\bar{o},
 \end{aligned} \tag{15}$$

for the prey and predator, respectively.

3.2.4.2 Restrictions on the range of success rate parameters

It is now possible to deduce further restrictions on the range of success rate parameters a_{ij} . These restrictions shall assure that the predators experience a real fitness trade-off with respect to the offense. By a real trade-off, I mean that for each phenotype there is the theoretical possibility to be selected for in an appropriate environment. In other words, the benefits of the offense must outweigh the costs in some environments but not in others.

Therefore, when all prey are undefended, induced predators must have a lower fitness than non-induced predators: $w_{p0} > w_{p1}|_{\bar{d}=0}$. This inequality yields

$$a_{01} < \frac{a_{00}}{1-c_0}. \quad (16)$$

Similarly, when all prey are defended, induced predators must have a higher fitness than non-induced predators: $w_{p0} < w_{p1}|_{\bar{d}=1}$, which yields

$$a_{11} > \frac{a_{10}}{1-c_o}. \quad (17)$$

Combining (16) and (17) with the assumptions made in the previous section leads to the following conditions for the range of success rate parameters:

1. $a_{10} < a_{00}$
 2. $a_{00} \leq a_{01} < \frac{a_{00}}{1-c_o}$; if $a_{00} < \frac{a_{10}}{1-c_o}$ then $\frac{a_{10}}{1-c_o} < a_{01} < \frac{a_{00}}{1-c_o}$
 3. $\frac{a_{10}}{1-c_o} < a_{11} \leq a_{01}$
- (18)

When choosing actual parameter values for the model, it is easiest to follow these steps in the given order. Note that there is no *a priori* relation between a_{00} and a_{11} .

3.2.4.3 The inducible counter-offense

The inducible counter-offense is triggered by the proportion of defended prey. The underlying genetics are analogous to those in the prey and follow the environmental threshold model. Each individual predator is assumed to have an induction threshold y , with the offense being induced if the proportion \bar{d} of defended prey is greater than y . That is the predator phenotype o is

$$o = \begin{cases} 0, & \bar{d} < y \\ 1, & \bar{d} \geq y \end{cases} \quad (19)$$

Like the prey threshold X , the predator threshold Y is normally distributed in the population with mean v , variance σ_p^2 , probability density function $g(y, v)$, and heritability h_p^2 . If a proportion \bar{d} of the prey is defended, a corresponding proportion

$$\bar{o} = G(\bar{d}, v) = \int_{-\infty}^{\bar{d}} g(y, v) dy \quad (20)$$

of the predators will express the counter-offense. Note that, since prey defense depends on predator density, predator offense ultimately is a function of predator density, too.

To illustrate the model assumptions one might imagine the following life cycles: The phenotypes of prey and predator are determined in a short period at the beginning of each generation. First, prey develop their defense in response to predator density. In a second step, predators develop their offense in response to the proportion of defended prey. After the initial period, both defense and offense are irreversible and cannot be readjusted for the rest of the generation. In particular, predators are not allowed to increase their offense when the proportion of undefended prey is reduced by predation.

The selection differentials for prey and predator are

$$\begin{aligned} S_n &= \frac{\sigma_n^2}{\bar{w}_n} f(P_t, \mu_t)(w_{n0} - w_{n1}) \\ S_p &= \frac{\sigma_p^2}{\bar{w}_p} g(\bar{d}(P_t), v_t)(w_{p0} - w_{p1}) \end{aligned} \quad (21)$$

and the dynamics of the model can be summarized by

$$\begin{aligned} \mu_{t+1} &= \mu_t + h_n^2 S_n \\ v_{t+1} &= v_t + h_p^2 S_p \\ N_{t+1} &= \bar{w}_n N_t \\ P_{t+1} &= \bar{w}_p P_t \end{aligned} \quad (22)$$

Model 2 reduces to model 1 for $v \rightarrow \infty$ and $h_p^2 = 0$. In this case a_{00} corresponds to a_0 , and a_{10} corresponds to a_1 .

3.2.4.4 Model 2a: Combination of inducible and constitutive offense

Model 2a is a variant of model 2 where the inducible counter-offense of the predator is complemented by a constitutive offense that is based on a major locus allele (i.e. on a one-locus-two-allele model). In this scenario, each predator has a quantitative locus determining the induction threshold for the inducible offense *and* a major locus determining the expression of the constitutive offense.

The major locus has two alleles, C^+ and C^- . I will assume that the genetics are diploid and that the C^+ allele is dominant. Therefore, C^+C^+ and C^+C^- genotypes express the offense independently of the prey's induction frequency \bar{d} . C^-C^- genotypes express the offense only if \bar{d} exceeds their individual induction threshold y . In other words, C^+C^+ and C^+C^- genotypes display the offense constitutively, whereas C^-C^- genotypes are phenotypically plastic.

The major locus alleles and the induction thresholds are assumed to evolve independently. Let q be the frequency of the C^+ allele in the predator population. The fraction of the predator population that displays the offense constitutively due to the C^+ allele is

$$\alpha = q^2 + 2q(1 - q) \quad (23)$$

Furthermore, a fraction

$$\beta = G(\bar{d}, v) = \int_{-\infty}^{\bar{d}} g(y, v) dy \quad (24)$$

displays the offense due to phenotypic plasticity, that is because \bar{d} exceeds the individual induction threshold y . As these two fraction overlap, the total proportion of predators with offense is given by

$$\bar{d} = \alpha + \beta - \alpha\beta. \quad (25)$$

Let w_α denote the mean fitness of predators carrying the C^+ allele and $w_{1-\alpha}$ the mean fitness of predators without this allele. Similarly, let w_β be the mean fitness of predators with induction thresholds below \bar{d} and $w_{1-\beta}$ the mean fitness of predators with induction thresholds above \bar{d} . Then

$$\begin{aligned} w_\alpha &= w_{p1} \\ w_{1-\alpha} &= (1-\beta)w_{p0} + \beta w_{p1} \\ w_\beta &= w_{p1} \\ w_{1-\beta} &= (1-\alpha)w_{p0} + \alpha w_{p1} \end{aligned} \quad (26)$$

with w_{p0} , w_{p1} and \bar{w}_p defined as in eq. (14) and (15).

The dynamics of model 2a can be described by

$$\begin{aligned} q_{t+1} &= \frac{(q_t^2 + q_t(1-q_t))w_\alpha}{(1-\alpha)w_{1-\alpha} + \alpha w_\alpha} \\ v_{t+1} &= v_t + h_p^2 S_p \quad \text{with} \quad S_p = \sigma_p^2 g(\bar{d}, v_t) \frac{w_{1-\beta} - w_\beta}{(1-\beta)w_{1-\beta} + \beta w_\beta} \end{aligned} \quad (27)$$

and

$$\begin{aligned} N_{t+1} &= N_t \\ P_{t+1} &= P_t \\ \mu_{t+1} &= \mu_t + h_n^2 S_n \end{aligned}$$

as in eq. (22).

The equation for v_{t+1} is analogous to eq. (9). The equation for q_{t+1} is adopted from Hartl (1997, p. 219). It corresponds to ‘‘viability selection’’, where fitness is proportional to the probability of surviving to maturity. Note that this is a very simplified way to

model the dynamics of allele frequencies. In contrast to the above assumption, the logic of the Nicholson-Bailey model implies that predator fitness is determined by the number of offspring produced per individual, which in turn is proportional to the number of consumed prey. Similarly, costs of the offense are typically thought of as reduced reproduction. A plausible scenario reconciling this “fecundity selection” with eq. (27) might be a population of mass-spawners where individual reproductive success is proportional to the number of gametes produced per individual, which in turn is proportional to the number of prey consumed, corrected for costs of the offense. (This scenario eliminates the problem that, with distinct mating pairs, one must determine the number of joint offspring produced by say a male with offense and a female without offense.)

3.2.5 Analysis and implementation

Analytical and numerical analysis was performed using Maple V Release 4 (Waterloo Maple Inc., Waterloo, Ontario, Canada). In case the built-in procedures from Maple could not be applied, I calculated function roots using the *regula falsi* method described in Carnahan et al. (1969, pp. 179+191) and function minima using Brent’s method according to Press et al. (Press et al. 2001, pp. 395 ff). Simulation runs were conducted by means of Excel spreadsheets or C++ implementations.

3.3 Results

3.3.1 Kinds of equilibria

Model 1 is at equilibrium if

$$\begin{aligned}
 N_{t+1} &= N_t = N^* \\
 P_{t+1} &= P_t = P^* \\
 \mu_{t+1} &= \mu_t = \mu^*
 \end{aligned}
 \tag{28}$$

Without evolution ($h_n^2 = 0$), an equilibrium requires

$$\bar{w}_n = \bar{w}_p = 1 \quad (29)$$

and will be referred to as *ecological equilibrium*. With evolution ($h_n^2 > 0$), an equilibrium requires

$$w_{n0} = w_{n1} = \bar{w}_p = 1 \quad (30)$$

and will be referred to as *evolutionary equilibrium*. In addition, there is always the *trivial equilibrium* where both species are extinct ($N^* = P^* = 0$).

For model 2, the general equilibrium condition (28) is complemented by $v_{t+1} = v_t = v^*$, the condition for an ecological equilibrium remains $\bar{w}_n = \bar{w}_p = 1$, and the condition for an evolutionary equilibrium is $w_{n0} = w_{n1} = w_{p0} = w_{p1} = 1$.

Furthermore, I will use the term *ecological stability* for the stability of the ecological equilibrium, and *evolutionary stability* for the stability of the evolutionary equilibrium. Note that evolutionary stability is not used in the sense of evolutionarily stable strategies and that it implies stability of the population dynamics, too. Similarly, *ecological dynamics* will refer to the dynamics without evolution ($h_n^2 = 0$, $h_p^2 = 0$), and *evolutionary dynamics* to the dynamics with evolution, including the population dynamics.

3.3.2 Some notes on the environmental threshold model

Before presenting my results, I will point out two important properties of the environmental threshold model, which tend to be counter-intuitive. My discussion will be restricted to the prey, but the conclusions are equally valid for the predator.

First, although it is easy to see that the “optimal” induction threshold for the prey would be

$$x_{\text{opt}} = \frac{\ln(1 - c_d)}{a_1 - a_0}$$

(because $w_{n0} \leq w_{n1}$ for $P \leq x_{\text{opt}}$, and $w_{n0} \geq w_{n1}$ for $P \geq x_{\text{opt}}$), the mean induction threshold μ does not evolve to this value. Instead, in a spatially and temporarily homogeneous environment, μ evolves towards $+\infty$ for $P > x_{\text{opt}}$ and towards $-\infty$ for $P < x_{\text{opt}}$. This is because, due to the normal distribution of induction thresholds, it is impossible for *all* individuals to have the phenotype which confers higher fitness. For a two-patch environment with fixed predator densities $P_1 < x_{\text{opt}}$ and $P_2 > x_{\text{opt}}$, Hazel and Smock (1993) showed that μ evolves towards an equilibrium value

$$\mu^* = \frac{P_1 + P_2}{2} + \frac{\sigma_n^2}{P_2 - P_1} \ln \left(\frac{q}{1-q} \cdot \frac{w_{n0}(P_1) - w_{n1}(P_1)}{w_{n1}(P_2) - w_{n0}(P_2)} \right).$$

Here q is the probability for an individual to live in the patch with predator density P_1 . Thus, μ^* increases (and the average propensity of expressing the defense decreases) with increasing probability of experiencing a low risk of predation. In other words, the equilibrium induction threshold is biased towards the more frequent environment (for $q = 1/2$, $\mu^* = (P_1 + P_2)/2$). The same principal applies if predator density varies temporarily rather than spatially. However, in temporally heterogeneous environments, there cannot be a stable equilibrium (see below).

Second, the environmental threshold model is discrete at the level of individuals but continuous at the level of populations. In the following, therefore, I will distinguish between the *individual reaction norm* $d(P)$, which is a step function of predator density, and the *population-level reaction norm* $\bar{d}(P)$, which is continuous and has the shape of a cumulative normal distribution. As I shall show, the population-level reaction norm strongly influences the dynamic behavior of the model, which is governed by population properties such as induction frequency and mean fitness. In contrast, the discrete nature of the individual reaction norm is reflected in the conditions required for an evolutionary equilibrium.

Furthermore, I will use the slope of the population-level reaction norm as a measure for the *realized plasticity* in the population, that is the responsiveness of the population to variation in the environment. This terminology is based on the notion that an individual with an induction threshold outside the range of environmental variation is plastic in

theory, but *in practice* it will always express the same phenotype. Thus, prey with induction thresholds less than 0 will always be defended, and prey with induction thresholds that exceeds the maximal possible number of predators will never be defended. If one of these situations applies to a large proportion of prey, the *realized plasticity* in the prey population is low.

In two limiting cases, the realized plasticity in the population declines to zero (although plasticity at the individual-level is unchanged). In the first case, the mean induction threshold $\mu \rightarrow \pm\infty$, and the induction frequency \bar{d} approaches 0 or 1, respectively. In the second case, the variance $\sigma_n^2 \rightarrow \infty$. Any induction frequency is possible, depending on the mean induction threshold μ , but \bar{d} no longer depends on predator density P . This is because any possible variability in P becomes negligible with respect to the variance of the induction thresholds and, therefore, each individual's induction threshold is either always or never exceeded by the cue. (For this conclusion, it is necessary to assume that P is restricted to a finite interval. Note that, in order to achieve $\bar{d} \neq 1/2$, μ must diverge, too, if $\sigma_n^2 \rightarrow \infty$.) Despite the loss of realized plasticity, evolution of μ and, therefore, adaptive change in \bar{d} , remains perfectly possible for arbitrary large σ_n^2 . Therefore, choosing a large σ_n^2 is a way to “switch off” plasticity but preserve evolution.

Similarly, evolution can be “switched off” and phenotypic plasticity preserved by setting $h_n^2 = 0$. This setting implies that the variability of the induction threshold is exclusively based on environmental variance and non-additive genetic variance. While such a scenario might appear unrealistic, there is an alternative interpretation that makes it possible to look at the model from a purely ecological point of view. In this interpretation, the prey population is genetically homogeneous, but induction is stochastic. The population-level reaction norm $\bar{d}(P)$ is reinterpreted as an individual reaction norm that specifies each prey's probability to express the defense as a function of predator density.

3.3.3 Model 1: Plasticity in the prey

3.3.3.1 Ecological equilibria

3.3.3.1.1 Ecological equilibria and the prey's mean fitness function

Under the conditions of model 1 without evolution, it is not possible to derive analytical expressions for the equilibrium population densities N^* and P^* . Therefore, the following discussion will rely largely on numerical results and graphical arguments. The non-trivial ecological equilibria of model 1 are best discussed in terms of the prey's mean fitness function $\bar{w}_n(P)$.

The graph of $\bar{w}_n(P)$ is located between the graphs of $w_{n0}(P)$ and $w_{n1}(P)$, the fitness functions for undefended and defended prey, respectively. As the induction frequency \bar{d} increases with P , \bar{w}_n is close to w_{n0} if P is small, and close to w_{n1} if P is large (Fig. 8 A).

The equilibrium predator density P^* is determined by the condition $\bar{w}_n(P^*) = 1$. If the population-level reaction norm is steep enough (i.e., σ_n^2 is small), there may be a range of P where \bar{w}_n increases with predator density. This happens if the increased defense level in the prey population more than offsets the increased encounter rate with the predator. In this case, there may be three alternative ecological equilibria (Fig. 8 B): A low equilibrium with most of the prey undefended, an high equilibrium with most of the prey defended, and an intermediate equilibrium in the region where mean prey fitness increases with predator density. As I shall show below, the intermediate equilibrium is always unstable and, therefore, has no biological relevance. The high equilibrium does not exist for $a_1 = 0$ (complete defense), because, in this case, the fitness of the defended prey is independent of predator density and does not decrease to zero for large P (Fig. 8 C). Note that the number of ecological equilibria depends solely on the number of solutions for $\bar{w}_n(P) = 1$. This is because predator fitness \bar{w}_p is linear in N and, therefore, any predator population can be sustained by an appropriately sized prey population (i.e., there is always a solution to the second equilibrium condition $\bar{w}_p = 1$).

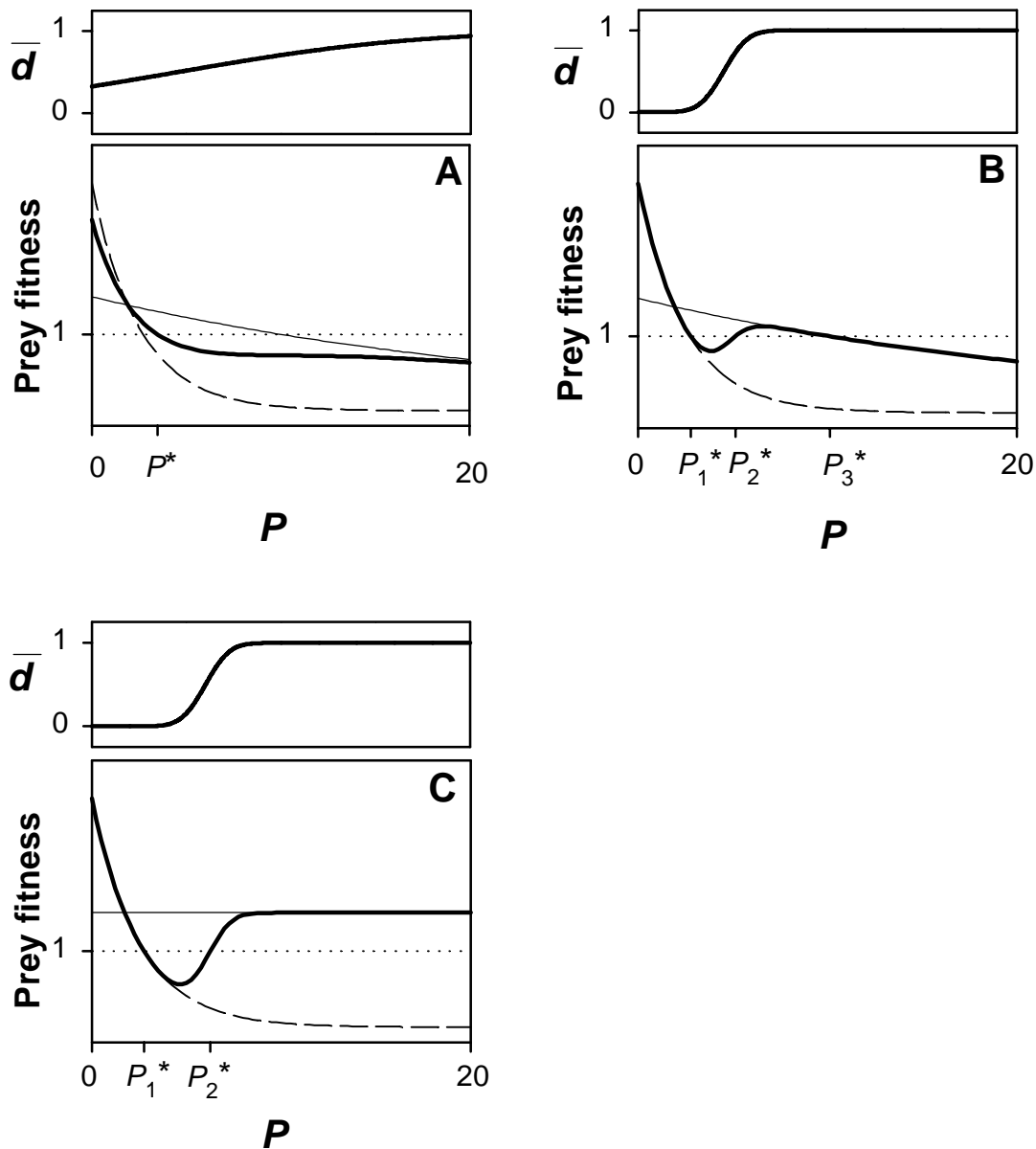


Fig. 8. Model 1 without evolution: The prey's mean fitness function.

In each plot, the upper panel shows the proportion \bar{d} of defended prey as a function of predator density P . The lower panels show w_{n0} , the fitness of undefended prey (dashed line), w_{n1} , the fitness of defended prey (thin solid line), and \bar{w}_n , the mean fitness of the prey (thick solid line).

In **A**, the variance σ_n^2 of the prey's induction threshold is high, and there is only one equilibrium predator density P^* . In **B**, σ_n^2 is small, and there are three alternative ecological equilibria with predator densities P_1^* (low equilibrium), P_2^* (intermediate equilibrium), and P_3^* (high equilibrium). In **C**, σ_n^2 is small, too. However, the prey's defense provides complete protection ($a_1 = 0$), and the high equilibrium is missing. Model 1. Parameters: **A**) $a_0 = 0.4$, $a_1 = 0.04$, $b = 0.4$, $c_d = 0.5$, $h_n^2 = 0$, $\lambda = 3$, $\mu = 4.5$, $\sigma_n^2 = 100$; **B**) as in **A**, but $\sigma_n^2 = 1$; **C**) as in **A**, but $a_1 = 0$, $\mu = 6$, $\sigma_n^2 = 1$, $\sigma_n^2 = 1$.

w_{n0} and w_{n1} intersect at

$$\hat{P} = \frac{\ln(1-c_d)}{a_1 - a_0} . \quad (31)$$

For $P < \hat{P}$ undefended prey have higher fitness than defended prey, whereas for $P > \hat{P}$ defended prey have higher fitness than undefended prey (\hat{P} is equivalent to x_{opt} in section 3.2).

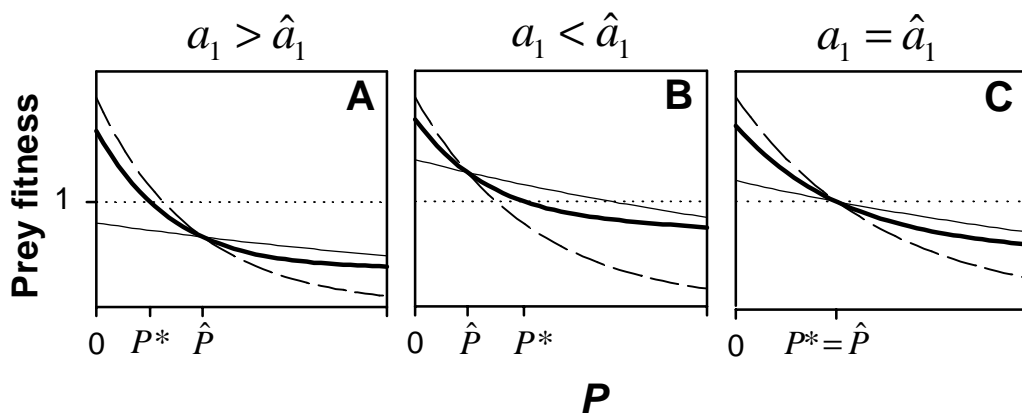


Fig. 9. Model 1 without evolution: The fitness of undefended and defended prey at the ecological equilibrium.

The relationship between the fitness of undefended and defended prey at the ecological equilibrium, depending on the intersection point between w_{n0} and w_{n1} . In **A**, undefended prey are favored at equilibrium, whereas in **B**, defended prey are favored at equilibrium. In **C**, both prey phenotypes have the same fitness at equilibrium. The three cases may be distinguished by the relation between a_1 and \hat{a}_1 (eq. 32).

The figures show w_{n0} , the fitness of undefended prey (dashed line), w_{n1} , the fitness of defended prey (thin solid line), and \bar{w}_n , the mean fitness of the prey (thick solid line) as a function of predator density P . Model 1. Parameters: **A**) $a_0 = 0.3$, $a_1 = 0.05$, $b = 0.4$, $c_d = 0.6$, $h_n^2 = 0$, $\lambda = 2$, $\mu = 5$, $\sigma_n^2 = 64$; **B**) $a_0 = 0.25$, $a_1 = 0.05$, $b = 0.4$, $c_d = 0.3$, $h_n^2 = 0$, $\lambda = 2$, $\mu = 2.5$, $\sigma_n^2 = 49$; **C**) $a_0 = 0.2$, $a_1 = 0.052606881$, $b = 0.4$, $c_d = 0.4$, $h_n^2 = 0$, $\lambda = 2$, $\mu = 4$, $\sigma_n^2 = 100$; The P -axis scales from 0 to 10.

If

$$a_1 > \hat{a}_1 = a_0 \frac{\ln(\lambda(1-c_d))}{\ln \lambda} \quad (32)$$

then prey fitness at the intersection point, $\bar{w}_n(\hat{P})$, is less than 1. This implies that the equilibrium predator density P^* is less than \hat{P} (because $\bar{w}_n(P^*)=1$, but $\bar{w}_n(P) < \bar{w}_n(\hat{P}) < 1$ for all $P > \hat{P}$; Fig. 9 A). Accordingly, $P^* > \hat{P}$ if $a_1 < \hat{a}_1$ (Fig. 9 B). In consequence, defended prey are favored at equilibrium if the defense is strong, and are disfavored if the defense is weak. Only if $a_1 = \hat{a}_1$ both predator morphs have the same equilibrium fitness, and this is the only case where model 1 can have an evolutionary equilibrium (see below; Fig. 9 C). Note also, that multiple equilibria are only possible for $a_1 < \hat{a}_1$, because \bar{w}_n is monotonically decreasing for $P < \hat{P}$.

3.3.3.1.2 The effect of the defense parameters on the ecological equilibria

In the following, I will investigate how the number of ecological equilibria and the values of N^* and P^* depend on the defense parameters μ , σ_n^2 , c_d and a_1 . First, I will explore the domain of multiple ecological equilibria.

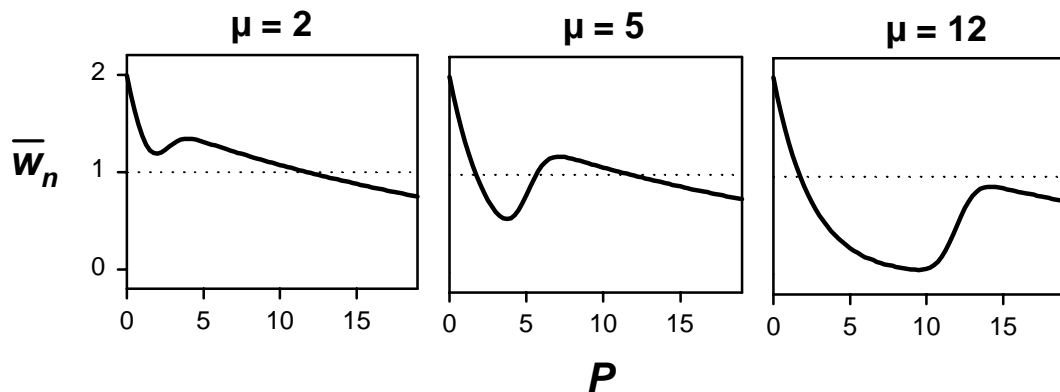


Fig. 10. Model 1 without evolution: Multiple ecological equilibria and the mean induction threshold.

The number of ecological equilibria in model 1 depends on the prey's mean induction threshold μ . The figures show \bar{w}_n , the mean fitness of the prey as a function of predator density P for various values of μ . An equilibrium exists whenever $\bar{w}_n(P)=1$. Model 1. Parameters: $a_0 = 0.4$, $a_1 = 0.02$, $b = 0.4$, $c_d = 0.2$, $h_n^2 = 0$, $\lambda = 2$, $\sigma_n^2 = 1$.

As shown in Fig. 8 B, multiple ecological equilibria require that the fitness function $\bar{w}_n(P)$ has a minimum followed by a maximum (except for $a_1 = 0$). Under this condition, the number of equilibria depends on the mean induction threshold μ (Fig. 10). If μ is small, the minimum of $\bar{w}_n(P)$ is greater than 1 and only the high equilibrium exists

($\mu = 2$ in Fig. 10). For intermediate μ , the minimum is less than 1 and the maximum is greater than 1. In consequence, the system has three alternative equilibria ($\mu = 5$ in Fig. 10). For large μ , the maximum becomes less than 1, too, and only the low equilibrium remains ($\mu = 12$ in Fig. 10).

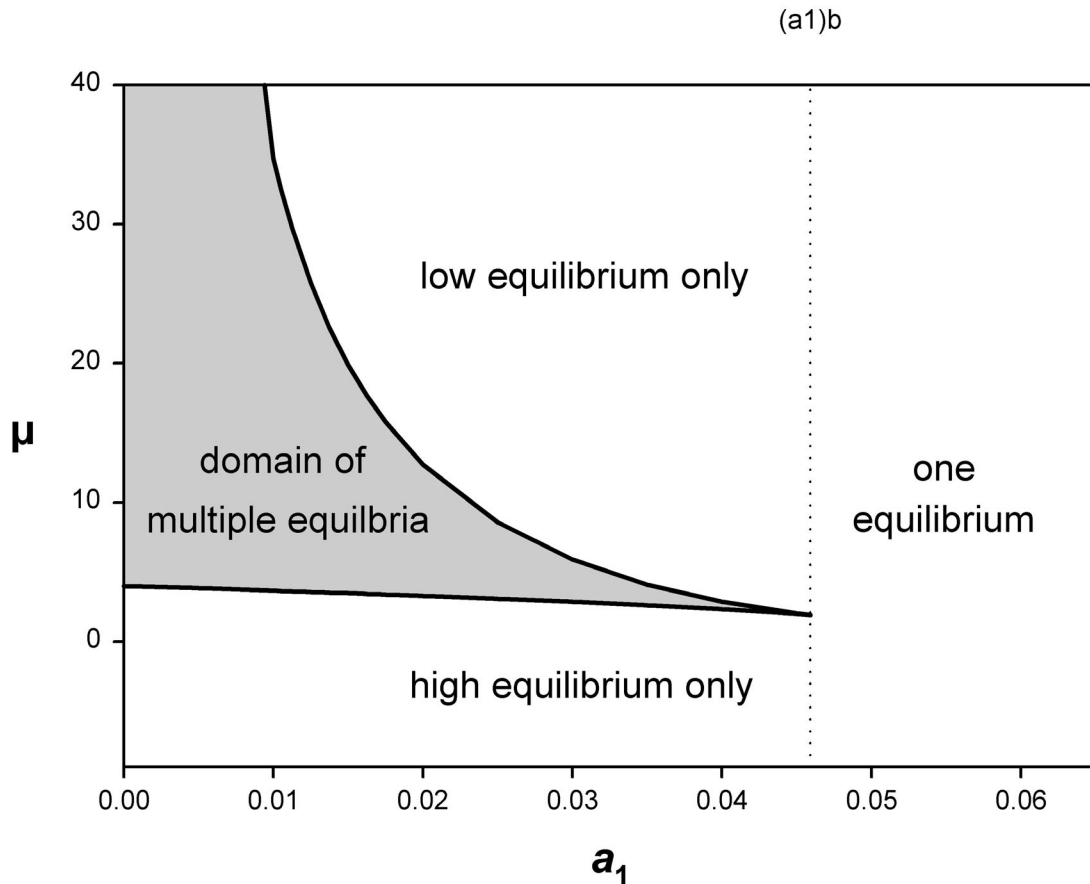


Fig. 11. Model 1 without evolution: The domain of multiple ecological equilibria.

Schematic overview of the domain of multiple ecological equilibria (shaded area) in the a_1 versus μ plane. The dashed line marks $(a_1)_b$, the maximal value of a_1 that allows for multiple equilibria. The upper boundary of the domain of multiple equilibria approaches the ordinate for $\mu \rightarrow \infty$. a_1 is the success rate of predators feeding on defended prey, and μ is the prey's mean induction threshold. See Fig. 10 and text. Model 1. Parameters: $a_0 = 0.4$, $b = 0.4$, $c_d = 0.2$, $h_n^2 = 0$, $\lambda = 2$, $\sigma_n^2 = 25$.

Fig. 11 shows the domain of multiple equilibria as a function of μ and a_1 . For each value of a_1 , the graph shows the minimal and maximal value of μ allowing for multiple equilibria. The lower boundary can be determined by numerically calculating μ such that the minimum of $\bar{w}_n(P)$ equals 1. Similarly, the upper boundary can be determined by finding μ such that the maximum of $\bar{w}_n(P)$ equals 1. The range of μ allowing for

multiple equilibria decreases in size with increasing a_1 . Finally, the two boundary lines meet at $a_1 = (a_1)_b$. $(a_1)_b$ and the corresponding value of μ can be found numerically by considering that, at this point, the minimum of $\bar{w}_n(P)$ merges with the maximum or, in other words, that $\bar{w}_n(P)$ has a saddle point at $\bar{w}_n = 1$. For $a_1 > (a_1)_b$, no multiple equilibria are possible.

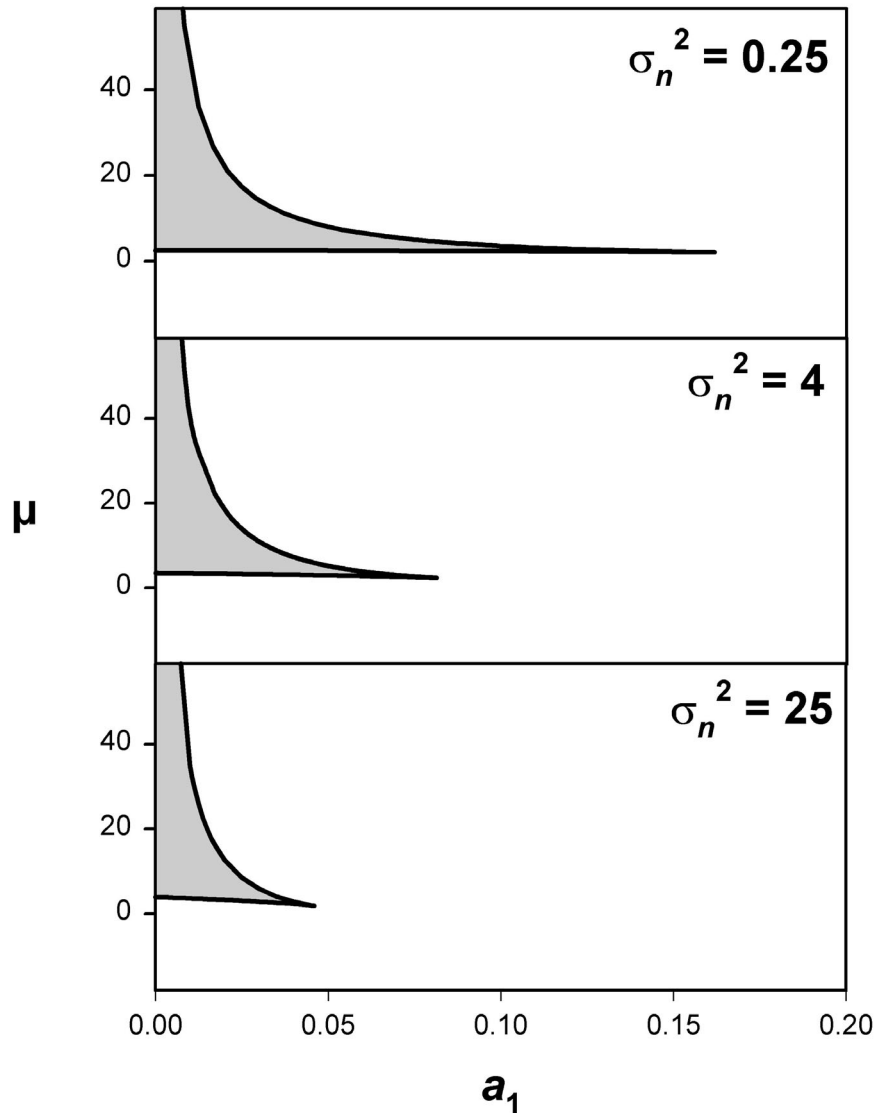


Fig. 12. Model 1 without evolution: The domain of multiple ecological equilibria and the variance of the prey's induction threshold.

The domain of multiple equilibria (shaded area) in the a_1 versus μ plane for three values of σ_n^2 , the variance of the prey's induction threshold. The domain of multiple equilibria decreases in size as σ_n^2 increases. In particular, $(a_1)_b$, the maximal value of a_1 that allows for multiple equilibria (see Fig. 11), decreases with increasing σ_n^2 . a_1 is the success rate of predators feeding on defended prey, and μ is the mean induction threshold of the prey. Model 1. Parameters: $a_0 = 0.4$, $b = 0.4$, $c_d = 0.2$, $h_n^2 = 0$, $\lambda = 2$.

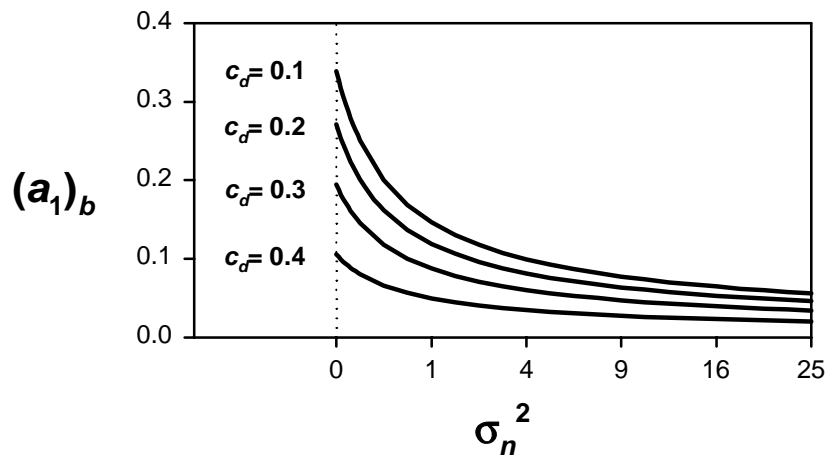


Fig. 13. Model 1 without evolution: $(a_1)_b$ as a function of σ_n^2 and c_d .

$(a_1)_b$, the maximal value of a_1 that allows for multiple equilibria (see Fig. 11), as a function of σ_n^2 , the variance of the prey's induction threshold, for various values of the defense costs c_d . The value of c_d is indicated inside the graphs. $(a_1)_b$ decreases with both σ_n^2 and c_d . a_1 is the success rate of predators feeding on defended prey. Note the quadratic scale of the abscissa. Model 1. Parameters: $a_0 = 0.4$, $b = 0.4$, $h_n^2 = 0$, $\lambda = 2$.

Fig. 12 shows similar diagrams for three values of σ_n^2 . With decreasing σ_n^2 , the domain of multiple equilibria is extended and $(a_1)_b$ increases. Therefore, $(a_1)_b$ can be used as a measure for the size of the domain of multiple equilibria. In Fig. 13, $(a_1)_b$ is plotted against σ_n^2 for various values of c_d , showing that the domain of multiple equilibria decreases in size with both parameters.

The previous results can be explained in terms of the prey's mean fitness function $\bar{w}_n(P)$. A comparison of Fig. 8 A and B shows that multiple equilibria are favored by small values of the variance σ_n^2 , which cause a rapid increase in the proportion of defended prey around $P = \mu$. Similarly, multiple equilibria are favored by low values of a_1 and c_d , because these make sure that $w_{n1} > 1$ for a large range of P , increasing the likelihood that the maximum of \bar{w}_n is greater than 1.

I will now investigate the effect of the defense parameters on the values of P^* and N^* . Note that P^* is the predator density needed for exact regulation of the prey population and N^* is the prey density needed to sustain this predator population. Fig. 14 shows all possible equilibrium predator densities as a function of a_1 for various values of c_d (note

that μ has been chosen such that $a_1 = 0$ is inside the domain of multiple equilibria). In the low and high equilibrium, P^* decreases with both parameters, whereas the reverse is true for the intermediate equilibrium. Thus, in the biologically meaningful equilibria, the predator density that is needed to prevent net growth of the prey population decreases if the defense becomes less effective or more costly. The corresponding plot for the equilibrium prey density N^* looks qualitatively similar (not shown), reflecting the fact that a smaller predator population can be sustained by fewer prey (and vice versa).

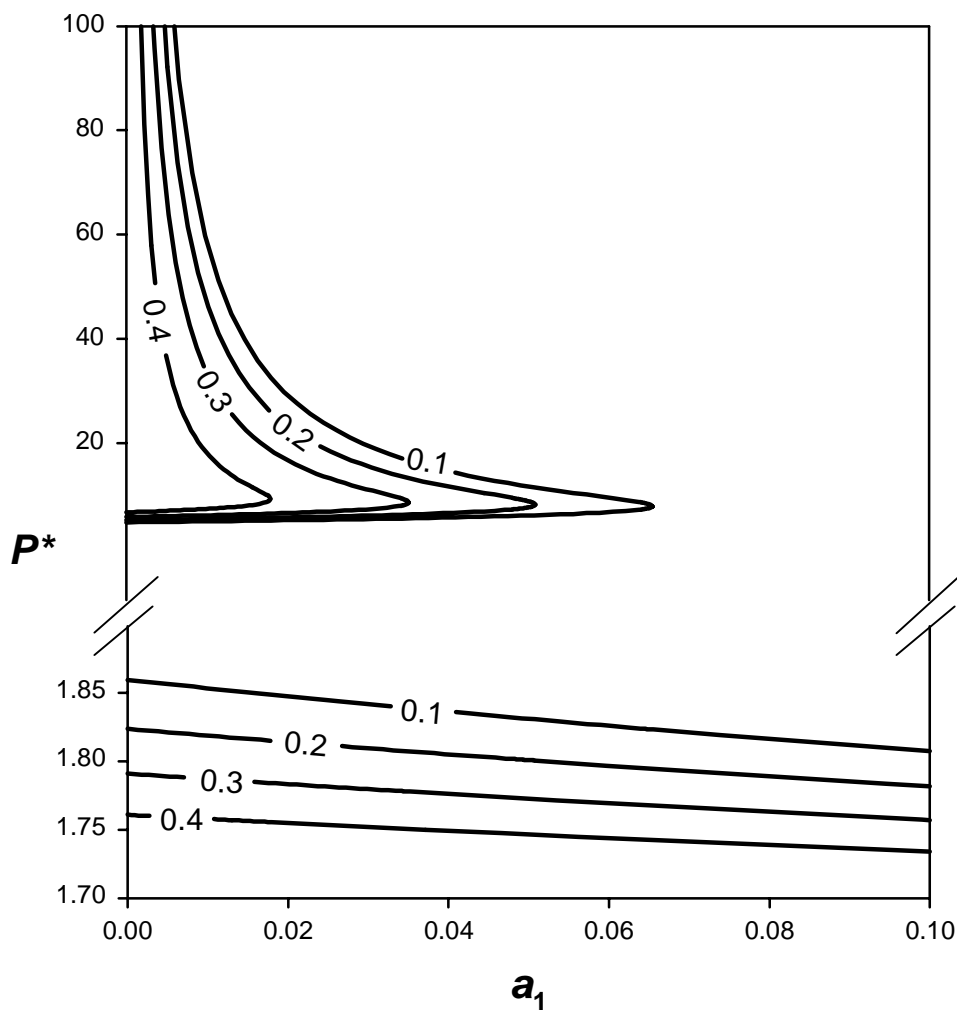


Fig. 14. Model 1 without evolution: Predator density at the ecological equilibrium as a function of a_1 and c_d .

The equilibrium predator density P^* as a function a_1 , the success rate of the predator when feeding on defended prey, for various values of the defense costs c_d . The value of c_d is given inside the graphs. For $a_1 < (a_1)_b$, there are three alternative equilibria. Note that parameters have been chosen such that $a_1 = 0$ is inside the domain of multiple equilibria (see Fig. 11). Model 1. Parameters: $a_0 = 0.4$, $b = 0.4$, $h_n^2 = 0$, $\lambda = 2$, $\mu = 5$, $\sigma_n^2 = 4$.

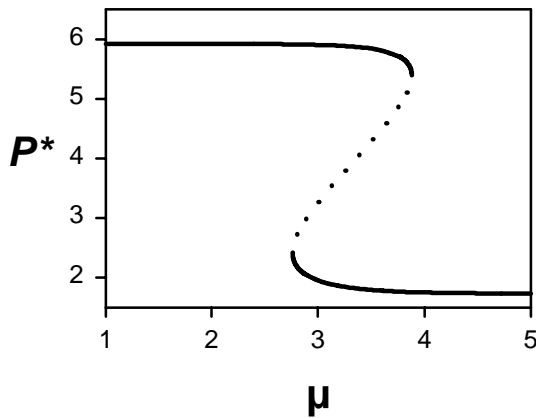


Fig. 15. Model 1 without evolution: Predator density at the ecological equilibrium as a function of μ .

Alternative equilibrium predator densities P^* as a function of the prey's mean induction threshold μ . The high and low equilibria are linked by the always unstable intermediate equilibrium (dotted line), resulting in a typical hysteresis loop. See Fig. 10. Model 1. Parameters: $a_0 = 0.4$, $a_1 = 0.1$, $b = 0.4$, $c_d = 0.1$, $h_n^2 = 0$, $\lambda = 2$, $\sigma_n^2 = 1$.

Next, I will regard variation in the mean induction threshold μ . Inside the domain of multiple equilibria, a plot of P^* against μ shows a typical hysteresis loop (Fig. 15), where two (potentially) stable equilibria are linked by an unstable equilibrium. At the low and high equilibrium, P^* decreases with μ , whereas at the intermediate equilibrium, P^* increases with μ .

Fig. 16 shows the same type of plot for various values of σ_n^2 in the case $a_1 < \hat{a}_1$. As σ_n^2 increases, the hysteresis loop disappears, and only one equilibrium remains, where P^* decreases with μ (see also Fig. 8). All curves in Fig. 16 intersect at a point where $P^* = \mu$ and $\bar{d} = 1/2$. This point is independent of σ_n^2 due to the symmetry of the normal distribution. Above the intersection point, P^* decreases with σ_n^2 at the low and high equilibrium, whereas it increases with σ_n^2 at the intermediate equilibrium. Below the intersection point, the reverse is true. For $\sigma_n^2 \rightarrow \infty$, $\bar{d} \rightarrow 1/2$ and $P^* \rightarrow \mu$ for all μ . For $\sigma_n \rightarrow 0$, $\bar{w}_n \rightarrow w_{n0}$ for $P < \mu$, and $\bar{w}_n \rightarrow w_{n1}$ for $P > \mu$. Therefore, the low equilibrium approaches the solution of $w_{n0}(P) = 1$, the high equilibrium approaches the solution of $w_{n1}(P) = 1$, and the intermediate equilibrium approaches μ . Again, the corresponding plot for the equilibrium prey density N^* looks qualitatively similar, that is a change in μ causes N^* and P^* to change into the same direction.

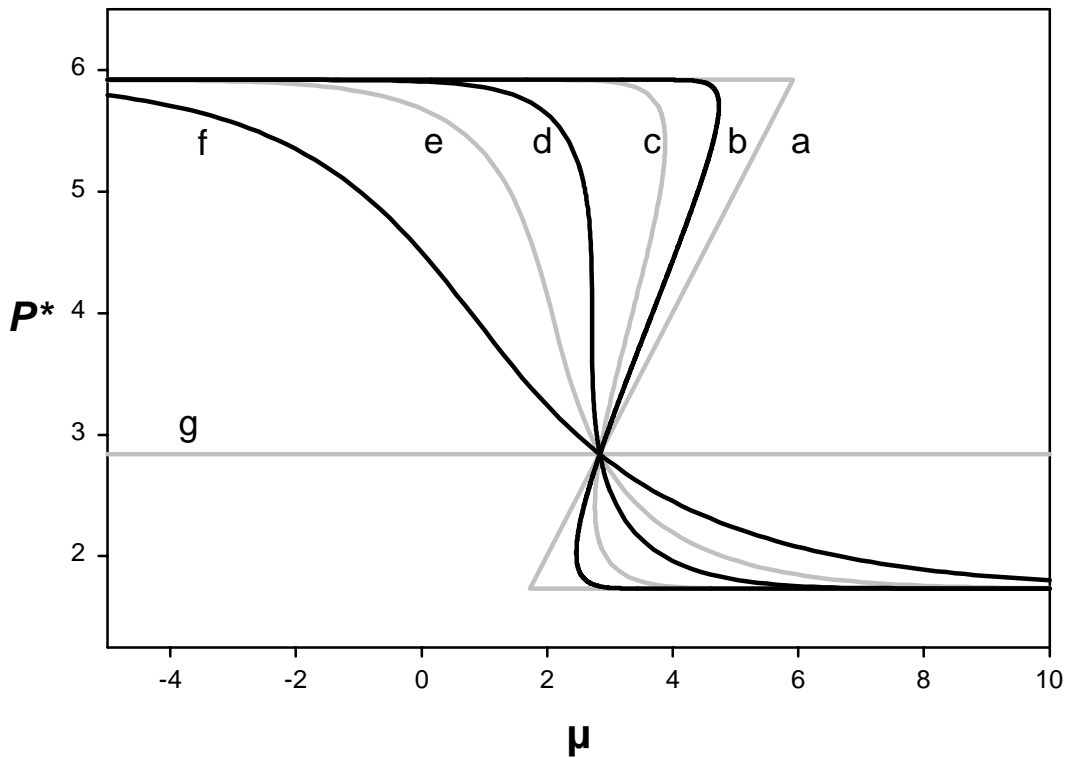


Fig. 16. Model 1 without evolution: Predator density at the ecological equilibrium as a function of μ and σ_n^2 .

Alternative equilibrium predator densities P^* as a function of the prey's mean induction threshold μ for various values of the variance σ_n^2 . **a)** $\sigma_n^2 \rightarrow 0$, **b)** $\sigma_n^2 = 0.25$, **c)** $\sigma_n^2 = 1$, **d)** $\sigma_n^2 = 4$, **e)** $\sigma_n^2 = 9$, **f)** $\sigma_n^2 = 16$, **g)** $\sigma_n^2 \rightarrow \infty$. For small σ_n^2 , there are three alternative equilibria, and the graph shows an hysteresis loop (see Fig. M8). For the given value of a_1 , the multiple equilibria disappear for $\sigma_n^2 \geq 4$. Model 1. Parameters: $a_0 = 0.4$, $a_1 = 0.1$, $b = 0.4$, $c_d = 0.1$, $h_n^2 = 0$, $\lambda = 2$.

However, the relation between prey and predator density at equilibrium becomes more complex for larger values of the defense parameter a_1 . Fig. 17 shows three principal possibilities outside the domain of multiple equilibria. For $a_1 < \hat{a}_1$, both N^* and P^* decrease with μ . For $a_1 > \hat{a}_1$, P^* increases with μ , whereas N^* continues to decrease with μ . Finally, for very large a_1 , N^* increases with μ , too. Fig. 18 shows, how $N^*(\mu)$ changes from a monotonically increasing to a monotonically decreasing function within a narrow range of a_1 . The proportion of defended prey \bar{d}^* always decreases from 1 to 0 as μ increases from $-\infty$ to $+\infty$.

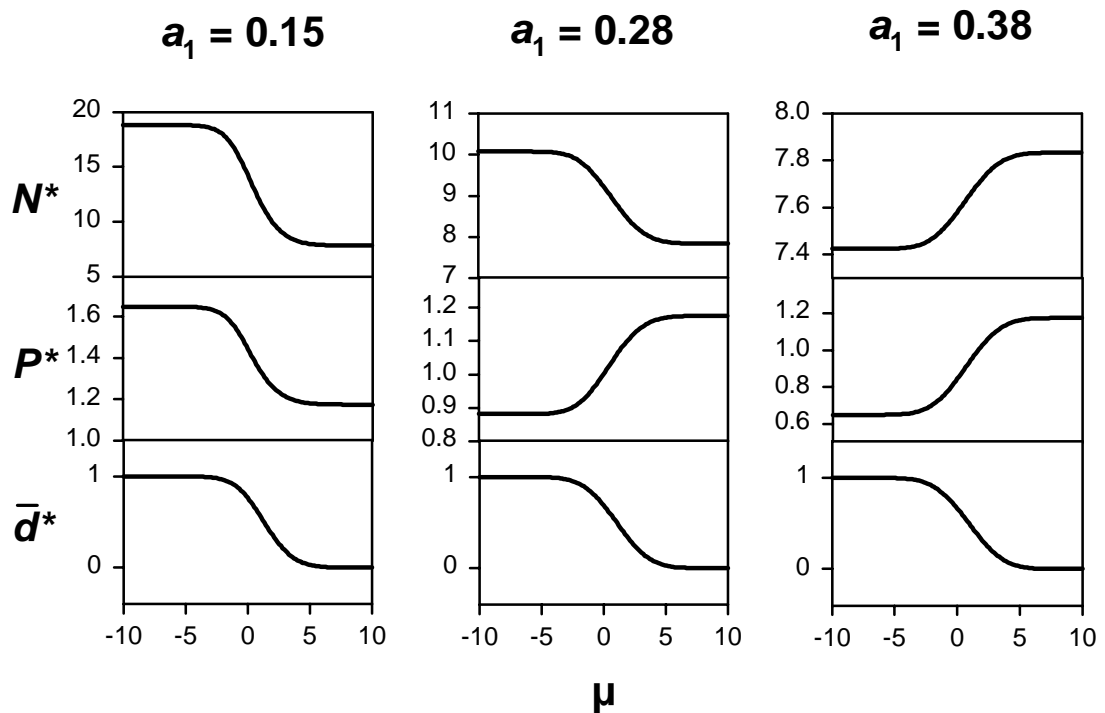


Fig. 17. Model 1 without evolution: The relationship between predator and prey density at the ecological equilibrium.

The equilibrium prey density N^* , equilibrium predator density P^* , and the equilibrium proportion of defended predators \bar{d}^* as a function of the mean induction threshold μ for three values of a_1 , the success rate of predators feeding on defended prey. With increasing μ , N^* and P^* may change into the same or the opposite direction, depending on the relation between a_1 and \hat{a}_1 (the threshold value of a_1 that determines which prey type is favored at equilibrium, see eq. (32) and Fig. 9). For the chosen parameters, $\hat{a}_1 = 0.2101$. See text for further details. Model 1. Parameters: $a_0 = 0.4$, $b = 0.4$, $c_d = 0.2$, $h_n^2 = 0$, $\lambda = 1.6$, $\sigma_n^2 = 4$.

Biologically, these findings can be interpreted as follows. First, P^* decreases with μ for $a_1 < \hat{a}_1$, because in this case, the defense is beneficial for the prey at equilibrium and, therefore, a decreased induction frequency means that the prey population can tolerate fewer predators. Similarly, P^* increases with μ for $a_1 > \hat{a}_1$ because, in this case, the defense is detrimental for the prey and a decreased induction frequency means that the prey population can tolerate more predators. Second, N^* , the density of prey needed to sustain the predator population, increases with P^* and with the proportion of defended prey \bar{d}^* . For $a_1 < \hat{a}_1$, both P^* and \bar{d}^* increase with μ , and, hence, N^* decreases with μ , too. For $a_1 > \hat{a}_1$, \bar{d}^* still decreases with μ , but P^* now increases with μ . Note however, that the amount of change in P^* depends on a_1 . P^* ranges from $\ln(\lambda(1-c_d))/a_1$

(the solution of $w_{n1}(P)=1$) for $\mu \rightarrow -\infty$ to $\ln(\lambda)/a_0$ (the solution of $w_{n0}(P)=1$) for $\mu \rightarrow \infty$. The magnitude of the difference between these two limits increases with $|a_1 - \hat{a}_1|$. Therefore, if a_1 is not too much greater than \hat{a}_1 the effect of the decrease in \bar{d}^* overrides the effect of the increase in P^* and, consequently, N^* decreases with μ . However, for very large values of a_1 , the effect of P^* becomes dominant over the effect of \bar{d}^* , causing N^* to increase with μ .

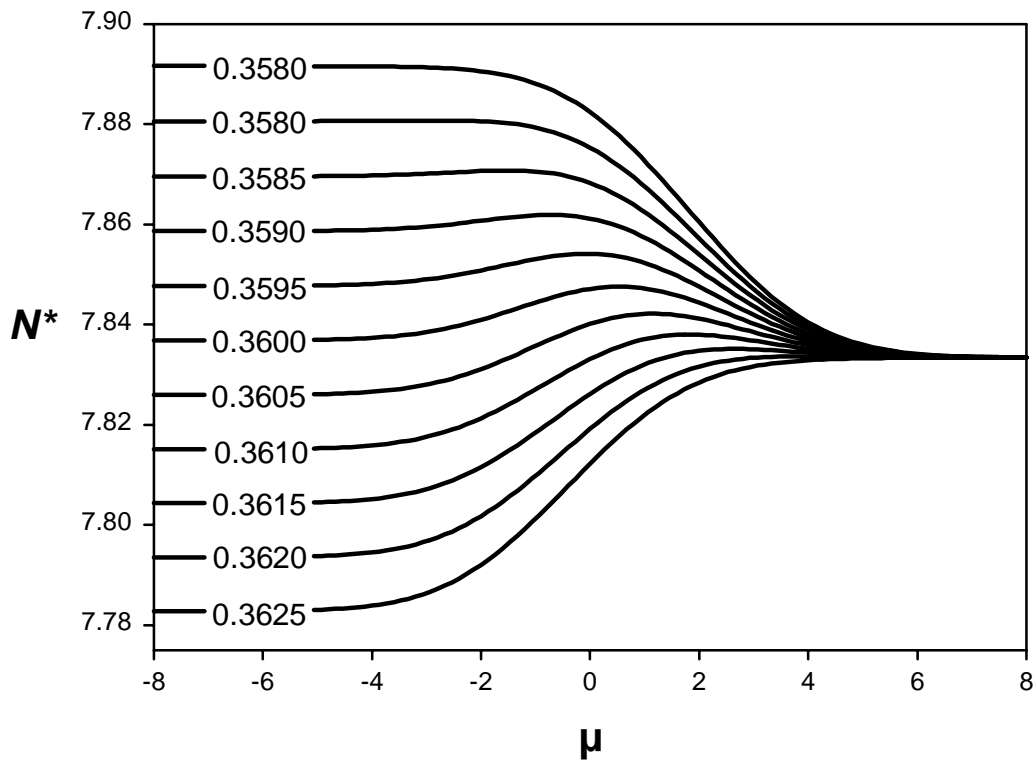


Fig. 18. Model 1 without evolution: Prey density at the ecological equilibrium as a function of μ and a_1 . The equilibrium prey density N^* as a function of the prey's mean induction threshold μ for various values of a_1 , the success rate of predators feeding on defended prey. The figure illustrates the transition between the two situations shown in Fig. 17 by demonstrating how $N^*(\mu)$ changes from a monotonically increasing to a monotonically decreasing function if a_1 becomes very large. See text for further explanations. Parameters are the same as in Fig. 17. Model 1. Parameters: $a_0=0.4$, $b=0.4$, $c_d=0.2$, $h_n^2=0$, $\lambda=1.6$, $\sigma_n^2=4$.

It is possible to derive an analytical expression for the smallest value of a_1 where $N^*(\mu)$ is monotonically increasing for all μ (see Fig. 18). First, N^* can be written as a function of P^* by solving $\bar{w}_n = 1$ for $\exp(-a_0 P)$ and inserting the solution into $\bar{w}_p = 1$, yielding

$$N^* = \frac{\lambda P^*}{b(\lambda - 1 - c_d \lambda \bar{d}^* \exp(-a_1 P^*))}, \quad (33)$$

where \bar{d}^* is a function of P^* . From $\bar{w}_n = 1$, it can be deduced that

$$\bar{d}^*(P^*) = \frac{\lambda \exp(-a_0 P^*) - 1}{\lambda(\exp(-a_0 P^*) - (1 - c_d) \exp(-a_1 P^*))} \quad (34)$$

Note that, for $a_1 > \hat{a}_1$, P^* increases with μ . Therefore, N^* increases with μ , too, if the relation between P^* and N^* is positive. Without giving a formal proof, I infer from Fig. 18 that, with increasing a_1 , N^* becomes an increasing function μ first for small μ and last for large μ . Therefore, in order to calculate the value of a_1 where N^* increases with μ for *all* μ , it is sufficient to regard the limiting case $\mu \rightarrow \infty$, that is $\bar{d}^* = 0$ and $P^* = \ln(\lambda)/a_0$.

Taking the first derivative of N^* (eq. 33), substituting $\bar{d}^* = 0$ and $P^* = \ln(\lambda)/a_0$, and eliminating all positive factors yields:

$$\text{signum}(\partial N^* / \partial P^*) = \text{signum} \left(\frac{\lambda^{a_1/a_0} - \lambda(1 - c_d) - c_d \ln \lambda - \lambda^{(a_1 - a_0)/a_0} + 1 - c_d}{\lambda^{(a_1 - a_0)/a_0} - 1 + c_d} \right) \quad (35)$$

For $a_1 > \hat{a}_1 = a_0 \frac{\ln(\lambda(1 - c_d))}{\ln \lambda}$, $\lambda^{(a_1 - a_0)/a_0} - 1 + c_d$ is positive. Hence, the denominator on the right-hand side of eq. (35) can be discarded, and the numerator can be rearranged to yield the following condition:

For $P^* = \ln(\lambda)/a_0$ there is a positive relationship between N^* and P^* (implying that N^* increases with μ) if and only if

$$a_1 > \tilde{a}_1 = \frac{a_0}{\ln \lambda} \ln \left(1 - c_d + c_d \frac{\ln \lambda}{\lambda - 1} \right) + a_0. \quad (36)$$

It can be shown that \tilde{a}_1 is always between \hat{a}_1 and a_0 for biologically reasonable parameters ($\lambda > 1$, $a_0 > 0$, $0 < c_d < 1$). Therefore, N^* will always increase with μ for sufficiently small a_1 and decrease with μ for sufficiently large a_1 .

Finally, the parameter b has no influence on P^* (as it has no effect on prey fitness) and is inversely proportional to N^* (eq. 33).

3.3.3.2 Stability of the ecological equilibria

I will now explore the stability of the ecological equilibria of model 1. I will first provide some very general analytical results (which also apply to model 2) and then present a more specific numerical analysis.

3.3.3.2.1 General analytical results for ecological stability

It is generally not possible to deduce analytical expressions defining the domain in parameter space where the ecological equilibria are stable. Here, I will only derive some very general statements, based solely on the following model assumptions: (1) Prey fitness is not density-dependent, and (2) mean fitness of predator and prey at equilibrium is equal to 1. That is, I analyze a general system of the form:

$$\begin{aligned} N_{t+1} &= N_t \bar{w}_n(P_t) \\ P_{t+1} &= P_t \bar{w}_p(N_t, P_t) \end{aligned} \quad (37)$$

This model structure is independent of the presence or absence of phenotypic plasticity in either predator or prey. It applies to the standard Nicholson-Bailey model (eq. 1) as well as to model 1 and model 2 of this study (for $h_n^2 = 0$ and $h_p^2 = 0$).

Using the standard technique of local linear stability analysis (e.g. Kot 2001) and skipping the time indices, the Jacobian of the above system is

$$J = \begin{pmatrix} \frac{\partial N \bar{w}_n(P)}{\partial N} & \frac{\partial N \bar{w}_n(P)}{\partial P} \\ \frac{\partial P \bar{w}_p(N, P)}{\partial N} & \frac{\partial P \bar{w}_p(N, P)}{\partial P} \end{pmatrix} = \begin{pmatrix} \bar{w}_n(P) & N \frac{\partial \bar{w}_n(P)}{\partial P} \\ \frac{P}{N} \bar{w}_p(N, P) & \bar{w}_p(N, P) + P \frac{\partial \bar{w}_p(N, P)}{\partial P} \end{pmatrix} \quad (38)$$

At equilibrium, this is

$$J^* = \begin{pmatrix} 1 & N^* \frac{\partial}{\partial P} \bar{w}_n(P^*) \\ \frac{P^*}{N^*} & 1 + P^* \frac{\partial}{\partial P} \bar{w}_p(N^*, P^*) \end{pmatrix}.$$

As the fitness functions only appear as derivatives with respect to P , I will simplify notation by writing $\partial / \partial P (\bar{w}_n(P^*)) = \bar{w}_n'$ and $\partial / \partial P (\bar{w}_p(N^*, P^*)) = \bar{w}_p'$. Thus, J^* becomes

$$J^* = \begin{pmatrix} 1 & N^* \bar{w}_n' \\ \frac{P^*}{N^*} & 1 + P^* \bar{w}_p' \end{pmatrix} \quad (39)$$

An equilibrium is stable if both eigenvalues of J^* have magnitude less than one. This condition can be verified by applying the Jury test, which uses the trace and the determinant of J^* :

$$\begin{aligned} \text{tr}(J^*) &= 2 + P^* \bar{w}_p' \\ \det(J^*) &= 1 + P^* (\bar{w}_p' - \bar{w}_n') \end{aligned} \quad (40)$$

The Jury test states that three conditions must be satisfied for stability:

$$\text{Condition 1: } 1 - \text{tr}(J^*) + \det(J^*) > 0 \Leftrightarrow \bar{w}_n' < 0.$$

$$\text{Condition 2: } \det(J^*) < 1 \Leftrightarrow \bar{w}_p' < \bar{w}_n'. \quad (41)$$

$$\text{Condition 3: } 1 + \text{tr}(J^*) + \det(J^*) > 0 \Leftrightarrow \bar{w}_p' > \frac{1}{2}\bar{w}_n' - \frac{2}{P^*}.$$

Taken together, these conditions state that stability requires

$$\frac{1}{2}\bar{w}_n' - \frac{2}{P^*} < \bar{w}_p' < \bar{w}_n' < 0. \quad (42)$$

Note that the first term need not necessarily be less than the third one.

Condition 1 states that stability is only possible if the equilibrium predator density P^* is inside the range where an increase in P reduces the mean fitness of the prey. This proves that, in the case of multiple equilibria, the intermediate equilibrium can never be stable. Condition 2 has a very intuitive interpretation: Stability requires that the within-species effect of an increase in predator density (increased competition for prey) must be stronger than the between-species effect (increased predation pressure exerted on prey). This condition can never be met in the basic Nicholson-Bailey model, which is why this model is always unstable. However, stability is made possible by the inducible prey defense, which weakens the intraspecific effect of predator density and intensifies the interspecific effect. Condition 3, by giving a lower boundary for \bar{w}_p' relative to \bar{w}_n' , shows that stability can be lost again if the intraspecific effect becomes too strong. As I shall show below, this may be the case if the prey's population-level reaction norm is very steep (small σ_n^2).

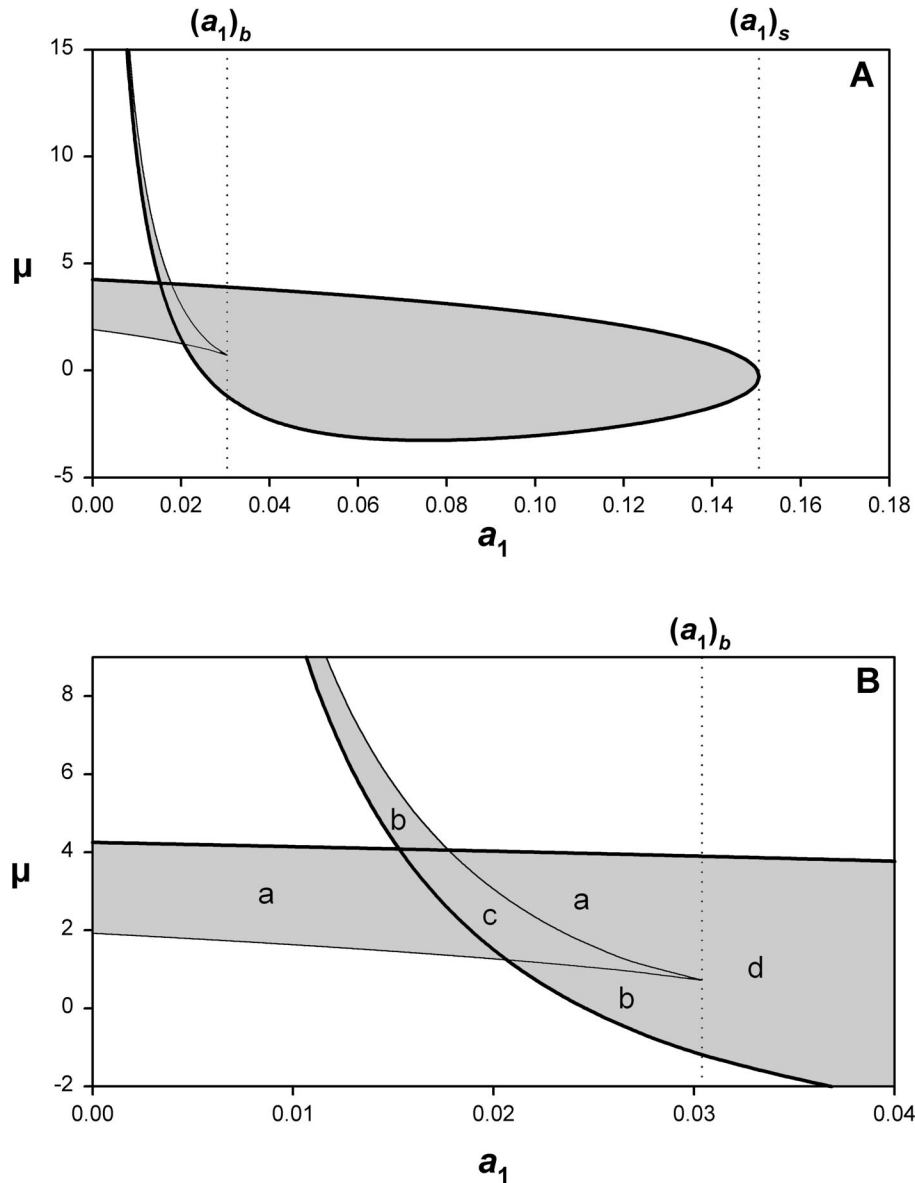


Fig. 19. Model 1 without evolution: The domain of ecological stability.

A) The domain of ecological stability in the a_1 versus μ plane. In the shaded area, the ecological equilibrium of model 1 is locally stable. The thick line marks the boundaries of the domain of stability. The maximal value of a_1 that allows for stability is termed $(a_1)_s$. It is a measure for the minimal efficiency the defense must have in order to stabilize the population dynamics. The thin line marks the boundaries of the domain of multiple ecological equilibria, and is delimited by $(a_1)_b$ (see Fig. 11). For $\mu \rightarrow \infty$, both boundary lines approach the ordinate.

B) A detailed view on the relationship between the domain of ecological stability and the domain of multiple ecological equilibria. **a)** low equilibrium stable, **b)** high equilibrium stable, **c)** low and high equilibrium stable, **d)** stable equilibrium for $a_1 > (a_1)_b$.

a_1 is the success rate of predators feeding on defended prey, and μ is the prey's mean induction threshold. Model 1. Parameters: $a_0 = 0.4$, $b = 0.4$, $c_d = 0.4$, $h_n^2 = 0$, $\lambda = 2$, $\sigma_n^2 = 6.25$.

Usually, it is not possible to derive analytical results regarding the effect of the various model parameters on the stability of the ecological equilibrium. The one exception is the parameter b , the number of new predators obtained per consumed prey. It can be shown that b has no influence on the domain of ecological stability at all. The prove is straightforward and, basically, relies on the fact that \bar{w}_n is independent of N_t and b , whereas \bar{w}_p is linear in both N_t and b . This causes N^* and several components of the Jacobian J^* to be linear in b , but in the characteristic polynomial all instances of b cancel, leaving the eigenvalues of J^* unchanged. Note, however, that b does have an influence on non-equilibrium dynamics.

3.3.3.2 Numerical stability analysis

In the following, I will use numerical methods to explore the domain of ecological stability as a function of the parameters μ , a_1 , σ_n^2 , c_d , and λ . The boundaries of the domain of stability can be calculated by finding parameter values such that the dominant eigenvalue of the Jacobian J^* has magnitude equal to 1.

Fig. 19 shows the domain of ecological stability in an a_1 vs. μ plane for a rather large value of σ_n^2 . It is delimited by a loop-shaped boundary line. For $a_1 < (a_1)_b$, there are separate stability domains for the low and the high equilibrium, respectively. The low equilibrium is stable if μ is not too large, and the high equilibrium is stable if μ is not too small. If a_1 is close to $(a_1)_b$, both equilibria can be stable simultaneously. For $a_1 > (a_1)_b$, the single ecological equilibrium is stable for intermediate values of μ . If a_1 exceeds another critical value, which I will term $(a_1)_s$, no stable equilibrium is possible for any μ . As a large value of a_1 is equivalent to a weak defense, $(a_1)_s$ can be interpreted as the minimum efficiency the defense must have in order to stabilize the system.

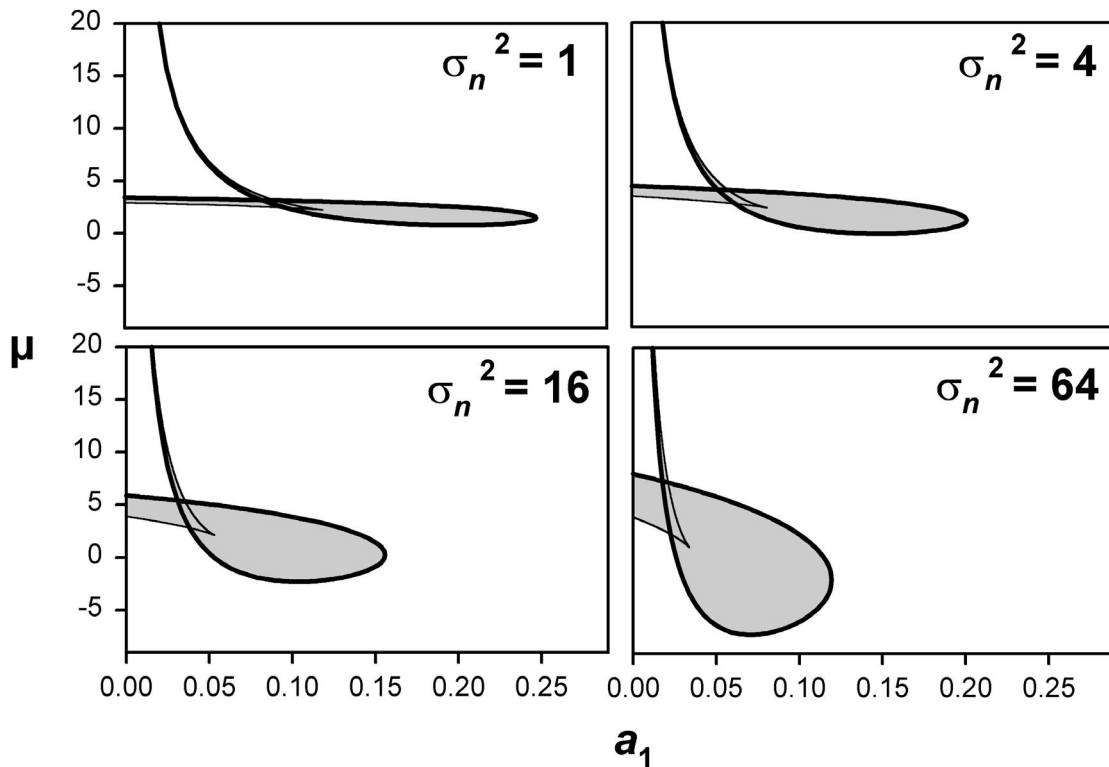


Fig. 20. Model 1 without evolution: The domain of ecological stability as a function of σ_n^2 .

The domain of ecological stability (shaded area) in the a_1 versus μ plane for various values of σ_n^2 , the variance of the prey's induction threshold. With increasing σ_n^2 , the range of μ that enables stability increases for small a_1 , but $(a_1)_s$, the maximal value of a_1 where stability is possible, decreases. For an explanation of the diagram, see Fig. 19. Model 1. Parameters: $a_0 = 0.4$, $b = 0.4$, $c_d = 0.2$, $h_n^2 = 0$, $\lambda = 2$.

If σ_n^2 is increased, $(a_1)_s$ decreases (but stays positive), but for $a_1 < (a_1)_s$, the range of μ where stability is possible increases (i.e. the domain of stability becomes “shorter” but “higher”, Fig. 20, see also Fig. 24). However, the increase in the range of μ merely reflects the increased variance of the distribution of induction thresholds and has no deeper biological meaning. The effect disappears if μ is normalized and divided by σ_n^2 (Fig. 21).

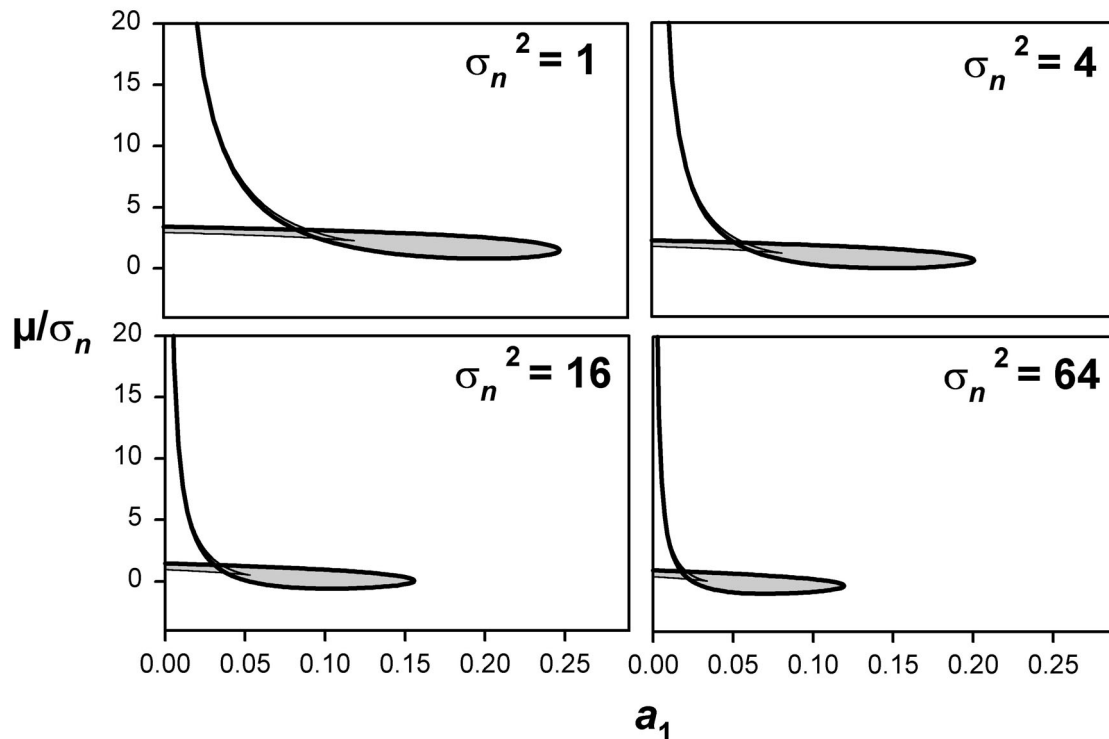


Fig. 21. Model 1 without evolution: The domain of ecological stability as a function of σ_n^2 with normalized μ .

The domain of ecological stability (shaded area) in the a_1 versus μ/σ_n plane for various values of σ_n^2 , the variance of the prey's induction threshold. Data are the same as in Fig. 20, but the prey's mean induction threshold μ has been divided by the standard deviation σ_n in order to achieve normalization. A comparison with Fig. 20 shows that the differences in the "height" of the domain of stability disappear and only the differences in $(a_1)_s$ remain. $(a_1)_s$ is the maximal value of a_1 where stability is possible. For an explanation of the diagram, see Fig. 19. Model 1. Parameters: $a_0 = 0.4$, $b = 0.4$, $c_d = 0.2$, $h_n^2 = 0$, $\lambda = 2$.

Fig. 22 (next page). Model 1 without evolution: The domain of ecological stability as a function of the prey's fecundity λ

The domain of ecological stability (shaded area) in the a_1 versus μ plane for various values of the prey's fecundity λ . With increasing λ , the range of μ that enables stability decreases, although $(a_1)_s$, the maximal value of a_1 where stability is possible, increases slightly. For an explanation of the diagram, see Fig. 19. Model 1. Parameters: $a_0 = 0.4$, $b = 0.4$, $c_d = 0.4$, $h_n^2 = 0$, $\sigma_n^2 = 6.25$.

Fig. 23 (next page). Model 1 without evolution: The domain of ecological stability as a function of the defense costs c_d

The domain of ecological stability (shaded area) in the a_1 versus μ plane for various values of the cost parameter c_d . With increasing defense costs, the range of μ that enables stability increases, although $(a_1)_s$, the maximal value of a_1 where stability is possible, decreases slightly. For an explanation of the diagram, see Fig. 19. Model 1. Parameters: $a_0 = 0.4$, $b = 0.4$, $h_n^2 = 0$, $\lambda = 2$, $\sigma_n^2 = 6.25$.

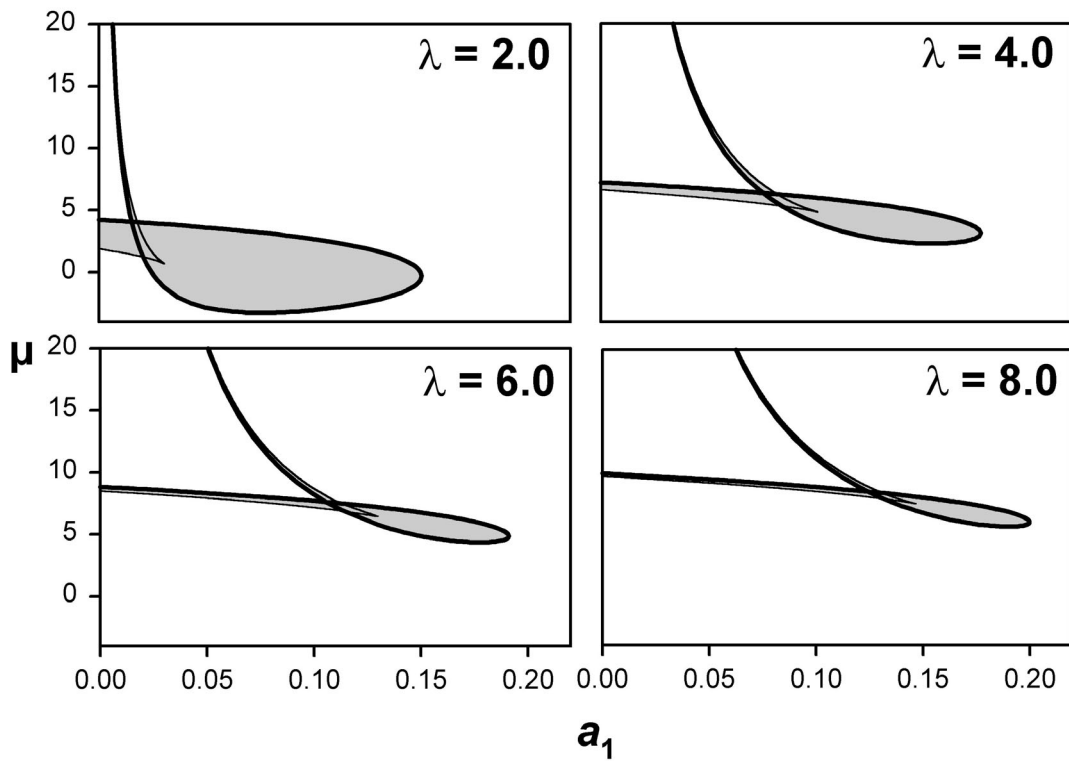


Fig. 22: For legend see previous page.

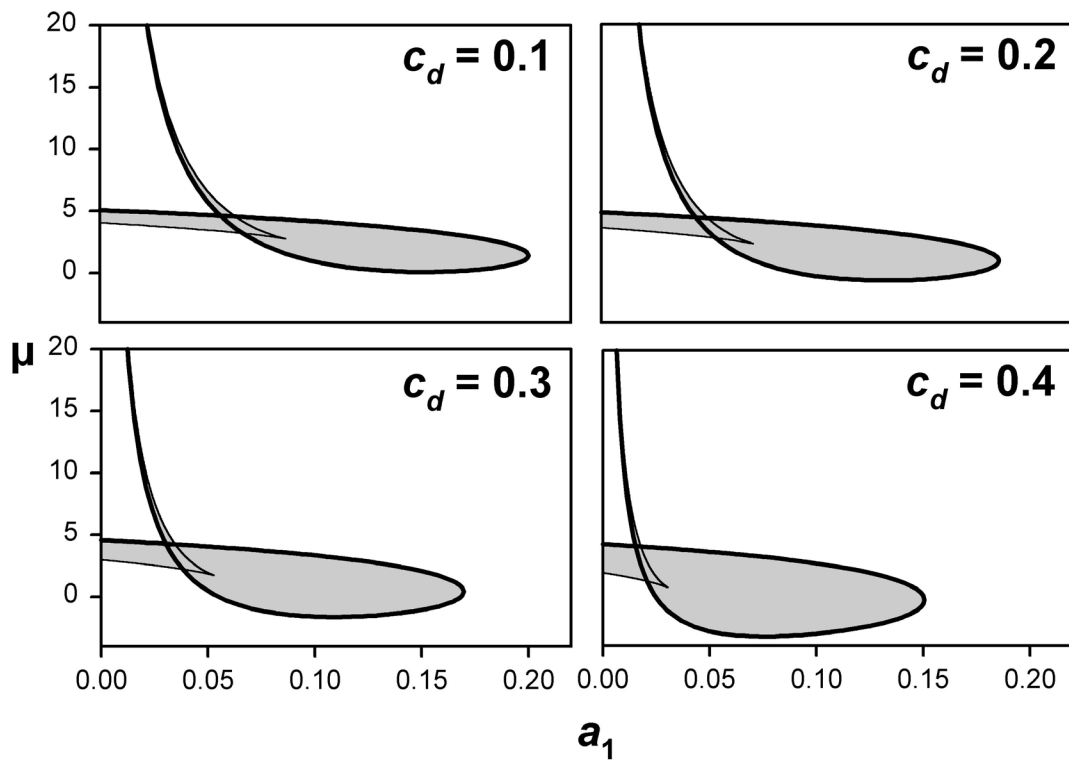


Fig. 23: For legend see previous page.

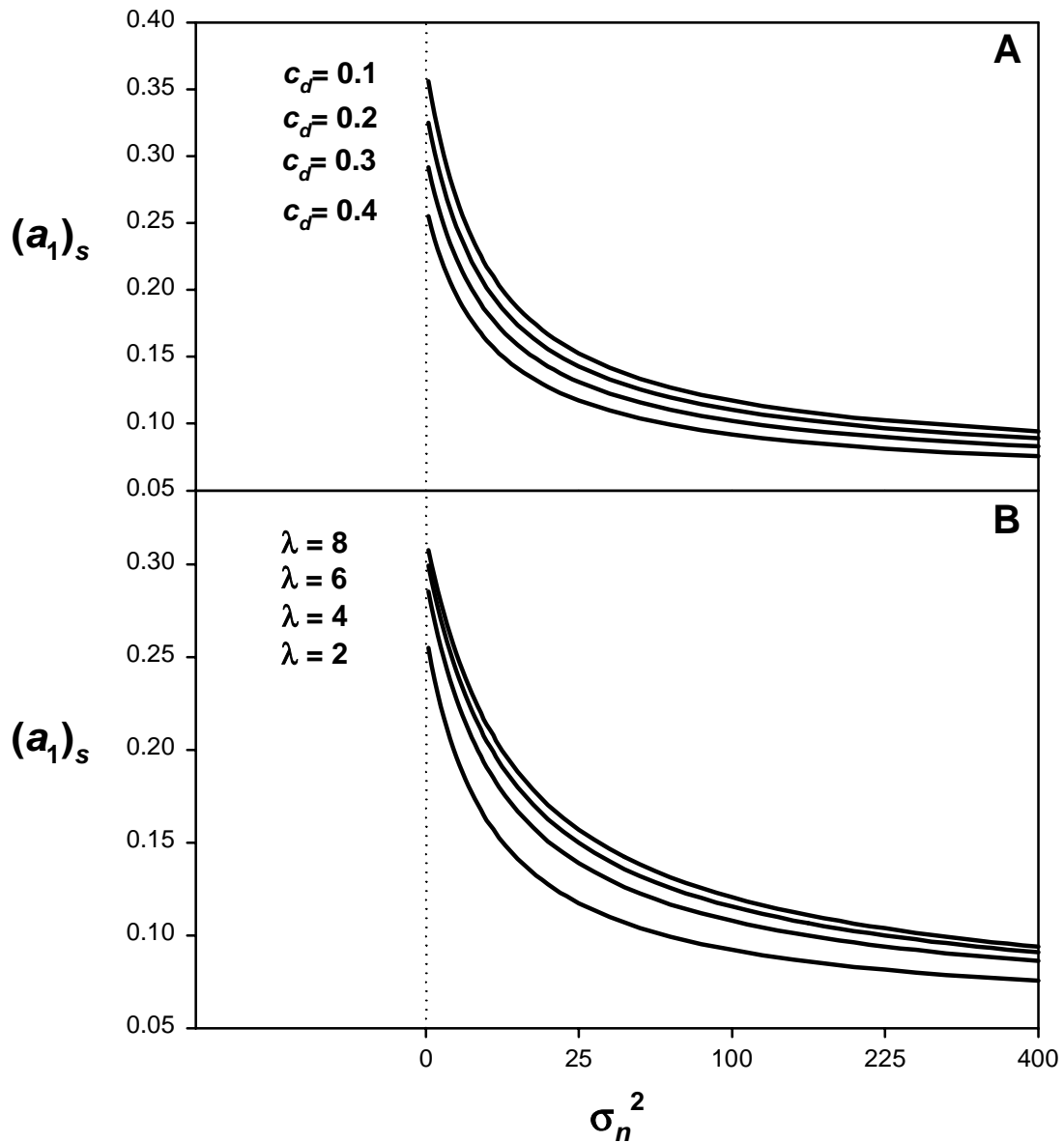


Fig. 24: $(a_1)_s$ as a function of σ_n^2 , c_d and λ

$(a_1)_s$, the maximal value of a_1 that allows for a stable equilibrium, as a function of σ_n^2 , the variance of the prey's induction threshold μ , for various values of the defense costs c_d (A) and the prey's fecundity λ (B). a_1 is the success rate of predators feeding on defended prey. $(a_1)_s$ is a measure for the capacity of the inducible defense to stabilize the dynamics of the predator-prey system. A high value of $(a_1)_s$ means that even a weak defense can stabilize the interaction, provided the mean induction threshold μ has an appropriate value. If σ_n^2 is increased further than shown in the figures, $(a_1)_s$ approaches a positive limiting value. The data show that the stabilizing capacity of the defense decreases strongly with increasing σ_n^2 and decreases slightly with increasing c_d and decreasing λ . Note however, that an increase in c_d and a decrease in λ causes a marked reduction in the range of μ where stability is possible for $a_1 < (a_1)_s$ (see Fig. 23). For very small σ_n^2 , $(a_1)_s$ can no longer be calculated (see Fig. 28). Therefore, the smallest value of σ_n^2 in the present figures is 0.0001. Note the quadratic scale of the abscissae. Model 1. Parameters: $a_0 = 0.4$, $b = 0.4$, $c_d = 0.4$, $h_n^2 = 0$, $\lambda = 2$ (A).

In contrast, there is a “real” decrease in the range of μ that enables stability if the prey growth rate λ is increased (Fig. 22) or the cost parameter c_d is decreased (Fig. 23), although in both cases, there is also a slight increase in $(a_1)_s$ (Fig. 24). Apparently, the stabilizing power of the defense decreases if the net growth rate of the prey is high (i.e. high fecundity, low defense costs). The concomitant increase in $(a_1)_s$ may be due to the increased ability of the prey population to compensate for predator-induced mortality.

If $\sigma_n^2 \rightarrow \infty$, $(a_1)_s$ approaches a positive limiting value. Thus, a strong defense can stabilize the interaction even if the realized plasticity at the population-level is zero. As in all other cases, however, stability requires that both prey phenotypes are present at sufficiently high frequency (\bar{d}^* must not be too close to 0 or 1).

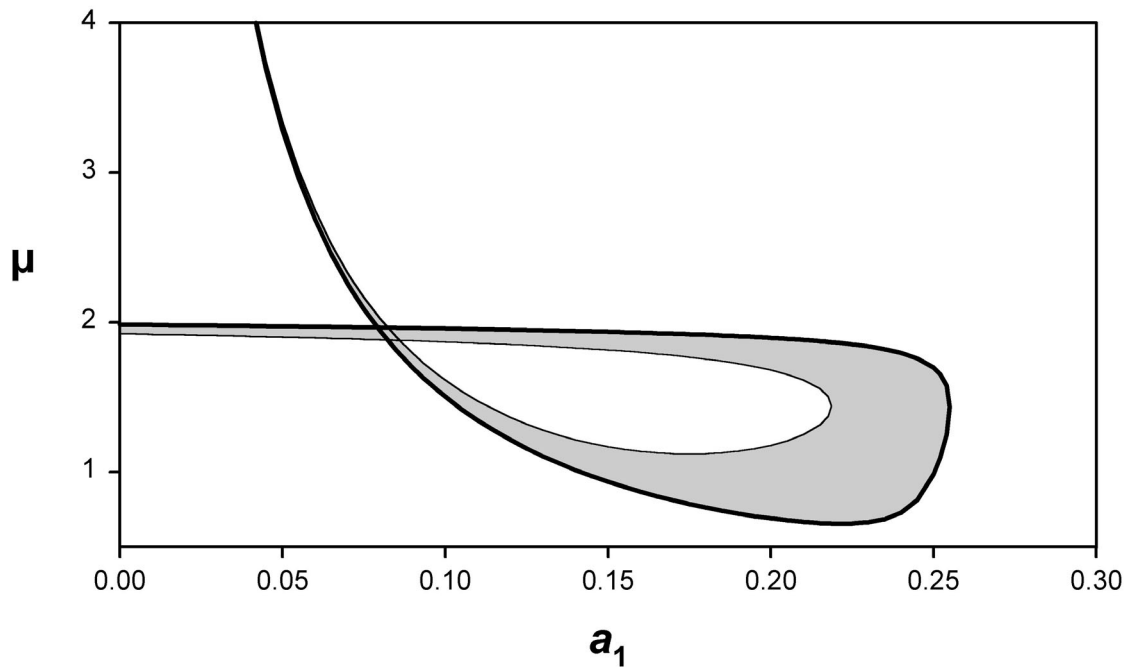


Fig. 25. Model 1 without evolution: The domain of ecological stability for small σ_n^2

The domain of ecological stability (shaded area) in the a_1 versus μ plane for a small value of σ_n^2 , the variance of the prey’s induction threshold. The parameters are the same as in Fig. 19, except for σ_n^2 , which has been decreased from 6.25 to 0.01. This reduction in σ_n^2 brings about a qualitative change in the structure of the domain of ecological stability. The thick (“outer”) boundary line corresponds to the one in Fig. 19. However, the thin (“inner”) boundary line is new and delimits a region on instability in the center of the stable domain. Note that the present figure does not show the boundaries of the domain of multiple equilibria (but see Fig. 26 for additional details). Model 1. Parameters: $a_0 = 0.4$, $b = 0.4$, $c_d = 0.4$ (**B**), $h_n^2 = 0$, $\lambda = 2$, $\sigma_n^2 = 0.01$.

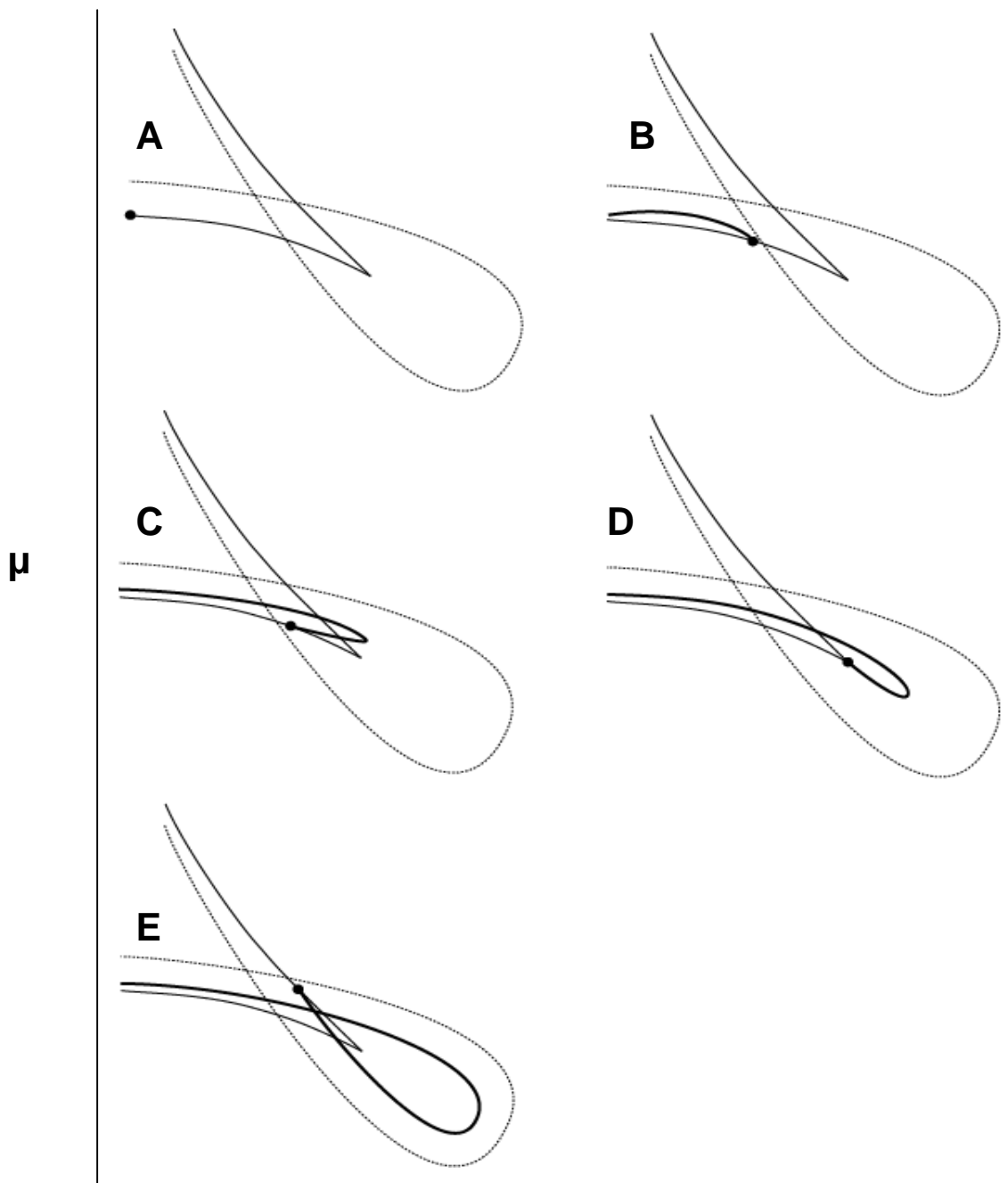


Fig. 26. Model 1 without evolution: The development of the “inner” stability boundary with decreasing σ_n^2 .

Schematic representations of the domain of ecological stability, illustrating the transition from the structure shown in Fig. 19 to that shown in Fig. 25. σ_n^2 , the variance of the prey’s induction threshold, decreases from A to F. For simplicity, the 5 graphs have been drawn together into a single coordinate system. The thin solid line represents the boundary of the domain of multiple equilibria, the dotted line represents the “outer” boundary of the domain of stability, and the thick solid line represents the “inner” stability boundary. (Note that these line styles differ from those in the previous figures.) A shows a situation analogous to that in Fig. 19. However, the inner stability boundary is just about to originate at the lower boundary of the domain of multiple equilibria (dot). With decreasing σ_n^2 , the structure of the domain of ecological stability more and more resembles that in Fig. 25 (F).

If σ_n^2 is decreased further than in the previous examples, the pattern shown in Fig. 19 changes qualitatively. A typical case is depicted in Fig. 25. The domain of ecological stability now has a second boundary line, which (in the “looped” part) is inside the first one. For $a_1 > (a_1)_b$, this means that there is a region of instability in the center of the stable domain. For $a_1 < (a_1)_b$, the low and high equilibrium now may be unstable close to the boundaries of the domain of multiple equilibria. (Note that these boundaries are not shown in Fig. 25, but see Fig. 26 for more details.)

Fig. 26 schematically shows the intermediate stages leading from the situation in Fig. 19 to that in Fig. 25 as σ_n^2 is successively decreased. It was necessary to use drawings that are not true to scale because, in the original data, the various lines are so close to each other that they cannot be clearly distinguished visually. Once σ_n^2 drops below a threshold, the second boundary line originates from the lower boundary of the domain of multiple equilibria. The threshold value for σ_n^2 increases with increasing defense costs c_d (Fig. 27). For $c_d = 0.4$ (as in Fig. 25 and 26), the second boundary line originates at $a_1 = 0$. However, if c_d is decreased, the point of origin moves towards $(a_1)_b$ (data not shown).

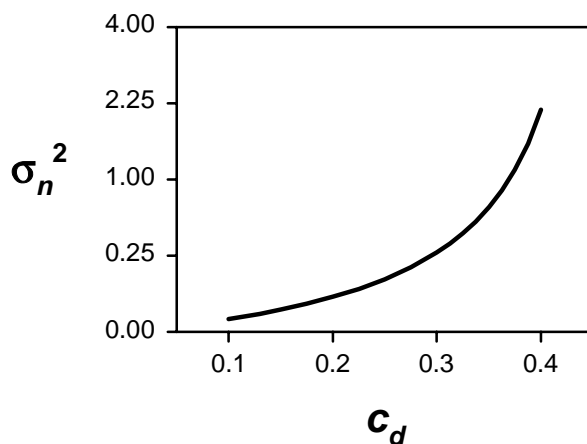


Fig. 27. Model 1 without evolution: The threshold value of σ_n^2 at the origin of the inner stability boundary. The threshold value of σ_n^2 where the inner stability boundary originates (see Fig. 26 A), as a function of the defense costs c_d . If the costs of the defense are high, the inner stability boundary is present already at relatively high values σ_n^2 . Note the quadratic scale of the ordinate. Model 1. Parameters: $a_0 = 0.4$, $b = 0.4$, $h_n^2 = 0$, $\lambda = 2$.

If σ_n^2 is decreased even further than in Fig. 25, the domain of ecological stability becomes more and more fragmented (Fig. 28). Finally, it vanishes completely as $\sigma_n^2 \rightarrow 0$. Stability is not possible for $\sigma_n^2 \rightarrow 0$ because, in this case, all prey have the same induction threshold and, thus, there can be only one prey type at equilibrium. For $\mu \neq P^*$, the model then reduces to the basic Nicholson-Bailey model which is always unstable. For $\mu = P^*$, linear stability analysis is not possible because $\bar{w}_n(P)$ is not differentiable at $P = P^*$. Numerical simulations suggest that the model is unstable in this case, too, with prey and predator showing chaotic oscillations but avoiding extinction.

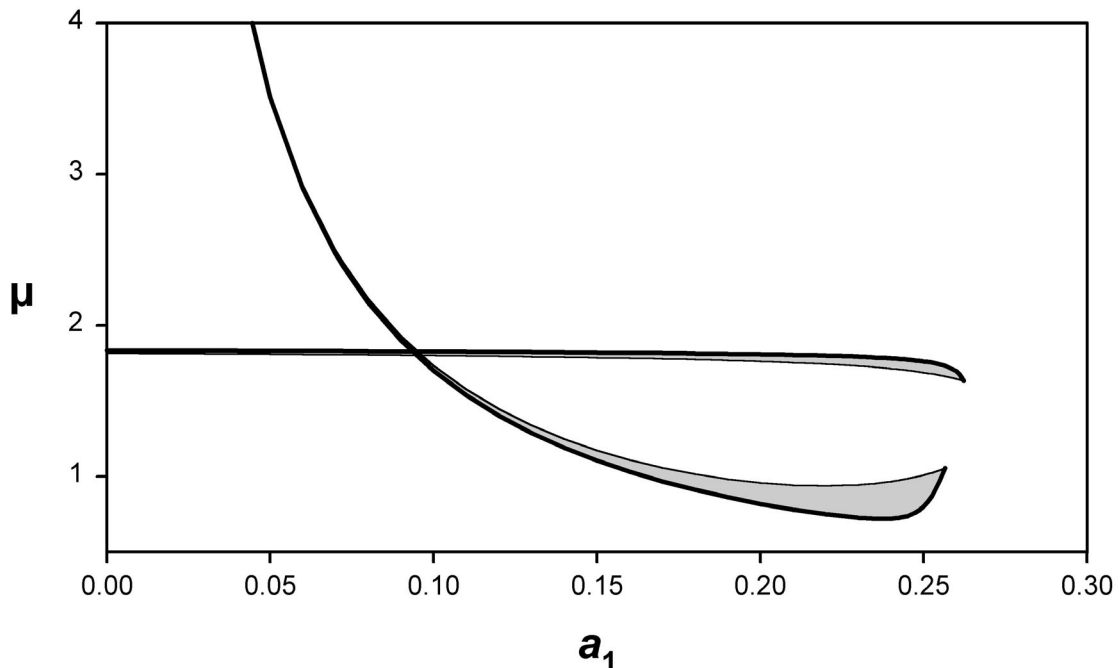


Fig. 28. Model 1 without evolution: Fragmentation of the domain of ecological stability for very small σ_n^2 .

The domain of ecological stability (shaded area) in the a_1 versus μ plane for a very small value of σ_n^2 , the variance of the prey's induction threshold. Parameters are the same as in Fig. 19 and 25, except for σ_n^2 , which has been further decreased to 0.001225. A comparison with Fig. 19 shows that the inner stability boundary (thin line) has “penetrated” the outer one (thick line), such that the domain of ecological stability has become fragmented. Note that the figure does not show the boundaries of the domain of multiple equilibria. Model 1. Parameters: $a_0 = 0.4$, $b = 0.4$, $c_d = 0.4$, $h_n^2 = 0$, $\lambda = 2$, $\sigma_n^2 = 0.001225$.

The two stability boundaries shown in Fig. 25 can be explained mechanistically by using the analytical results derived in the previous section (eq. 41). The outer boundary marks the case where the second Jury condition, $\bar{w}_p' < \bar{w}_n'$, is violated and predator density at equilibrium has a stronger impact on predator fitness than on prey fitness

(Fig. 29). Although violation of this condition can be prevented by the inducible defense, this is not possible if either the defense is too weak ($a_1 > (a_1)_s$) or the equilibrium induction frequency \bar{d}^* is too close to 0 or 1, which is the case for extreme values of μ (i.e. if μ is too far from P^*). In the latter case, the dynamics converges to those of the basic Nicholson-Bailey model, which is always unstable. The inner boundary marks the case where the third Jury condition, $\bar{w}_p' > \bar{w}_n'/2 - 2/P^*$, is violated and the effect of predator density on predator fitness is too strong relative to the effect on prey fitness (Fig. 29 B). This happens if the prey's population-level reaction norm at equilibrium is too steep, that is for small σ_n^2 and intermediate μ (leading to intermediate \bar{d}^*).

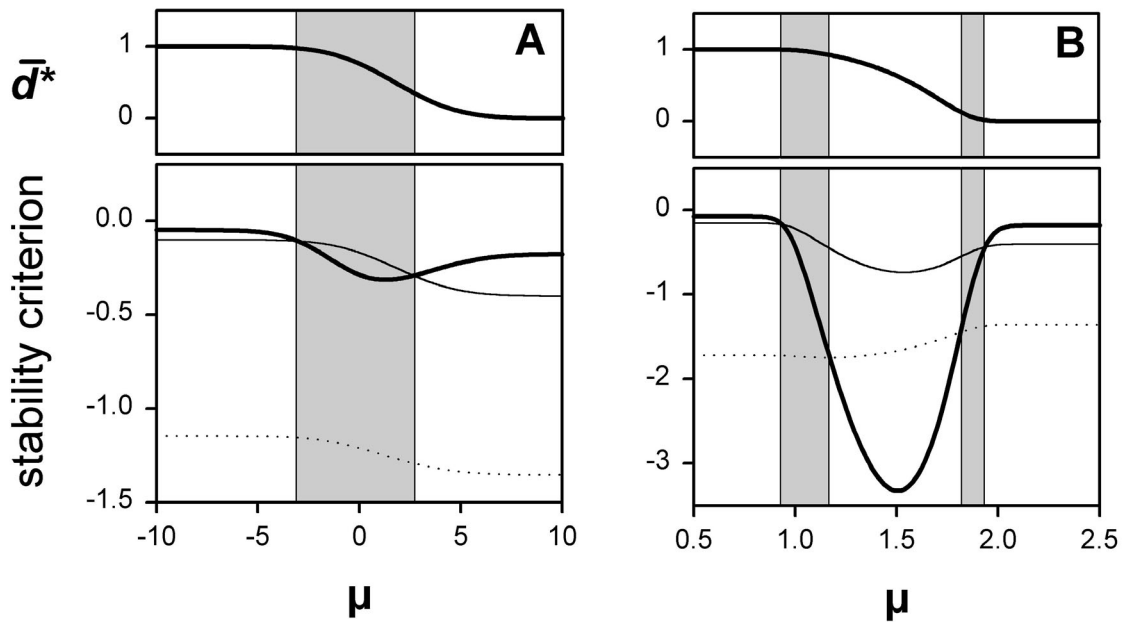


Fig. 29. Model 1 without evolution: Explaining the inner and outer stability boundary.

The two kinds of stability boundaries shown in Fig. 25 can be related to the analytical results summarized in eq. (41). The figures show the equilibrium induction frequency \bar{d}^* , and the quantities \bar{w}_n' (thick solid line), \bar{w}_p' (thin solid line), and $\bar{w}_n'/2 - 2/P^*$ (dotted line) on a gradient of the mean induction threshold μ . In **A**, the parameters are the same as in Fig. 19 at $a_1 = 0.1$, whereas in **B**, the parameters are those of Fig. 25 at $a_1 = 0.15$. The shaded area marks the range of μ where the ecological equilibrium is stable. The outer boundaries of this range (i.e. the outer stability boundaries) are defined by violation of the second Jury condition, $\bar{w}_p' < \bar{w}_n'$ (**A** and **B**), whereas the inner boundaries are defined by violation of the third Jury condition $\bar{w}_p' > \bar{w}_n'/2 - 2/P^*$ (only **A**). Model 1. Parameters: **A**) $a_0 = 0.4$, $a_1 = 0.1$, $b = 0.4$, $c_d = 0.4$, $h_n^2 = 0$, $\lambda = 2$, $\sigma_n^2 = 6.25$. **B**) $a_0 = 0.4$, $a_1 = 0.15$, $b = 0.4$, $c_d = 0.4$, $h_n^2 = 0$, $\lambda = 2$, $\sigma_n^2 = 0.01$.

3.3.3.3 Non-equilibrium population dynamics

Even if the inducible defense cannot completely stabilize the system, predator and prey may coexist by performing non-equilibrium population dynamics. As I shall show, these dynamics can be highly complex, and a full analysis is far beyond the scope of this study. Instead, I will present a series of figures, based on variation in μ , that give an overview of the possible behaviors.

If μ crosses the “outer” stability boundary (see Fig. 25) linear stability analysis predicts stable limit cycles that span several generations (Fig. 30 A; Gurney and Nisbet 1998, pages 60f). In contrast, μ crossing the “inner” stability boundary leads to overcompensation and creates a 2-cycle with the populations alternately overshooting and undershooting the equilibrium (Fig. 30 B). If μ is moved further away from the domain of stability, the system may undergo further bifurcations (qualitative changes of dynamics) that lead to very complex and “chaotic” behavior.

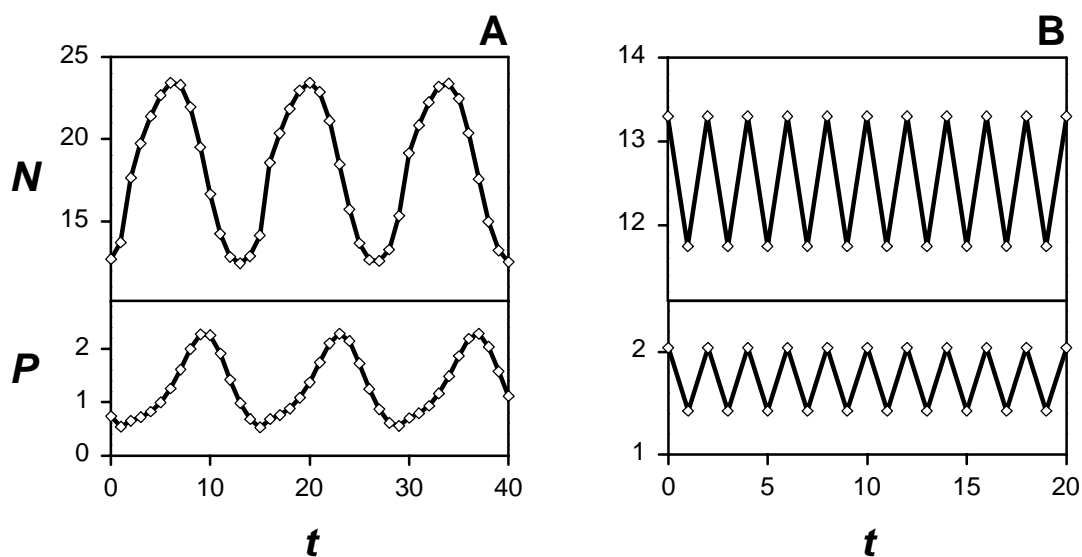


Fig. 30: Model 1 without evolution: Simple types of non-equilibrium dynamics near the domain of ecological stability.

Close to the domain of stability, model 1 (without evolution) displays a regular dynamic behavior. The graphs show prey density N and predator density P as a function of time t . Parameters are those of Fig. 25 at $a_1 = 0.15$. In **A**, $\mu = 0.55$ is outside the outer stability boundary, and the system displays stable limit cycles with a period of several generations. In **B**, $\mu = 1.8$ is inside the inner stability boundary, and the populations undergo regular two-cycles. Model 1. Parameters: $a_0 = 0.4$, $b = 0.4$, $c_d = 0.4$, $h_n^2 = 0$, $\lambda = 2$, $\sigma_n^2 = 0.01$.

Fig. 31 shows some possible attractors in the N vs. P phase plane. An attractor is the set of points (N, P) that the system reaches in its final dynamic state (after transient dynamics have been damped away). For $\mu = 3$, which is inside the domain of stability, the attractor is a single point (N^*, P^*) . After crossing the outer stability boundary, this equilibrium is replaced by a stable limit cycle ($\mu = 4$), which may take the form of a closed curve if its period is an irrational multiple of generation time (i.e. the system never exactly returns to its starting point). A cycle of integer period is shown for $\mu = 4.6$. With further increase in μ , the shape of the cycle becomes distorted. Finally, via a series of period doublings, it evolves to a “strange attractor” that reflects chaotic dynamics.

A more systematic way to display the dynamic behavior of model 1 as a function of μ is to use bifurcation diagrams. For each μ , these diagrams show all values of the predator density P that belong to the respective attractor (bifurcation diagrams using the prey density N instead of the predator density P look qualitatively similar). Fig. 32 shows bifurcation diagrams for a situation without an inner stability boundary. Furthermore, it illustrates the transition from the multiple to the single equilibria case. Fig. 33 shows a bifurcation diagram in a situation with two stability boundaries. Outside the outer stability boundary, the behavior of the system is similar to that shown in Fig. 31. Inside the inner boundary, the dynamics are extremely complex.

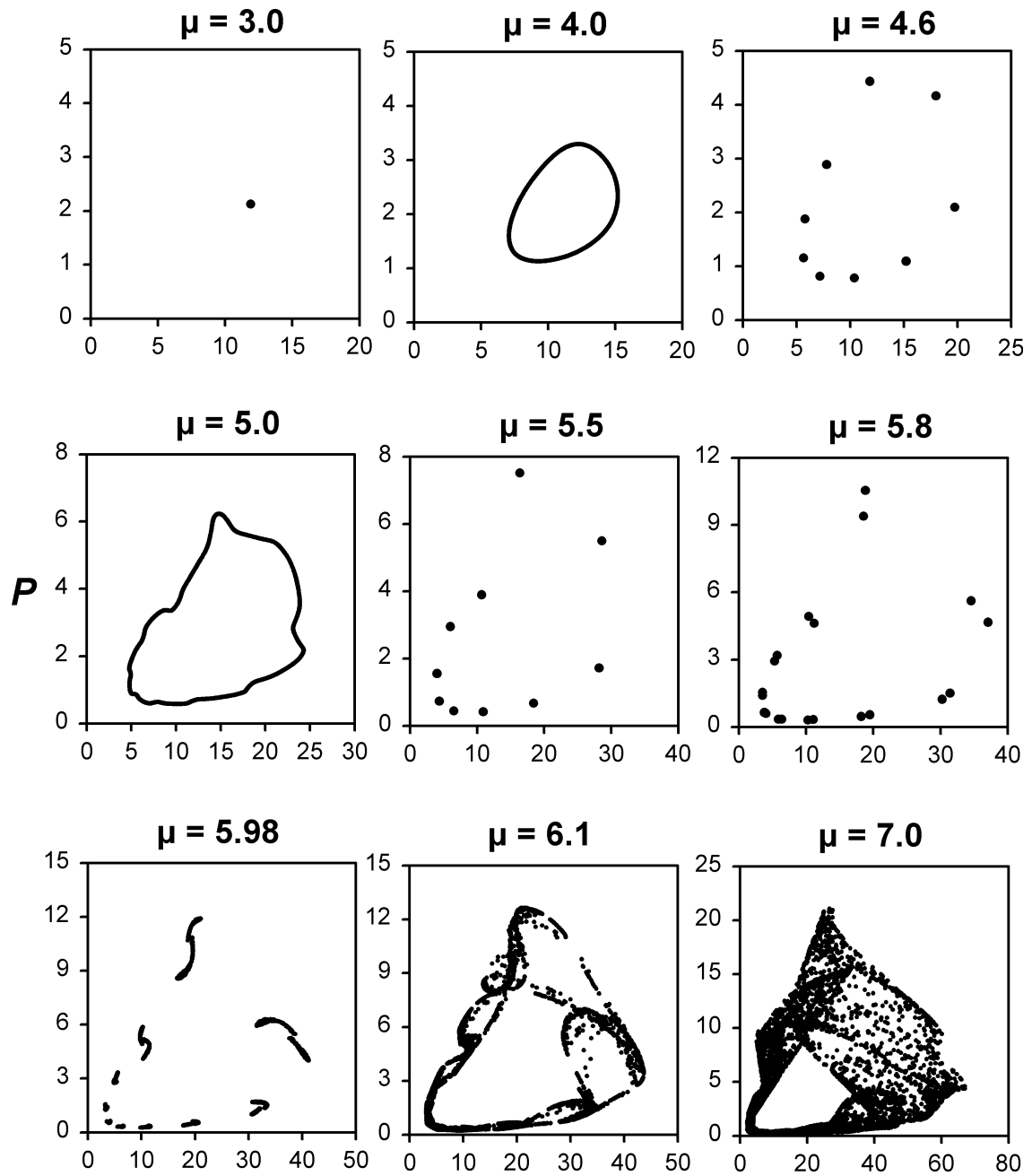


Fig. 31. Model 1 without evolution: Some types of non-equilibrium dynamics on a gradient of μ .

Phase plane diagrams for some types of non-equilibrium dynamic behavior of model 1 without evolution. The graphs show the combinations of prey density N and predator density P that occur in the system after transient dynamics have been damped away. For example, the graph shown for $\mu = 4$ is the phase plane representation of a stable limit cycle similar to the one in Fig. 30 A. As the mean induction threshold μ increases (and, thus, moves away from the domain of ecological stability), the dynamics change from a stable equilibrium (single point) to stable limit cycles with either integer (distinct points) or non-integer / irrational (closed curve) period and, finally, to “chaos” (complex, ragged plot). Model 1. Parameters: $a_0 = 0.4$, $a_1 = 0.1$, $b = 0.4$, $c_d = 0.2$, $h_n^2 = 0$, $\lambda = 2$, $\sigma_n^2 = 4$.

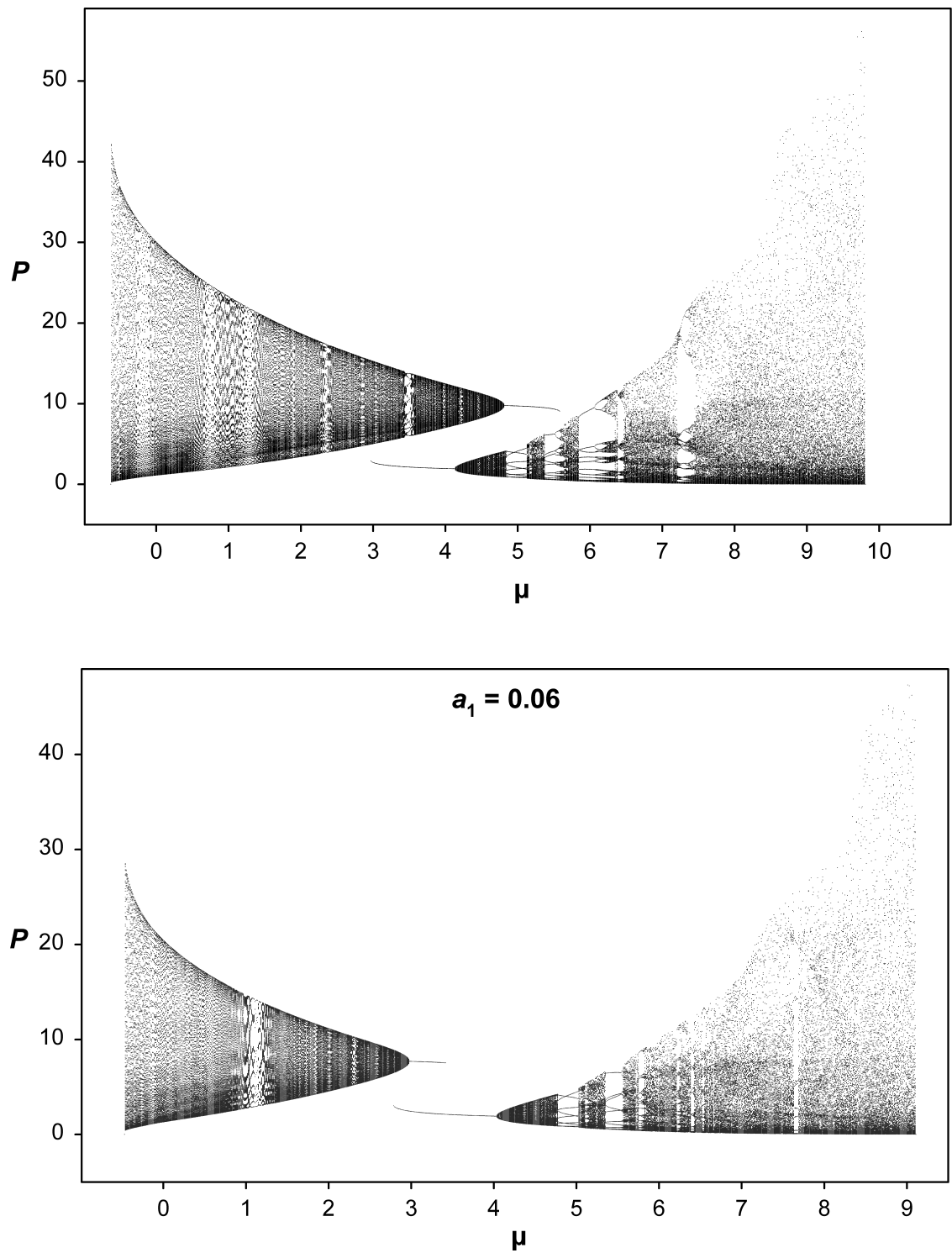


Fig. 32. For legend see next page.

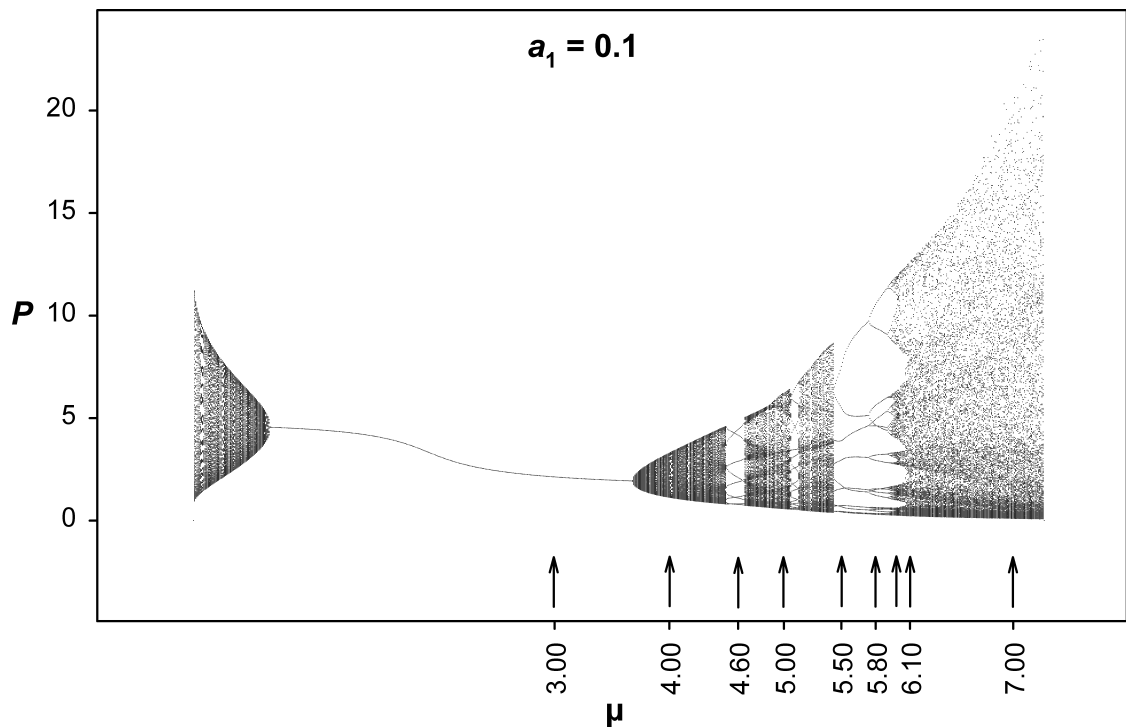


Fig. 32. Model 1 without evolution: Bifurcation diagrams for a situation without an inner stability boundary

Bifurcation diagrams for predator density P as a function of the prey's mean induction threshold μ . The graphs show the predator densities that occur in the system after transient dynamics are damped away. Single lines represent stable equilibria, multiple lines represent cycles with integer period, filled regions with clear-cut boundaries reflect cycles with non-integer or irrational period, and filled regions without clear boundaries point to chaotic dynamics.

The three graphs illustrate the transition from the multiple to the single equilibrium case in a situation with no inner stability boundary (i.e. the domain of stability looks similar to that in Fig. 19). In the first two cases shown, there are two alternative equilibria (the low and the high equilibrium), which are each stable for a certain range of μ before they are replaced by stable limit cycles or some more complex attractor. Both equilibria can be stable simultaneously for $a_1 = 0.06$, but not for $a_1 = 0.0475$. For $a_1 = 0.1$ (which is greater than $(a_1)_b$), the two equilibria have fused to yield a single equilibrium, which is stable for intermediate μ and unstable for low or high μ . The amplitude of the oscillations increases as μ is moved away from the domain of ecological stability. The arrows in the third figure point to the cases shown in Fig. 31. Model 1. Parameters: $a_0 = 0.4$, $b = 0.4$, $c_d = 0.2$, $h_n^2 = 0$, $\lambda = 2$, $\sigma_n^2 = 4$.

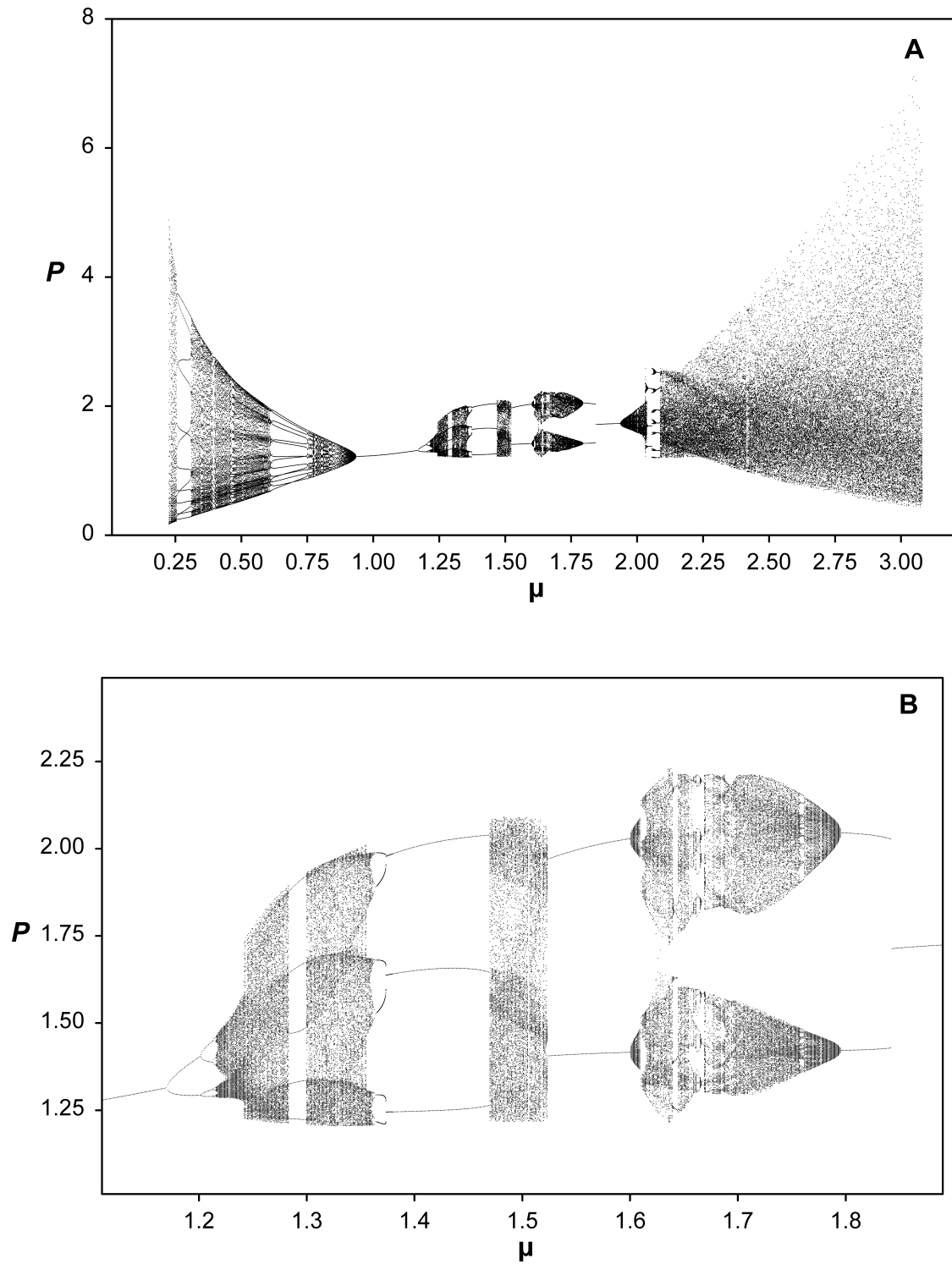


Fig. 33. For legend see next page.

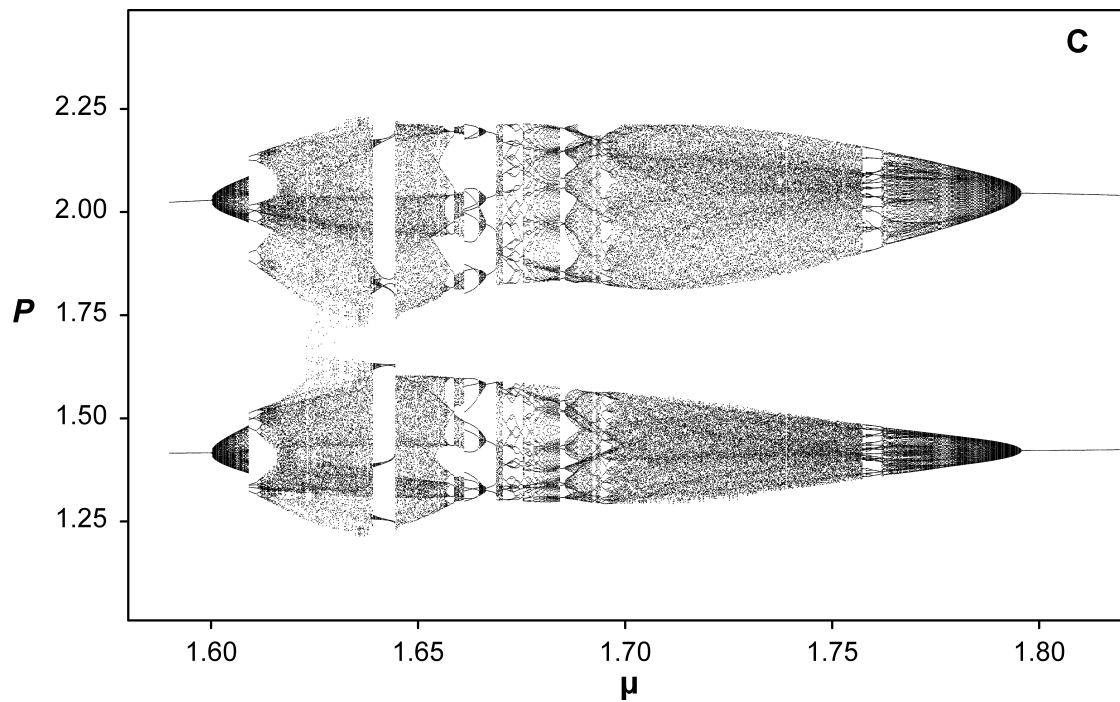


Fig. 33. Model 1 without evolution: Bifurcation diagrams for a situation with an inner stability boundary. Bifurcation diagrams for predator density P as a function of the prey's mean induction threshold μ (see Fig. 32) in a situation with an inner stability boundary, but outside the domain of multiple ecological equilibria. The graphs highlight the wealth of complex non-equilibrium behavior that may be observed outside the domain of ecological stability. Parameters are those of Fig. 25 at $a_1 = 0.15$. In **A**, the full range of μ is shown. **B** shows the range inside the inner stability boundary in greater detail, and **C** is a magnification of the “right-hand” part of this range. Model 1. Parameters: $a_0 = 0.4$, $a_1 = 0.15$, $b = 0.4$, $c_d = 0.4$, $h_n^2 = 0$, $\lambda = 2$, $\sigma_n^2 = 0.01$.

3.3.3.4 Evolution

3.3.3.4.1 Evolutionary stability of model 1

As shown in section 3.3.3.1.1, model 1 has an evolutionary equilibrium only if $a_1 = \hat{a}_1$ (eq. 32), because only in this case, the condition $w_{n0} = w_{n1} = 1$ can be satisfied (see Fig. 9 C). If $a_1 = \hat{a}_1$, an evolutionary equilibrium exists for each value of the mean induction threshold μ , with $\hat{P} = P^* = \ln(1 - c_d)/(a_1 - a_0)$ being independent of μ and N^* increasing with decreasing μ .

Linear stability analysis for this equilibrium (see eq. 10) yields the following results: First, it is easy to show that at equilibrium

$$\begin{aligned} \frac{\partial N_{t+1}}{\partial N_t} &= \frac{\partial N_t \bar{w}_n}{\partial N_t} = \bar{w}_n = 1 \\ \frac{\partial \mu_{t+1}}{\partial N_t} &= 0 \\ \frac{\partial N_{t+1}}{\partial \mu_t} &= 0 \\ \frac{\partial \mu_{t+1}}{\partial \mu_t} &= 1 \end{aligned} \tag{42}$$

The first two equalities reflect the lack of density-dependence in the prey, whereas the last two equalities are due to the fact that at equilibrium, both prey types have the same fitness. Consequently, the Jacobian is of the form

$$J^* = \begin{pmatrix} 1 & J_{12} & 0 \\ J_{21} & J_{22} & J_{23} \\ 0 & J_{32} & 1 \end{pmatrix}. \tag{43}$$

It follows directly from the characteristic polynomial that any such matrix has one eigenvalue equal to 1. In consequence, the linearized version of the model is either unstable, or – if the other two eigenvalues have magnitude less than 1 – neutrally stable. In

the latter case, stability of the full non-linear model must be investigated by numerical simulations. These simulations show that an equilibrium indeed is reached, but its exact location (in terms of the values of N^* and μ^*) depends upon the initial conditions.

3.3.3.4.2 Non-equilibrium dynamics of model 1 with evolution

In the general case $a_1 \neq \hat{a}_1$, model 1 does not have an evolutionary equilibrium. However, non-equilibrium dynamics may lead to infinite persistence of the system if the mean induction threshold μ is kept at intermediate values by cyclic evolutionary dynamics.

In the following, I will give a preliminary analysis of this scenario. I will focus on parameter combinations that ensure an high overall stability of the system. In particular, I will consider the case $\sigma_n^2 = 1$ and $c_d = 0.4$.

With evolution (i.e. $h_n^2 > 0$) the simplest behavior of the system is a stable limit cycle where predator-prey oscillations drive cyclical changes in the mean induction threshold μ . An example is provided in Fig. 34: μ increases when $P < \hat{P}$ and decreases when $P > \hat{P}$ (\hat{P} is the predator density where both prey types have equal fitness, see eq. 31). The stabilizing action of this negative feedback between μ and P is further illustrated in Fig. 35.

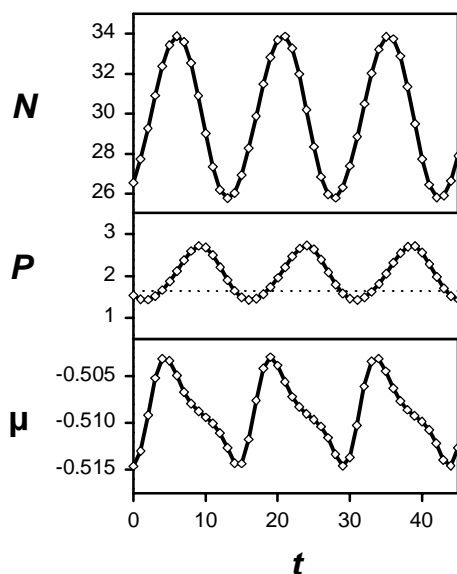


Fig. 34. Model 1 with evolution: Stable limit cycles.

Prey density N , predator density P , and the prey's mean induction threshold μ as a function of time t . Phenotypic plasticity is maintained, because predator-prey cycles drive corresponding cycles in μ . μ decreases when P is high, but increases again whenever P drops below the threshold density \hat{P} (dotted line, see eq. 31). Model 1. Parameters: $a_0 = 0.4$, $a_1 = 0.09$, $b = 0.4$, $c_d = 0.4$, $h_n^2 = 1$, $\lambda = 2$, $\sigma_n^2 = 1$.

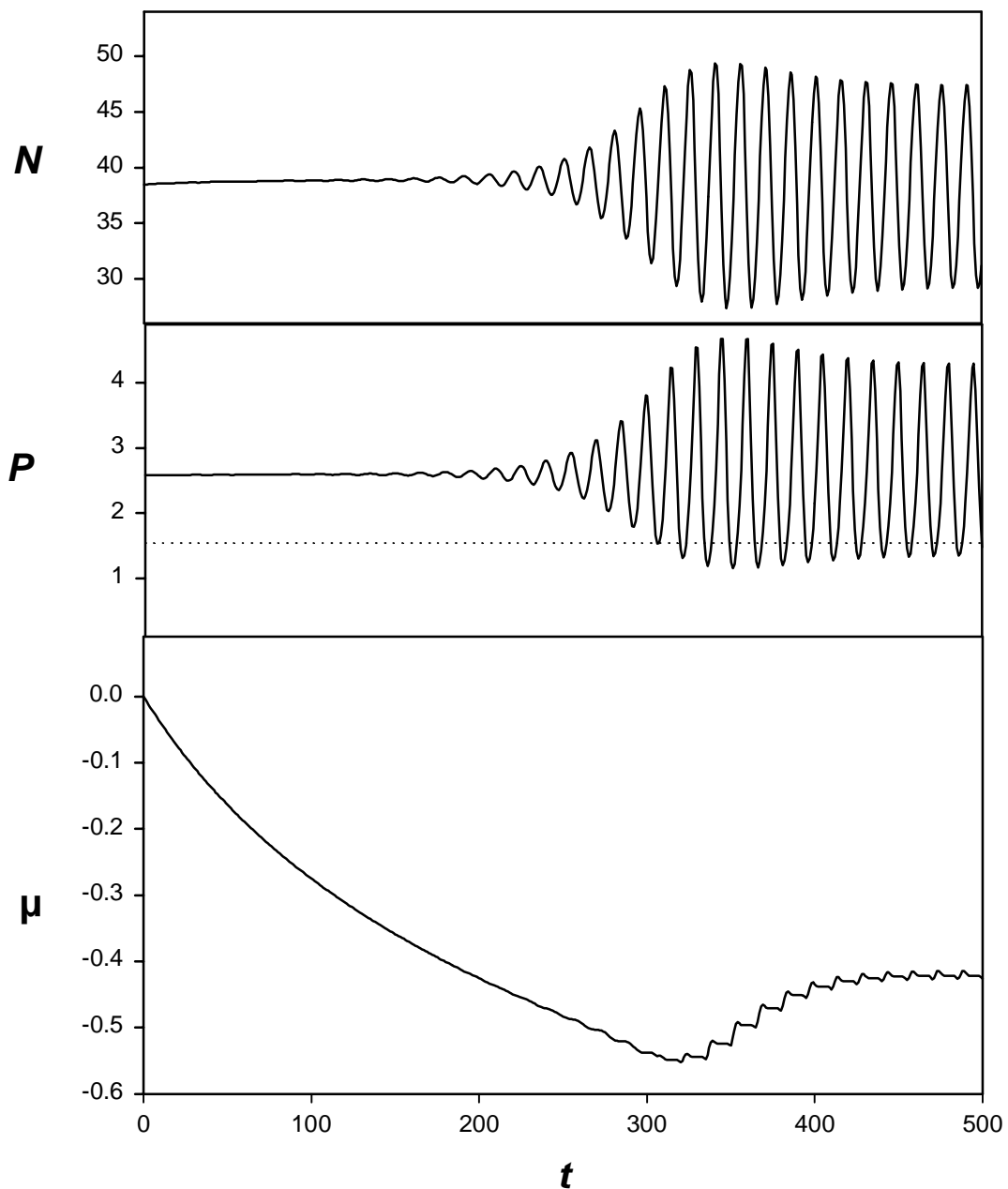


Fig. 35. Model 1 with evolution: Stabilization of the prey's induction threshold by predator-prey cycles.

The Figure illustrates the interaction between predator-prey dynamics and the evolutionary dynamics of the prey's induction threshold. Prey density N , predator density P , and the prey's mean induction threshold μ are displayed as a function of time t . At the beginning of the simulation, predator and prey are at the ecological equilibrium for $\mu = 0$. When evolution is "switched on" μ starts to decrease, because defended prey have a higher fitness than undefended prey (as $P^* > \hat{P}$, see eq. 31). In consequence, the population dynamics are destabilized and the stable equilibrium is replaced by predator-prey cycles. Continuing decrease of μ results in an increase in the amplitude of the cycles, until predator density temporarily falls below \hat{P} (dotted line). Thus, the decrease of μ is stopped, and the dynamics converge to a stable limit cycle. (It should be noted that transient dynamics may be more complex than in this example!) Model 1. Parameters: $a_0 = 0.4$, $a_1 = 0.07$, $b = 0.4$, $c_d = 0.4$, $h_n^2 = 1$, $\lambda = 2$, $\sigma_n^2 = 1$.

The oscillations considered so far have been restricted to the ecological time-scale, that is the time scale of predator-prey cycles. However, the model may display more complex dynamics, too. In particular, the ecological-scale cycles may be superimposed by higher-order cycles that arise at a larger, evolutionary time-scale. Two examples are depicted in the following figures. Fig. 36 shows low-amplitude evolutionary-scale cycles that shift the location of the ecological cycles. These cycles seem to prevail if a_1 is either very small or very large. In Fig. 37, large-amplitude evolutionary-scale cycles drive the system into and out of the domain of ecological stability, leading to “pulsed” oscillations. Dynamics of this kind can be observed for $\sigma_n^2 > 1$ and a_1 close to \hat{a}_1 . Evolutionary-scale cycles are also frequently observed in transient dynamics.

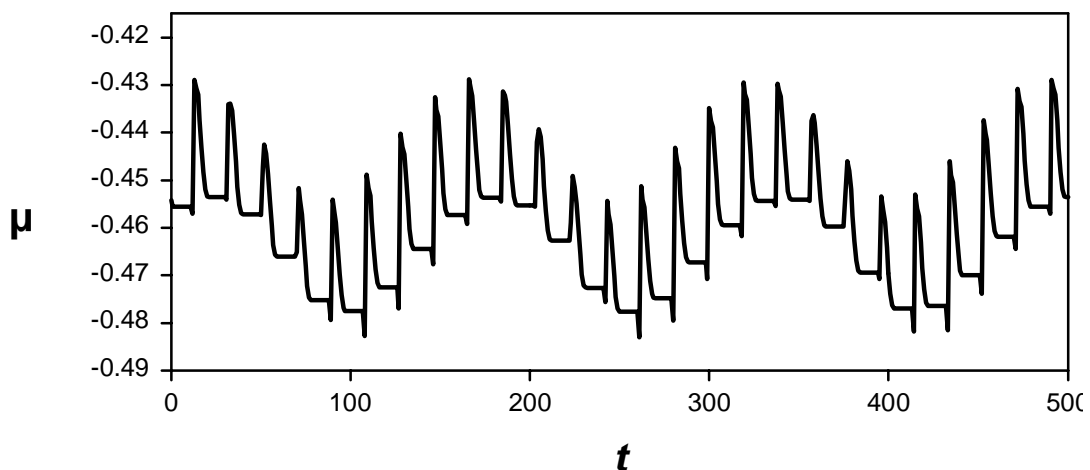


Fig. 36. Model 1 with evolution: Ecological-scale cycles in μ superseded by evolutionary-scale cycles.

Dynamics of the mean induction threshold μ as a function of time t . Parameters are those of Fig. 34, except for a_1 which now equals 0.01. Cycles at the time-scale of predator-prey cycles (see Fig. 34) are superimposed by low-amplitude cycles at a larger, evolutionary time-scale. The population dynamics of predator and prey (not shown) follow a similar pattern. Model 1. Parameters: $a_0 = 0.4$, $a_1 = 0.01$, $b = 0.4$, $c_d = 0.4$, $h_n^2 = 1$, $\lambda = 2$, $\sigma_n^2 = 1$.

Fig. 38 shows the location of stable limit cycles as a function of the parameter a_1 . For $a_1 < \hat{a}_1$, the average value of μ is low (corresponding to high induction frequencies \bar{d}) and the average prey population density N is high. The cycles decrease in amplitude as a_1 approaches \hat{a}_1 and, for $a_1 = \hat{a}_1$, converge to an equilibrium point with μ at the lower boundary of the region of neutral stability. When a_1 is increased further, another set of limit cycles starts off from the upper boundary of this stability region with high average

values of μ and low values of \bar{d} and N . For a_1 between about 0.03 and 0.14, the cycles are of the type shown in Fig. 34 (ecological time-scale only). For smaller or larger a_1 , there are cycles like those shown in Fig. 36 (ecological and evolutionary scale). For $a_1 < 0.01$ (not shown in Fig. 38) the dynamics are truly chaotic, with extremely high maximal values of N and P , and the curves delimiting the range of μ become “ragged”. Finally, for $a_1 \rightarrow 0$ or $a_1 > 0.17$ the predator population goes extinct.

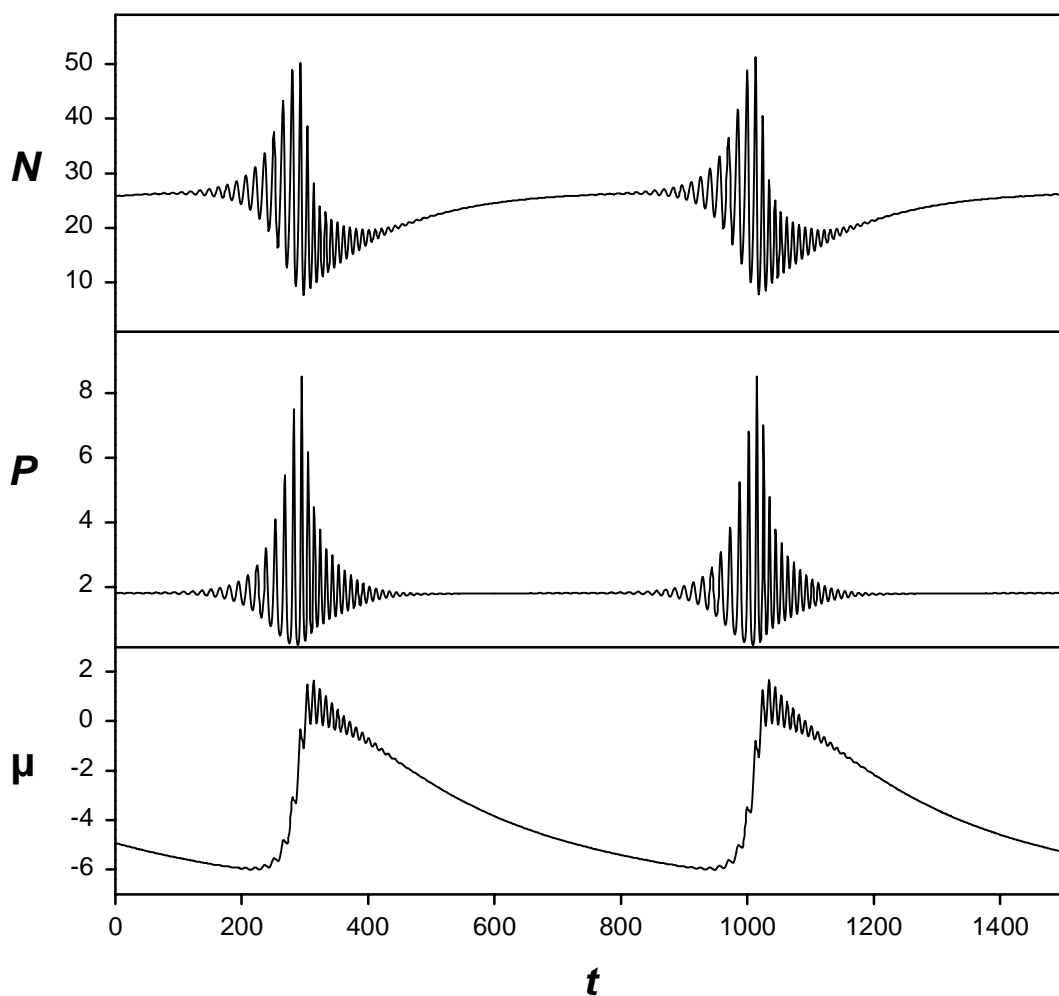


Fig. 37. Model 1 with evolution: Pulsed dynamics due to evolutionary-scale cycles.

Prey density N , predator density P , and the prey’s mean induction threshold μ as a function of time t . Large-amplitude evolutionary-scale cycles drive the system into and out of the domain of ecological stability, leading to “pulsed” oscillations at the ecological time-scale. Model 1. Parameters: $a_0 = 0.4$, $a_1 = 0.1$, $b = 0.4$, $c_d = 0.4$, $h_n^2 = 1$, $\lambda = 2$, $\sigma_n^2 = 12.25$.

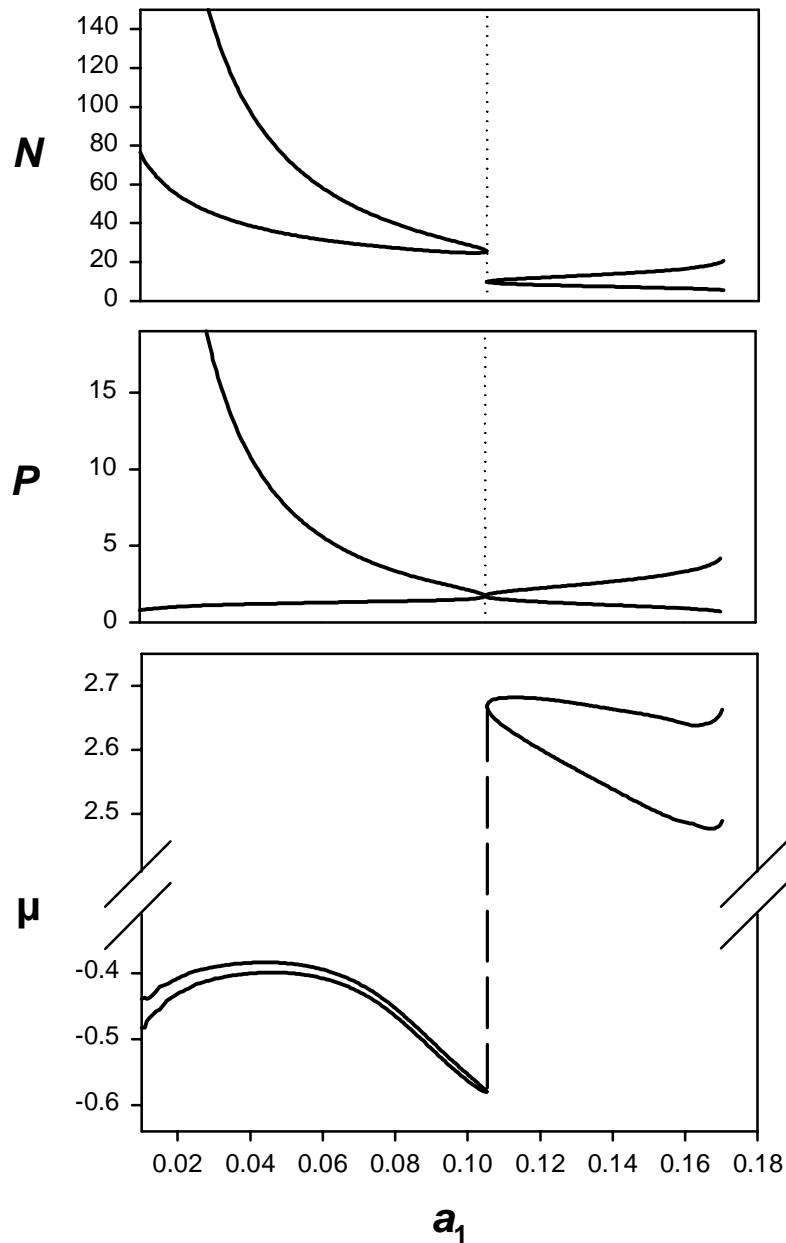


Fig. 38. Model 1 with evolution: Bifurcation diagrams

Overview of the dynamic behavior of model 1 with evolution as a function of the defense parameter a_1 . The figure shows the maximal and minimal values of N , P , and μ that occur in the system after transient dynamics have been damped away. N is prey density, P is predator density, and μ is the prey's mean induction threshold. In most cases, the dynamics are stable limit cycles spanning the range indicated in the plots (see Fig. 34). For very small or very large a_1 , the dynamics are more like those shown in Fig. 36. For $a_1 < 0.01$ (not shown), the system behaves in a truly chaotic manner, and the maximal population densities tend towards infinity.

The dotted line in the first two plots marks \hat{a}_1 , the value of a_1 where undefended and defended prey have equal fitness at the ecological equilibrium (eq. 32). This is the only case where an evolutionary equilibrium is possible. The evolutionary equilibrium is neutrally stable in the range of μ indicated by the dashed line. For $a_1 < \hat{a}_1$, the system displays cycles with low average μ (i.e. high average induction frequencies) and high average N . The reverse is true for $a_1 > \hat{a}_1$. Model 1. Parameters: $a_0 = 0.4$, $b = 0.4$, $c_d = 0.4$, $h_n^2 = 1$, $\lambda = 2$, $\sigma_n^2 = 1$.

3.3.4 Model 2: Plasticity in both prey and predator

3.3.4.1 Model 2 without evolution

An in depth analysis of model 2 without evolution (i.e. $h_n^2 = h_p^2 = 0$) is beyond the scope of this study. Here, I will only mention two aspects.

3.3.4.1.1 Multiple ecological equilibria

The addition of phenotypic plasticity in the predator increases the maximal number of alternative ecological equilibria – already three in model 1 – to five. Such a case is shown in Fig. 39, where $\bar{w}_n = 1$ has five solutions. However, this scenario seems to require very low values of both σ_n^2 and σ_p^2 . For most other parameter combination, there are either three equilibria or one. I will not pursue this question in further detail here.

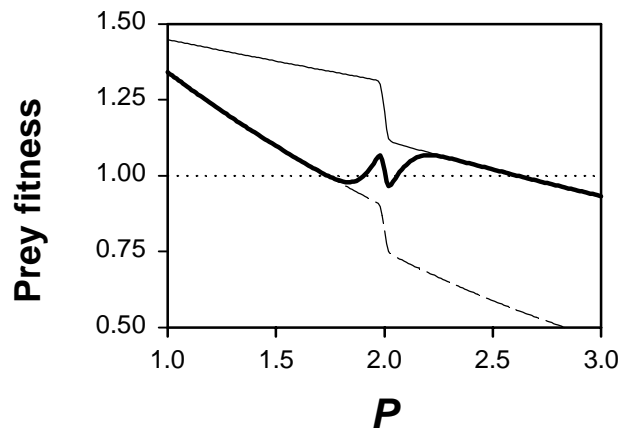


Fig. 39. Model 2 without evolution: 5 alternative ecological equilibria

In extreme cases, the combination of an inducible defense and an inducible counter-offense gives rise to five alternative ecological equilibria. The figure shows w_{n0} , the fitness of undefended prey (dashed line), w_{n1} , the fitness of defended prey (thin solid line), and \bar{w}_n , the mean fitness of the prey (thick solid line) as a function of predator density P . Note that $\bar{w}_n = 1$ has five solutions. Model 2. Parameters: $a_{00} = 0.4$, $a_{10} = 0.1$, $a_{01} = 0.49$, $a_{11} = 0.18$, $b = 0.4$, $c_d = 0.2$, $c_o = 0.2$, $h_n^2 = 0$, $h_p^2 = 0$, $\lambda = 2$, $\mu = 2$, $\nu = 2$, $\sigma_n^2 = 0.01$, $\sigma_p^2 = 0.0025$.

3.3.4.1.2 Ecological stability

In this section, I will give a brief overview of the effects that the predator's counter-offense can have on the stability of the predator-prey dynamics. I will focus on how the offense influences the capacity of the defense to stabilize the interaction.

For model 1, I have measured this capacity by means of the quantity $(a_1)_s$, the maximal value of a_1 that permits a stable equilibrium for appropriate values of μ (see Fig. 19). Similarly, I now define $(a_{10})_s$ as the maximal value of a_{10} that permits stability for appropriate μ in model 2. In the following, I will investigate how $(a_{10})_s$ is influenced by the inducible offense, in particular by the parameters a_{11} and c_o . I will not investigate the effect of v and σ_p^2 , but instead restrict myself to the case $v = 0.5$ and $\sigma_p^2 = 0.25$. In order to keep the following discussion as simple as possible, I will temporarily relax the assumption $a_{11} \geq 1/(1-c_o)$ (eq. 17) and only require $0 \leq a_{10} \leq a_{11} \leq a_{00}$. This does not change the conclusions of the analysis but avoids an additional source of complication.

Fig. 40 A shows $(a_{10})_s$ as a function of a_{11} . Together with the lines $a_{10} = a_{11}$, $a_{11} = a_{00}$ and $a_{10} = 0$, the graph of $(a_{10})_s$ delimits the domain in the a_{11} versus a_{10} plane where ecological stability is possible for appropriate values of μ . $(a_{10})_s$ decreases with a_{11} , which means that stability is not possible if the defense is too weak or the counter-offense is too strong.

The overall effect of the offense can be seen by comparing $(a_{10})_s$ with $(a_1)_s$ in the corresponding model 1 (i.e. model 1 with $a_0 = a_{00}$ and $a_1 = a_{10}$). As shown in Fig. 40 A, the offense tends to increase stability (i.e. $(a_{10})_s > (a_1)_s$) if a_{11} is small, but tends to decrease stability if a_{11} is large. Furthermore, Fig. 40 B shows that $(a_{10})_s$, and hence the stabilizing tendency, decreases as the cost parameter c_o increases.

These results demonstrate that the inducible offense can affect stability of the predator-prey dynamics in two different ways. On the one hand, it tends to have a destabilizing impact, because it reduces the stabilizing effect of the prey's defense. On the other hand, it tends to stabilize the interaction by imposing fitness costs on the predator in a density

dependent manner ($\bar{\sigma}$ ultimately is a function of P). Which of the two effects prevails depends on the relative magnitude of the parameters a_{11} and c_o . The destabilizing effect of predation efficiency increases with a_{11} , whereas the stabilizing effect of costs increases with c_o . Furthermore, stabilization due to the offense costs requires that the realized plasticity in the predator population is greater than zero. For $\sigma_p^2 \rightarrow \infty$, $(a_{10})_s \leq (a_1)_s$ for all a_{11} , with $(a_{10})_s = (a_1)_s$ for $a_{10} = a_{11}$ (not shown in Fig. 40).

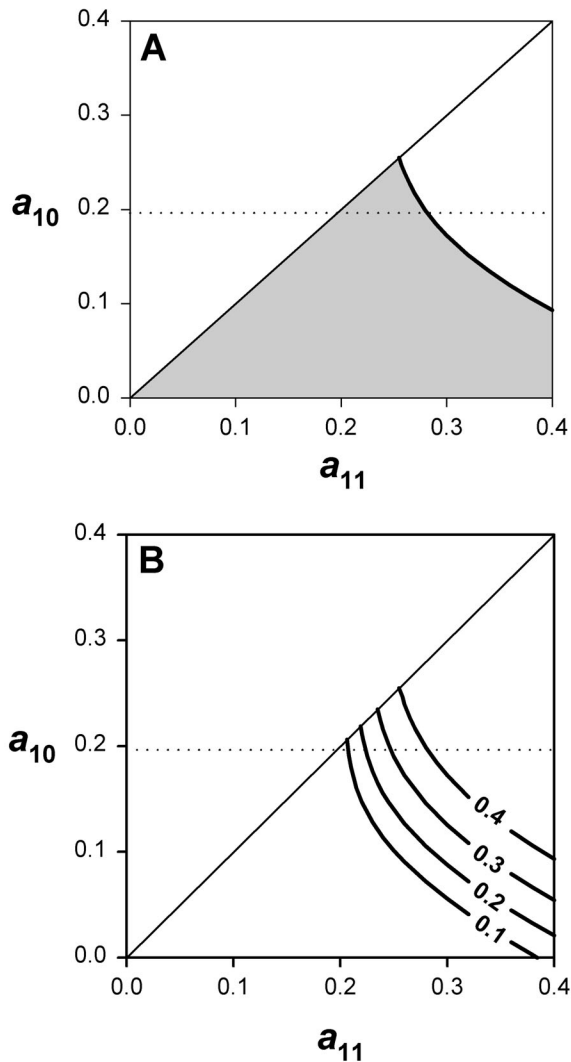


Fig. 40. Model 2 without evolution: The impact of the counter-offense on the stabilizing effect of the prey's defense.

Potential stability of model 2 (without evolution) as a function of the defense parameter a_{10} and the counter-offense parameter a_{11} . a_{10} is the success rate of non-induced predators feeding on defended prey, and a_{11} is the success rate of induced predators feeding on defended prey. Only cases where $a_{11} > a_{10}$ are considered. In **A**, the shaded area marks the domain in the a_{11} versus a_{10} plane where an ecological equilibrium is stable for appropriate values of the prey's mean induction threshold μ . The thick solid line marks $(a_{10})_s$, the maximal value of a_{10} where stability is possible for some μ . The dotted line shows the same value for the case that the counter-offense is completely absent (i.e. $v \rightarrow \infty$). This value is equivalent to $(a_1)_s$ in the corresponding model 1 (see Fig. 19). In **B**, $(a_{10})_s$ is compared for four different values of the offense costs c_o . The results show that the stabilizing power of the defense is increased with respect to model 1 if the counter-offense is weak and the offense costs are high, and decreased if the counter-offense is strong and the costs are low. Model 2. Parameters: $a_{00} = 0.4$, $a_{01} = 0.4$, $b = 0.4$, $c_d = 0.4$, $c_o = 0.4$ (**A**), $h_n^2 = 0$, $h_p^2 = 0$, $\lambda = 2$, $v = 0.5$, $\sigma_n^2 = 1$, $\sigma_p^2 = 0.25$.

When interpreting the above results, it is important to keep in mind that $(a_{10})_s$ and $(a_1)_s$, respectively, do not necessarily reflect the overall size of the domain of ecological stability. In contrast, as shown in Fig. 22 and 23, $(a_1)_s$ may increase while the size of the domain of ecological stability decreases. Therefore, the results should be viewed as revealing two potential mechanisms affecting stability without allowing to assess their respective importance.

3.3.4.2 The evolutionary equilibrium

In contrast to model 1, model 2 generally has an evolutionary equilibrium. This equilibrium is possible because the existence of two prey phenotypes allows for coexistence of the two predator phenotypes and vice versa. The equilibrium conditions $w_{n0} = w_{n1} = 1$ and $w_{p0} = w_{p1} = 1$ can be solved analytically to yield expressions for N^* , P^* , \bar{d}^* , and \bar{o}^* . The equilibrium induction thresholds μ^* and ν^* can then be obtained numerically from these values and the cumulative normal distribution.

In the following, I will frequently discuss the equilibrium in terms of the induction frequencies \bar{d}^* and \bar{o}^* , rather than the induction thresholds μ^* and ν^* . Note that \bar{d}^* and \bar{o}^* are independent of the genetic mechanism that creates the alternative phenotypes in prey and predator, respectively. In particular, \bar{d}^* and \bar{o}^* are independent of the parameters σ_n^2 , σ_p^2 , h_n^2 , and h_p^2 .

Here, I will only present analytical results for P^* and \bar{o}^* , as the expressions for N^* and \bar{d}^* are cumbersome and non-instructive:

$$P^* = \frac{r_0(a_{11} - a_{10}) - r_1(a_{01} - a_{00})}{a_{00}a_{11} - a_{01}a_{10}} \quad \text{with} \quad \begin{aligned} r_0 &= \ln \lambda \\ r_1 &= \ln(\lambda(1 - c_d)) \end{aligned} \quad (44)$$

$$\bar{o}^* = \frac{r_0 a_{10} - r_1 a_{00}}{r_0(a_{11} - a_{10}) - r_1(a_{01} - a_{00})}$$

In all of the following, I will only discuss the case $a_{01} = a_{00}$ (no effect of the offense if the prey is undefended). Thus, the above expressions simplify to

$$P^* = \frac{\ln(\lambda)}{a_{00}} \quad (45)$$

$$\bar{d}^* = \frac{r_0 a_{10} + r_1 a_{00}}{r_0 (a_{11} - a_{10})}$$

These results allow to determine the conditions for the existence of the evolutionary equilibrium. The equilibrium exists if \bar{d}^* is between 0 and 1, which is the case for

$$a_{10} \leq a_{00} \cdot r_1 / r_0 \leq a_{11}. \quad (46)$$

(Note that \bar{d}^* is between 0 and 1 if the conditions given in eq. (18) are satisfied.)

In the following, I will frequently display results in an a_{10} versus a_{11} plane (and for constant $a_{00} = a_{01}$). Combining eq. (46) with the restrictions given in eq. (18) yields:

$$0 \leq a_{10} \leq a_{00} \cdot r_1 / r_0 \quad (47)$$

$$\max(a_{00} \cdot r_1 / r_0, a_{00} / (1 - c_o)) \leq a_{11} \leq a_{00}$$

These conditions define the domain in the a_{10} versus a_{11} plane where the parameter values are in accordance with the basic model assumptions (in particular with regard to the trade-off in the predator) *and* an evolutionary equilibrium is possible (Fig. 41). I will call this domain the domain of evolutionary equilibrium.

Fig. 42 shows how the equilibrium values N^* , \bar{d}^* , and \bar{o}^* depend on the parameters a_{10} and a_{11} . I will explain the results one by one: First, as w_{n0} depends only on P , a_{00} , and λ , and because P^* must be the solution to $w_{n0} = 1$, $P^* = \ln(\lambda) / a_{00}$ is independent of both a_{10} and a_{11} (not shown in Fig. 42). Second, for given P^* , fulfillment of the condition $w_{n0} = w_{n1}$ depends solely on the predator's induction frequency \bar{o} . The condition is fulfilled if the offense neutralizes the benefit of the defense. As the benefit of the de-

fense increases with decreasing a_{10} and a_{11} , so does \bar{o}^* . \bar{o}^* equals 0 for $a_{10} = a_{00} \cdot r_1 / r_0$ and equals 1 for $a_{11} = a_{00} \cdot r_1 / r_0$. Third, for given P^* and \bar{o}^* , fulfillment of the condition $w_{p0} = w_{p1}$ depends on the prey's induction frequency \bar{d}^* . The benefit of the offense can be reduced by decreasing \bar{d}^* . As the benefit of the offense increases with increasing a_{10} and increasing a_{11} , \bar{d}^* must decrease with these parameters. \bar{d}^* equals 1 for $a_{11} = a_{10} / (1 - c_o)$. (Furthermore, $\bar{d}^* = 0$ for $a_{01} = a_{00} / (1 - c_o)$, but this case has not been investigated here.) Fourth and finally, N^* is the density of prey needed to sustain a predator population of density P^* for given \bar{o}^* and \bar{d}^* . N^* decreases with increasing predation efficiency, which is determined by a_{10} and a_{11} as well as by \bar{o}^* and \bar{d}^* . All effects combined, N^* decreases strongly with a_{11} and increases slightly with a_{10} . Thus, it is roughly proportional to \bar{d}^* .

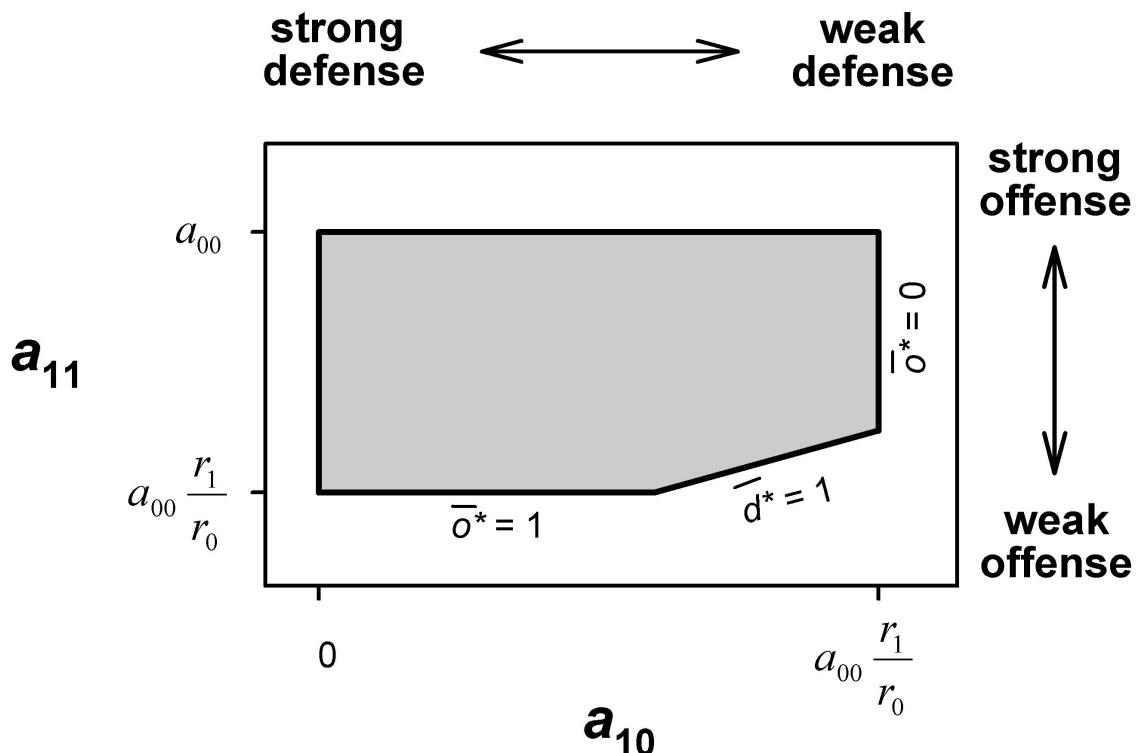


Fig. 41. Model 2 with evolution: The domain of evolutionary equilibrium

Schematic representation of the domain in the a_{10} versus a_{11} plane where (1) an evolutionary equilibrium exists and (2) both the defense and the offense are subject to a fitness trade-off (see eq. 47; shaded area). In addition, extreme values of the equilibrium induction frequencies of predator and prey, \bar{o}^* and \bar{d}^* , are given. See text for further details.

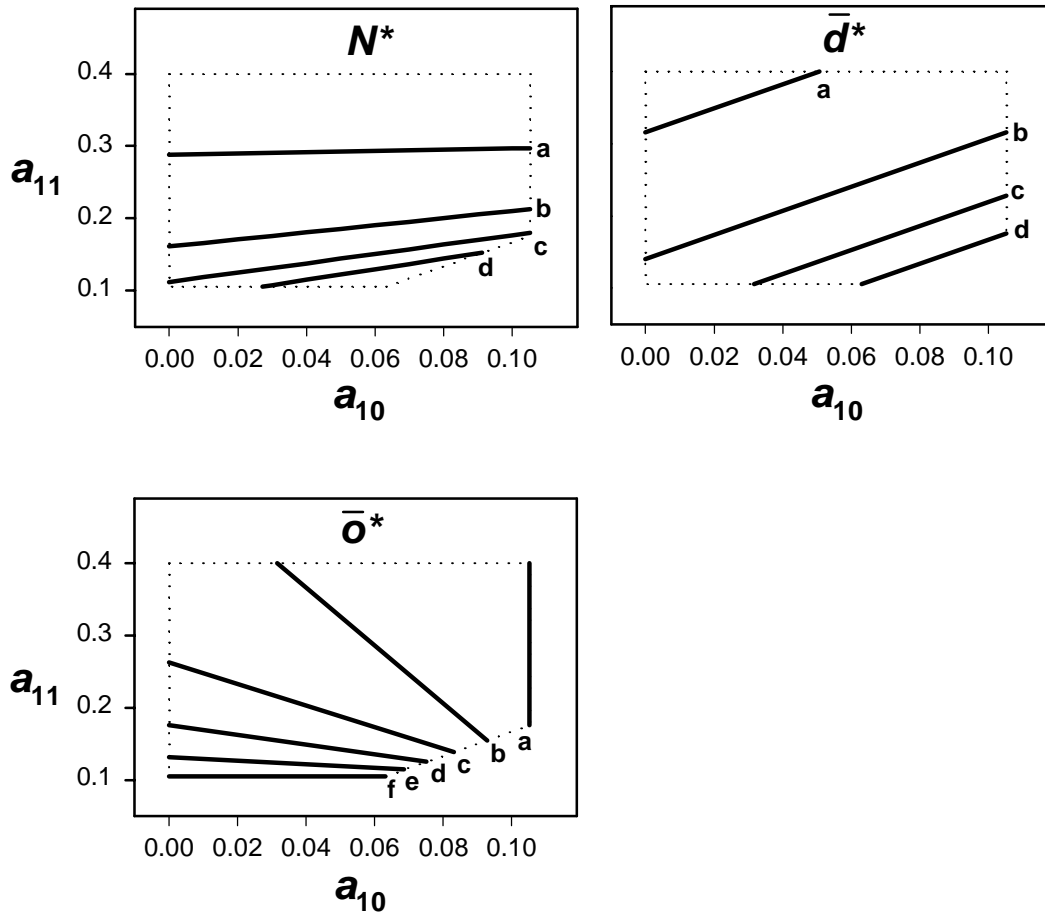


Fig. 42. Model 2 with evolution: The evolutionary equilibrium

Isoclines for the equilibrium induction frequencies of predator and prey, \bar{o}^* and \bar{d}^* , respectively, and for the equilibrium prey density N^* in the a_{10} versus a_{11} plane. Values of \bar{o}^* are **a**) 0.0, **b**) 0.2, **c**) 0.4, **d**) 0.6, **e**) 0.8, **f**) 1.0. Values for \bar{d}^* are **a**) 0.4, **b**) 0.6, **c**) 0.8, **d**) 1.0. Values for N^* are **a**) 15, **b**) 20, **c**) 25, **d**) 30. The equilibrium density of the predator, $P^* = 1.7329$, is independent of a_{10} and a_{11} .

The dotted line marks the domain of evolutionary equilibrium (see Fig. 41). a_{10} is the success rate of non-induced predators feeding on defended prey, and a_{11} is the success rate of induced predators feeding on defended prey. Model 2. Parameters: $a_{00} = 0.4$, $a_{01} = 0.4$, $b = 0.4$, $c_d = 0.4$, $c_o = 0.4$, $h_n^2 = 1$, $h_p^2 = 1$, $\lambda = 2$.

The limiting cases $a_{10} = a_{00} \cdot r_1 / r_0$ (i.e. $\bar{o}^* = 0$) and $a_{11} = a_{00} \cdot r_1 / r_0$ (i.e. $\bar{o}^* = 1$) can be reached only asymptotically, because they require $v^* \rightarrow \infty$ or $v^* \rightarrow -\infty$, respectively. As, in these cases, only one predator morph is present, the model reduces to a version of model 1. This model 1 has parameters $a_0 = a_{00}$ and $a_1 = a_{10}$ in the first case, and $a_0 = a_{01} = a_{00}$, $a_1 = a_{11}$, and $b_{\text{model 1}} = b_{\text{model 2}} \cdot (1 - c_o)$ in the second case. In both cases, $a_{00} \cdot r_1 / r_0 = a_0 \cdot r_1 / r_0$ is equivalent to \hat{a}_1 as defined in eq. (32). Hence, the condition

$a_1 = \hat{a}_1$ is satisfied, and an evolutionary equilibrium is possible. μ^* and \bar{d}^* , which are not uniquely defined in model 1 (see section 3.3.3.4.1), can be derived from the original model 2.

The limiting case $a_{11} = a_{10} / (1 - c_o)$ (i.e. $\bar{d}^* = 1$) can be reached asymptotically if $\mu^* \rightarrow \infty$. In this case, the model reduces to a Nicholson-Bailey model with one prey and two predator types, but without phenotypic plasticity.

In contrast to the ecological equilibria, the evolutionary equilibrium is unique. Furthermore, the associated ecological equilibrium (i.e. the ecological equilibrium for $\mu = \mu^*$ and $v = v^*$) is also unique. This can be seen from the fact that both w_{n0} and w_{n1} are strictly monotonically decreasing functions of P . Thus, because \bar{w}_n lies between w_{n0} and w_{n1} , $P < P^*$ implies $\bar{w}_n > 1$ and $P > P^*$ implies $\bar{w}_n < 1$. Consequently, $\bar{w}_n = 1$ cannot be satisfied for any $P \neq P^*$.

3.3.4.3 Stability of the evolutionary equilibrium

The evolutionary equilibrium is stable if both the population dynamics and the dynamics of the induction thresholds are stable. I will investigate stability of the evolutionary equilibrium by focusing on the domain of stability in the a_{10} versus a_{11} plane. The boundaries of the domain of evolutionary stability can be derived by numerically calculating parameter values such that the magnitude of the dominant eigenvalue of the Jacobian is equal to 1.

Fig. 43 (next page). Model 2 with evolution: The domain of evolutionary stability as a function of σ_n^2 (next page).

The domain of evolutionary stability (shaded area) in the a_{10} versus a_{11} plane for various values of σ_n^2 , the variance of the prey's induction threshold. The domain of evolutionary stability is largest for intermediate σ_n^2 and decreases in size for both low and high σ_n^2 . The dotted line marks the domain of evolutionary equilibrium (see Fig. 41). a_{10} is the success rate of non-induced predators feeding on defended prey, and a_{11} is the success rate of induced predators feeding on defended prey. Model 2. Parameters: $a_{00} = 0.4$, $a_{01} = 0.4$, $b = 0.4$, $c_d = 0.4$, $c_o = 0.4$, $h_n^2 = 1$, $h_p^2 = 1$, $\lambda = 2$, $\sigma_p^2 = 1$.

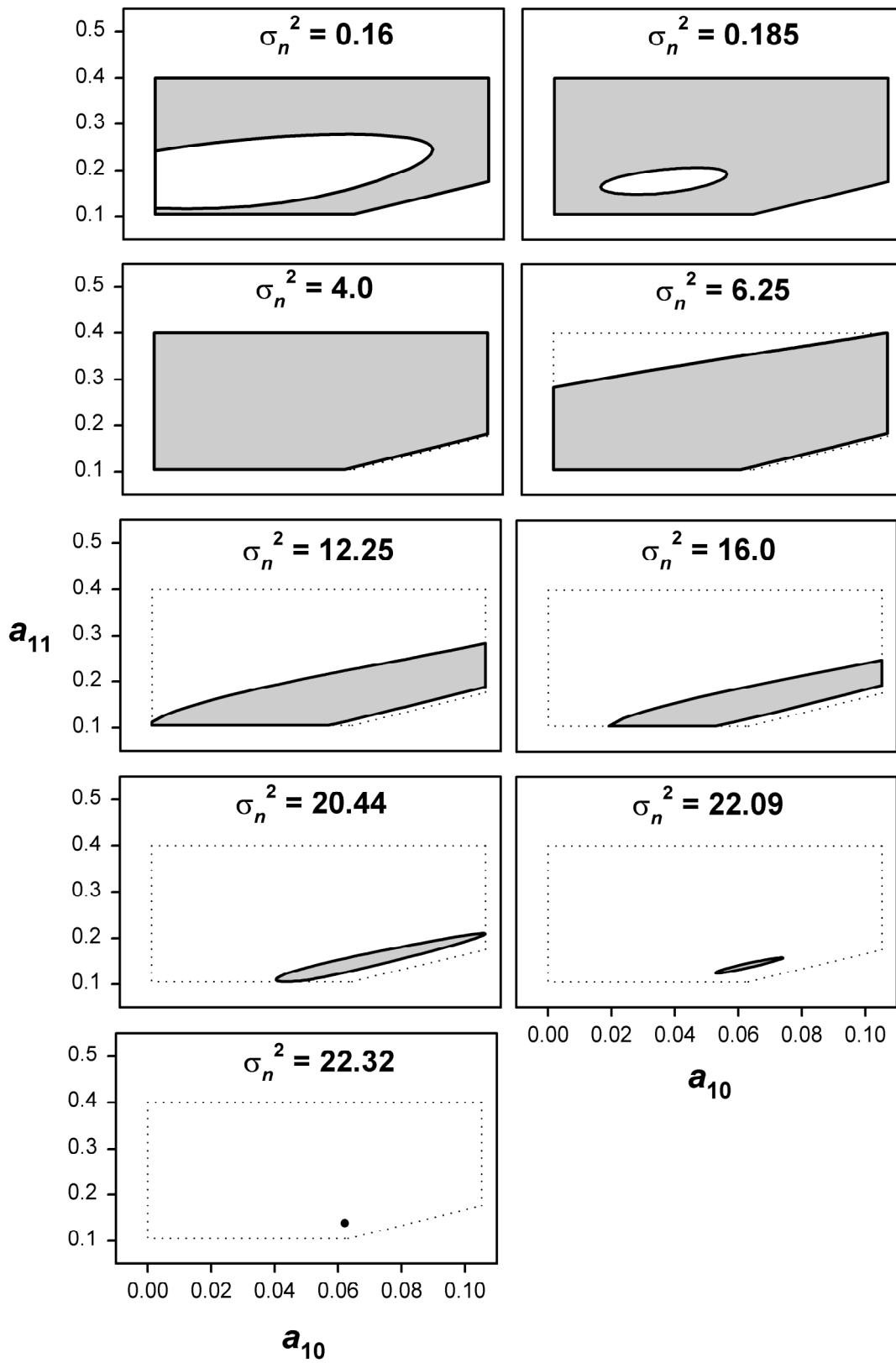


Fig. 43. For legend see previous page.

I will first discuss stability at the boundaries of the domain of evolutionary equilibrium (see Fig. 41). At the boundary defined by $a_{11} = a_{10}/(1-c_o)$ (i.e. $\bar{d}^* = 1$), the equilibrium is always unstable. In this case, the model reduces to a one-prey-two-predator model without phenotypic plasticity. As the stabilizing impact of the prey's defense is missing, this model is always unstable. Conversely, at the boundaries defined by $a_{10} = a_{00} \cdot r_1/r_0$ (i.e. $\bar{d}^* = 1$) and $a_{11} = a_{00} \cdot r_1/r_0$ (i.e. $\bar{d}^* = 0$), the model reduces to a version of model 1 (see previous section), and the dynamics may be neutrally stable, as discussed in section 3.3.3.4.1. Finally, for $a_{10} = 0$ and $a_{11} = a_{00}$, there are no restrictions on potential stability.

Fig. 43 shows the domain of stability for various values of σ_n^2 , the variance of the prey's induction threshold. Similar to the results for model 1 without evolution, stability is greatest if σ_n^2 is intermediate. For small σ_n^2 , the domain of stability has a "hole" at intermediate values of a_{10} and a_{11} . (For $\sigma_n^2 \rightarrow 0$, \bar{d} must be either 0 or 1 and, therefore, an evolutionary equilibrium with intermediate \bar{d}^* is not possible). The "hole" vanishes as σ_n^2 grows larger. With further increase in σ_n^2 , however, stability is lost at high values of a_{11} and low values of a_{10} . The boundaries of the domain of evolutionary stability are remarkably parallel to the boundary line defined by $a_{11} = a_{10}/(1-c_o)$ and, thus, to the isoclines of \bar{d}^* (see Fig. 42). With increasing σ_n^2 , the domain of evolutionary stability becomes more and more narrow and vanishes completely for $\sigma_n^2 > 22.3244$.

Fig. 44 (next page). Model 2 with evolution: The domain of evolutionary stability as a function of σ_p^2 . The domain of evolutionary stability (shaded area) in the a_{10} versus a_{11} plane for various values of σ_p^2 , the variance of the predators' induction threshold. For small σ_p^2 , the domain of stability is reduced for parameter combinations where \bar{d}^* , the equilibrium induction frequency of the predator, is intermediate (see Fig. 42). The dotted line marks the domain of evolutionary equilibrium (see Fig. 41). a_{10} is the success rate of non-induced predators feeding on defended prey, and a_{11} is the success rate of induced predators feeding on defended prey. Model 2. Parameters: $a_{00} = 0.4$, $a_{01} = 0.4$, $b = 0.4$, $c_d = 0.4$, $c_o = 0.4$, $h_n^2 = 1$, $h_p^2 = 1$, $\lambda = 2$, $\sigma_n^2 = 12.25$.

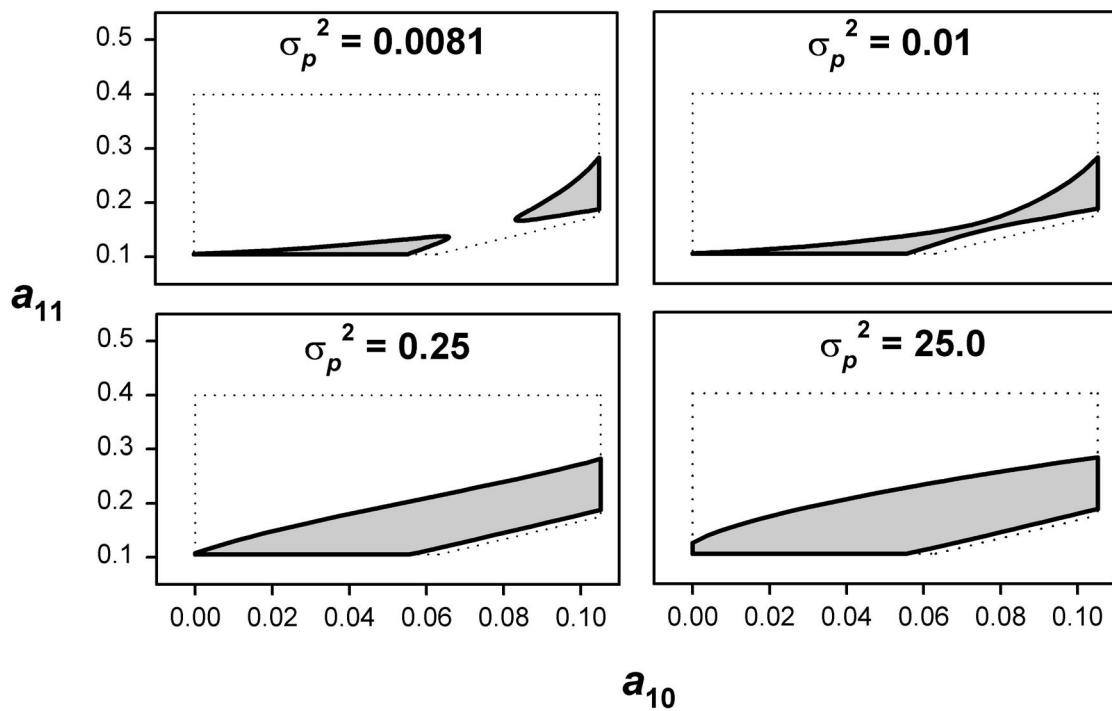


Fig. 44. For legend see previous page.

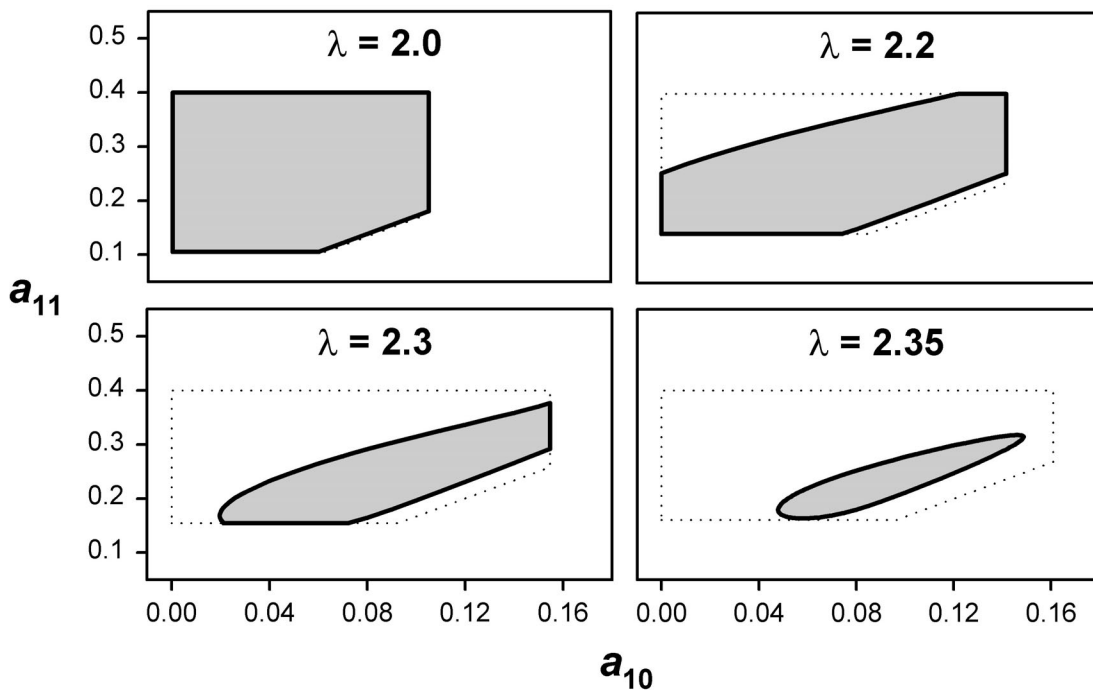


Fig. 45. Model 2 with evolution: The domain of evolutionary stability as a function of λ .

The domain of evolutionary stability (shaded area) in the a_{10} versus a_{11} plane for various values of the prey's fecundity λ . With increasing λ , the domain of evolutionary stability drastically decreases in size. The dotted line marks the domain of evolutionary equilibrium (see Fig. 41). Note that the shape of this domain changes with λ . a_{10} is the success rate of non-induced predators feeding on defended prey, and a_{11} is the success rate of induced predators feeding on defended prey. Model 2. Parameters: $a_{00} = 0.4$, $a_{01} = 0.4$, $b = 0.4$, $c_d = 0.4$, $c_o = 0.4$, $h_n^2 = 1$, $h_p^2 = 1$, $\sigma_n^2 = 12.25$, $\sigma_p^2 = 1$.

Fig. 44 shows the domain of evolutionary stability for various values of σ_p^2 , the variance of the predators' induction threshold. σ_n^2 was chosen such that the domain of evolutionary stability has no "hole" (see Fig. 43). The domain of evolutionary stability is largest if σ_p^2 is large. If σ_p^2 is decreased, stability is reduced in the region where \bar{d}^* is intermediate (see Fig. 42). In contrast, σ_p^2 has no influence on stability in the limiting cases where $\bar{d}^*=0$ or $\bar{d}^*=1$ (because in these cases, the realized plasticity in the predator is zero). In consequence, a decrease in σ_p^2 causes the boundaries of the domain of evolutionary stability to "curve inwards".

The following figures explore the domain of evolutionary stability as a function of the parameters λ , c_d , c_o , h_n^2 , and h_p^2 . In all examples, σ_n^2 has been chosen large enough such that the domain of evolutionary stability has no "hole", and σ_p^2 has been chosen large enough such that the boundaries of the domain of evolutionary stability are not "curved inwards". The domain of evolutionary stability decreases in size if the prey's fecundity λ increases (Fig. 45) or the cost parameters c_d (Fig. 46) and c_o (Fig. 47) decrease. In all cases, the boundaries remain approximately parallel to the isoclines of \bar{d}^* . Furthermore, stability is most persistent if both the defense and the counter-offense are comparatively weak (i.e. large for a_{10} and small a_{11}), that is if \bar{d}^* is large, but not too close to 1.

Fig. 46 (next page). Model 2 with evolution: The domain of evolutionary stability as a function of c_d .

The domain of evolutionary stability (shaded area) in the a_{10} versus a_{11} plane for various values of the defense costs c_d . The domain of evolutionary stability is smallest for low values of c_d . The dotted line encompasses the domain of evolutionary equilibrium (see Fig. 41). The shape of this domain changes as a function of c_d . a_{10} is the success rate of non-induced predators feeding on defended prey, and a_{11} is the success rate of induced predators feeding on defended prey. Model 2. Parameters: $a_{00}=0.4$, $a_{01}=0.4$, $b=0.4$, $c_o=0.4$, $h_n^2=1$, $h_p^2=1$, $\lambda=2$, $\sigma_n^2=12.25$, $\sigma_p^2=1$.

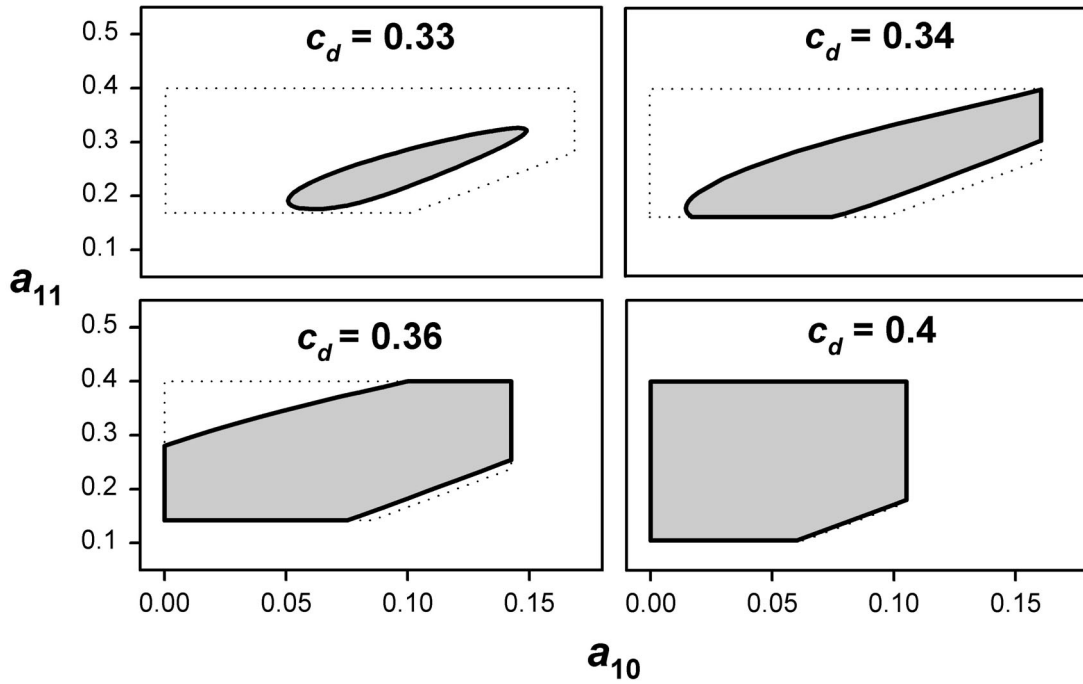


Fig. 46. For legend see previous page.

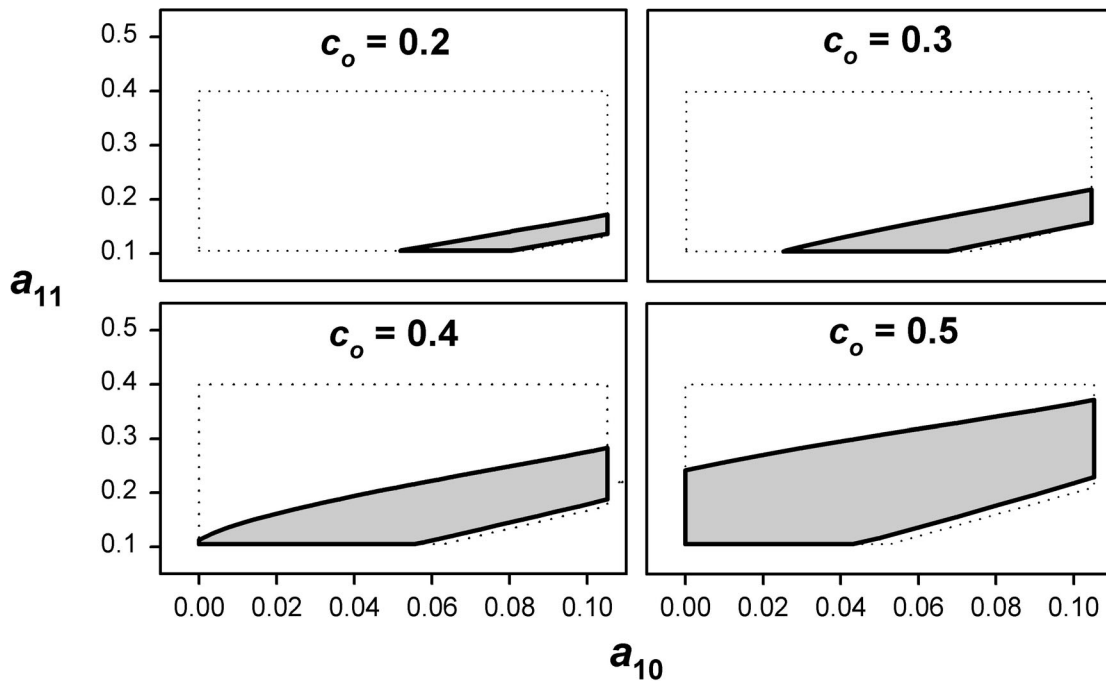


Fig. 47. Model 2 with evolution: The domain of evolutionary stability as a function of c_o .

The domain of evolutionary stability (shaded area) in the a_{10} versus a_{11} plane for various values of the offense costs c_o . The domain of stability is smallest for low values of c_o . The dotted line encompasses the domain of evolutionary equilibrium (see Fig. 41). The shape of this domain changes as a function of c_o . The shape of this domain changes as a function of c_d . a_{10} is the success rate of non-induced predators feeding on defended prey, and a_{11} is the success rate of induced predators feeding on defended prey. Model 2. Parameters: $a_{00} = 0.4$, $a_{01} = 0.4$, $b = 0.4$, $c_d = 0.4$, $h_n^2 = 1$, $h_p^2 = 1$, $\lambda = 2$, $\sigma_n^2 = 12.25$, $\sigma_p^2 = 1$.

The domain of evolutionary stability also decreases in size if the heritability of the induction thresholds in both species increases (Fig. 48). As demonstrated in Fig. 49, the heritability h_n^2 of the prey's induction threshold has a much stronger effect on stability than the heritability h_p^2 of the predator's induction threshold.

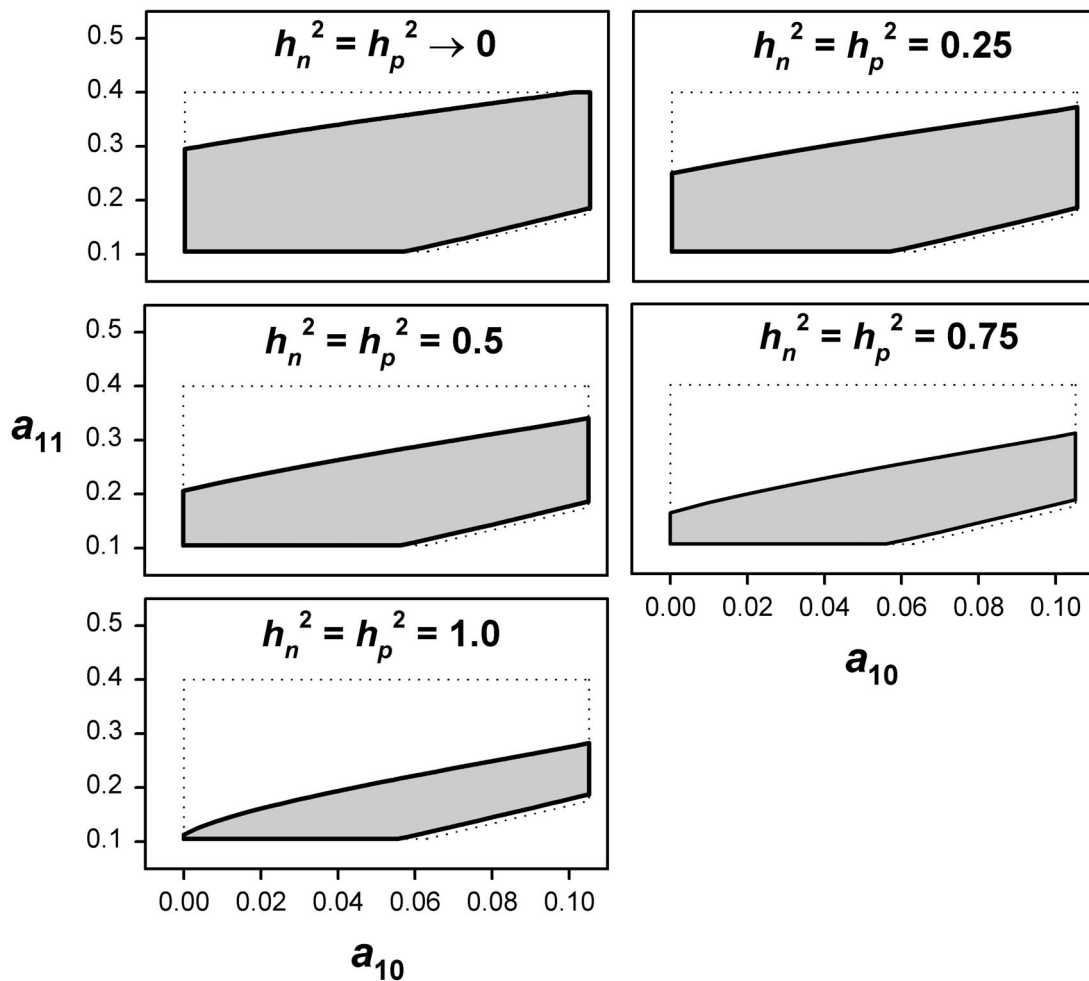


Fig. 48. Model 2 with evolution: The domain of evolutionary stability as a function of h_n^2 and h_p^2 .

The domain of evolutionary stability (shaded area) in the a_{10} versus a_{11} plane for various values of h_n^2 and h_p^2 , the heritabilities of the induction thresholds of prey and predator, respectively. In the figure, h_n^2 and h_p^2 always have the same value. See Fig. 49 for an attempt to separate the effects of the two parameters. The domain of evolutionary stability decreases with increasing h_n^2 and h_p^2 , that is evolution of the induction thresholds destabilizes the system. The dotted line encompasses the domain of evolutionary equilibrium (see Fig. 41). a_{10} is the success rate of non-induced predators feeding on defended prey, and a_{11} is the success rate of induced predators feeding on defended prey. Model 2. Parameters: $a_{00} = 0.4$, $a_{01} = 0.4$, $b = 0.4$, $c_d = 0.4$, $c_o = 0.4$, $\lambda = 2$, $\sigma_n^2 = 12.25$, $\sigma_p^2 = 1$.

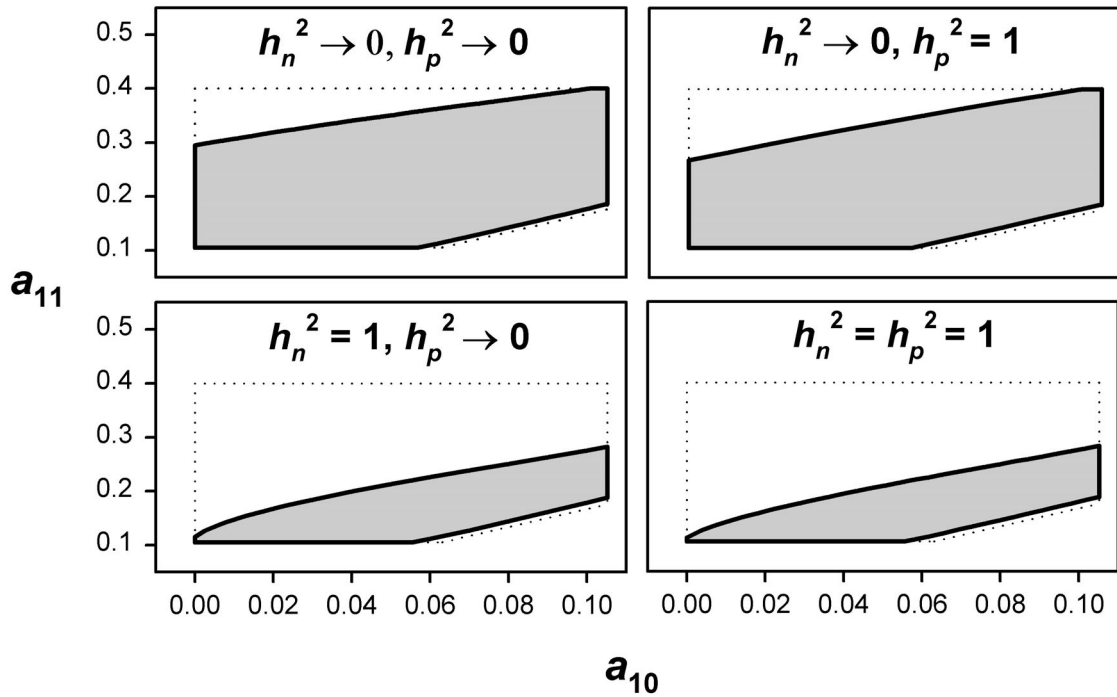


Fig. 49. Model 2 with evolution: The domain of evolutionary stability as a function of evolution in the prey *or* the predator.

The effect of the presence or absence of evolution in the two species on the domain of evolutionary stability (shaded area) in the a_{10} versus a_{11} plane. Evolution in the prey ($h_n^2 = 1$) strongly decreases stability, whereas evolution in the predator ($h_p^2 = 1$) only has a minor impact. h_n^2 and h_p^2 are the heritabilities of the induction thresholds of the prey and the predator, respectively. The dotted line encompasses the domain of evolutionary equilibrium (see Fig. 41). a_{10} is the success rate of non-induced predators feeding on defended prey, and a_{11} is the success rate of induced predators feeding on defended prey. Model 2. Parameters: $a_{00} = 0.4$, $a_{01} = 0.4$, $b = 0.4$, $c_d = 0.4$, $c_o = 0.4$, $\lambda = 2$, $\sigma_n^2 = 12.25$, $\sigma_p^2 = 1$.

I will now summarize the previous results and offer some possible interpretations:

1. The inducible defense of the prey stabilizes the evolutionary dynamics, provided that σ_n^2 , the variance of the prey's induction threshold, is not too small.
2. The inducible counter-offense of the predator tends to destabilize the evolutionary dynamics, especially if the costs c_o of the offense are low.
3. Stability seems to be very sensitive to the prey's fecundity λ (see also model 1). A slight increase in λ causes a strong reduction in the size of the domain of stability.

4. High defense costs c_d tend to stabilize the evolutionary dynamics, because they reduce the mean fecundity of the prey population. This effect is strongest if a large proportion of the prey population is induced. Therefore, stability is greatest for parameter combinations where \bar{d}^* is high, but not too close to 1.
5. As shown by the previous points, many parameters have similar impacts in the models with evolution and without evolution. This suggests, that the stability of the evolutionary equilibrium is largely determined by the stability of the underlying population dynamics.
6. Evolution of the prey's induction threshold destabilizes interaction between predator and prey. The reason for this effect is unclear. Intuitively, evolutionary changes in the mean induction threshold μ should increase the negative feedback between predator density and the proportion of defended prey \bar{d} , which is a key stabilizing mechanism in the model. However, whereas changes in \bar{d} due phenotypic plasticity are instantaneous, evolutionary changes involve a time lag of one generation, and time lags frequently have a destabilizing effect on population dynamics.

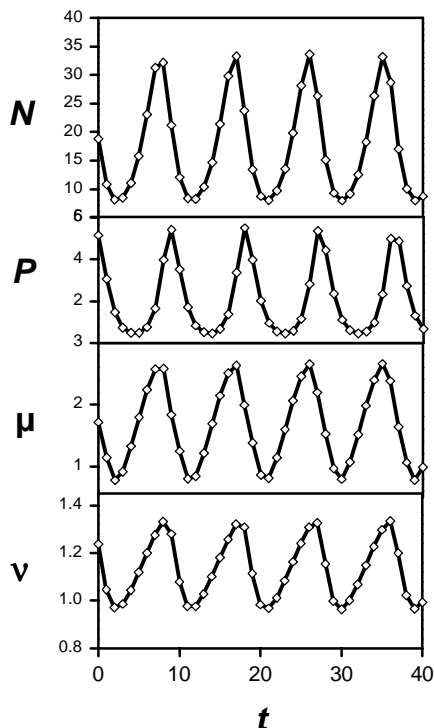


Fig. 50. Model 2 with evolution: Stable limit cycles.

Dynamics of prey density N , predator density P , and the mean induction thresholds μ and ν of prey and predator, respectively, as a function of time t . The system persists and intermediate induction threshold are maintained, because predator-prey cycles drive corresponding cycles in μ and ν . Model 2. Parameters: $a_{00} = 0.4$, $a_{10} = 0.06$, $a_{01} = 0.4$, $a_{11} = 0.24$, $b = 0.4$, $c_d = 0.4$, $c_o = 0.4$, $h_n^2 = 1$, $h_p^2 = 1$, $\lambda = 2$, $\sigma_n^2 = 12.25$, $\sigma_p^2 = 1$.

3.3.4.4 Non-equilibrium dynamics

Outside the domain of stability, the system may persist via non-equilibrium dynamics. The following figures depict three possible types of dynamics. In Fig. 50, predator-prey cycles are accompanied by cycles in the mean induction thresholds that occur at the same (ecological) time-scale. Fig. 51 shows cycles in the mean induction thresholds that span over a larger, evolutionary time-scale and drive “pulsed” oscillations in the population dynamics.

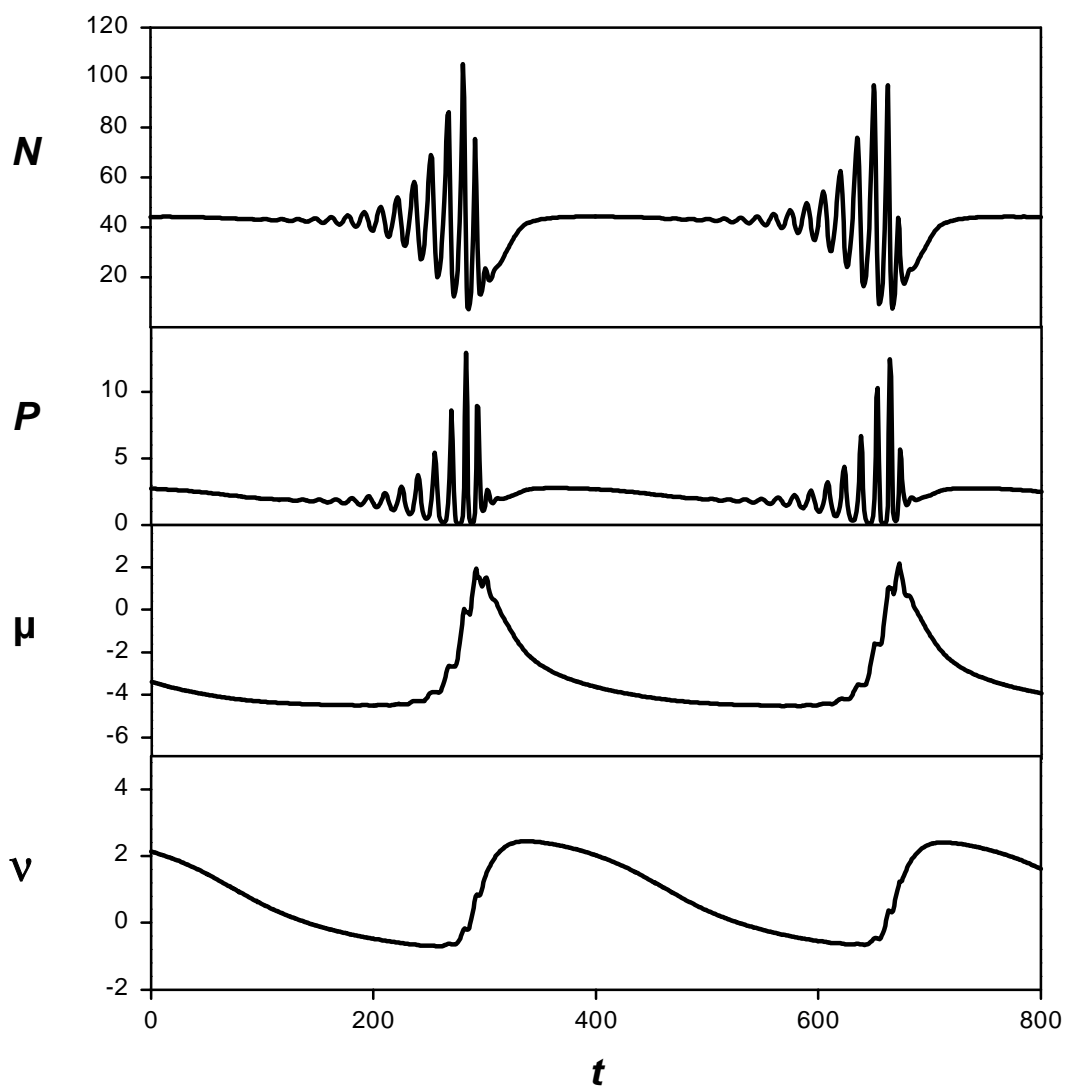


Fig. 51. Model 2 with evolution: Pulsed dynamics due to evolutionary-scale cycles.

Dynamics of prey density N , predator density P , and the mean induction thresholds μ and ν of prey and predator, respectively, as a function of time t . Large-amplitude evolutionary-scale cycles in the mean induction thresholds drive the system into and out of the domain of ecological stability, leading to “pulsed” oscillations at the ecological time-scale. Model 2. Parameters: $a_{00} = 0.4$, $a_{10} = 0.06$, $a_{01} = 0.4$, $a_{11} = 0.106$, $b = 0.4$, $c_d = 0.4$, $c_o = 0.4$, $h_n^2 = 1$, $h_p^2 = 1$, $\lambda = 2$, $\sigma_n^2 = 6.25$, $\sigma_p^2 = 1$.

In Fig. 52, the evolutionary equilibrium is unstable, and v , the mean induction threshold of the predator, evolves towards infinity. This is because the effect of the counter-offense (the difference between a_{11} and a_{10}) is very low, and this small advantage does not outweigh the costs of the offense, because, in the long run, the prey's induction frequency \bar{d} is not high enough. In consequence, the realized phenotypic plasticity in the predator reduces to zero, and the system approaches a dynamic state with pulsed dynamics similar to that shown in Fig. 37. The realized plasticity in the predator is also lost if $a_{10} \geq a_{00} \cdot r_1 / r_0$ or $a_{10} \leq a_{00} \cdot r_1 / r_0$ (i.e. if the equilibrium condition (46) is not satisfied). In the former case, v evolves towards plus infinity, and in the latter case, v evolves towards minus infinity (no figure).

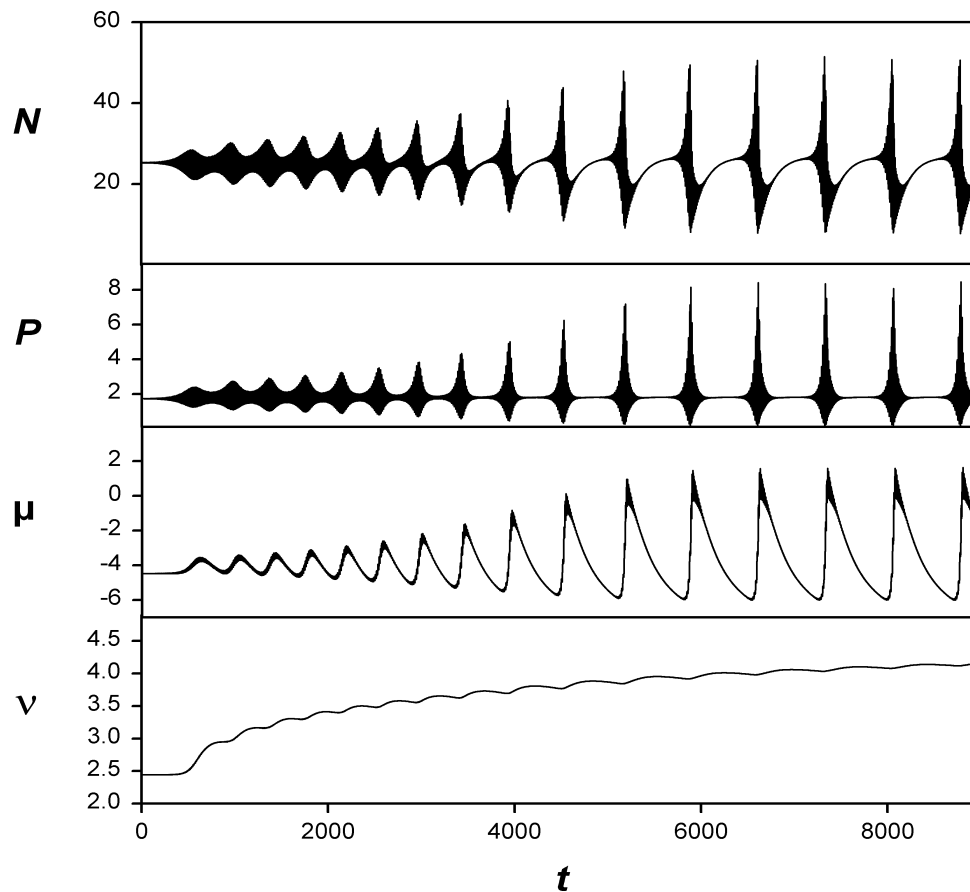


Fig. 52. Model 2 with evolution: Loss of plasticity in the predator.

Dynamics of prey density N , predator density P , and the mean induction thresholds μ and v of prey and predator, respectively, as a function of time t . The evolutionary equilibrium is unstable, as a_{11} is close to $a_{10}/(1-c_o)$ and \bar{d}^* is close to 1. The simulation is started close to the equilibrium. However, v , the mean induction threshold of the predator, increases towards infinity, such that phenotypic plasticity in the predator is lost. The system approaches pulsed dynamics similar to those shown in Fig. 37. Model 2. Parameters: $a_{00} = 0.4$, $a_{10} = 0.1$, $a_{01} = 0.4$, $a_{11} = 0.175$, $b = 0.4$, $c_d = 0.4$, $c_o = 0.4$, $h_n^2 = 1$, $h_p^2 = 1$, $\lambda = 2$, $\sigma_n^2 = 12.25$, $\sigma_p^2 = 1$.

3.3.4.5 Plastic versus constitutive offense – preliminary results for model 2a

In model 2a, the inducible counter-offense of the predator is complemented by a constitutive offense based on a major locus allele. This allows to compare the evolution of both types of offense. Preliminary results suggest the following conclusions:

First, it is important to note that in model 2a, the equilibrium is not unique. Eq. (44) determines only the overall proportion \bar{o}^* of predators with offense, but not the proportions α and β (see eq. 23 and 24) of predators with constitutive or inducible offense, respectively. At equilibrium, any combination of v and q (the frequency of the offense allele C^+) is possible if it assures $\bar{o} = \bar{o}^*$.

Numerical simulations were used to investigate which type of offense is favored by natural selection. Obviously, once an equilibrium is reached, there is no difference between a constitutive and an inducible offense. Therefore, within the domain of stability, the equilibrium values of v and q depend solely upon the initial conditions. (But note, that the domain of stability itself may be influenced by the relative frequencies of the two types of offense.) For parameter combinations outside the domain of stability, preliminary results indicate a very clear trend. In all examples with cyclic population dynamics that I have encountered, the frequency of the C^+ allele reduces steadily to zero, such that eventually only predators with inducible offense remain in the population (Fig. 53). In other words, natural selection favors the inducible offense over the constitutive one if the population dynamics are not at equilibrium.

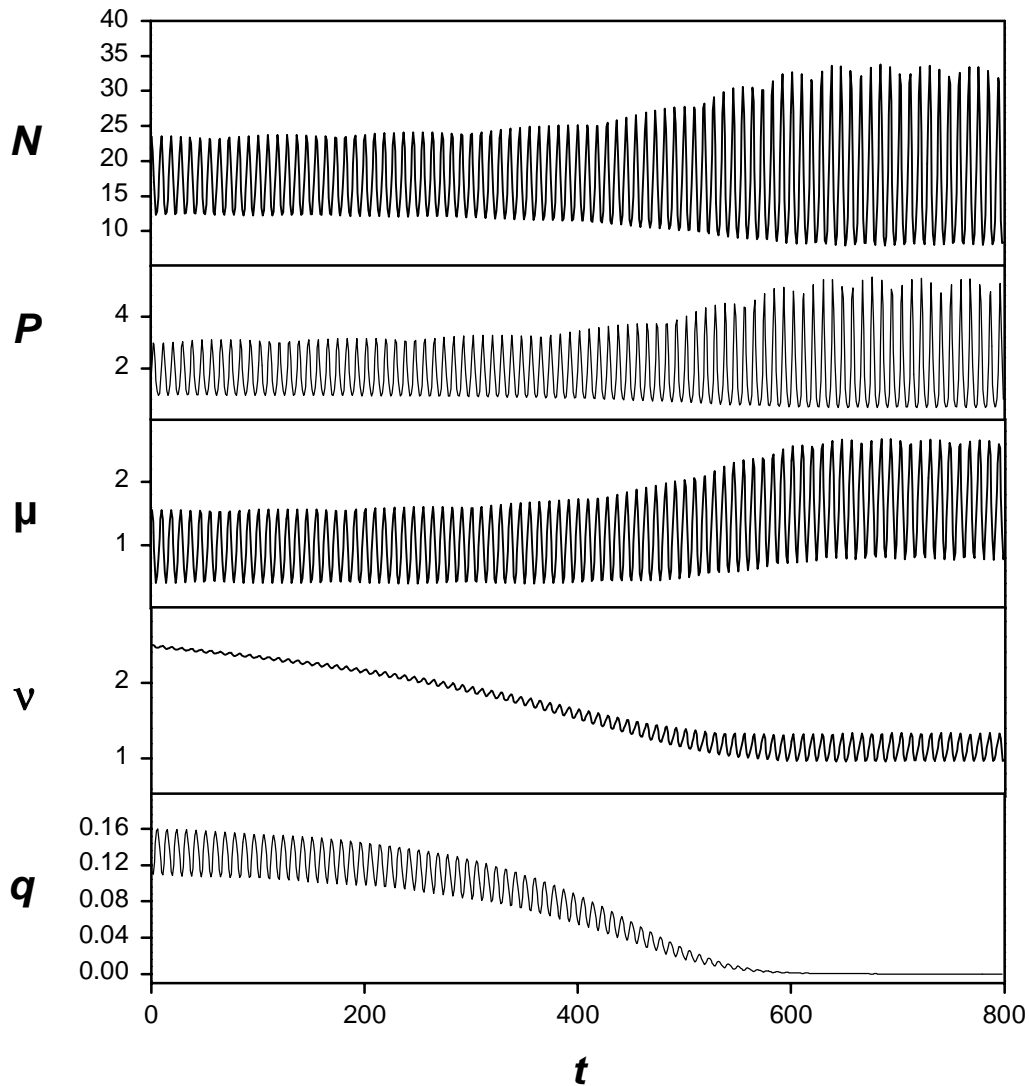


Fig. 53. Model 2a: Inducible versus constitutive offense.

The figure shows an example for the dynamics of model 2a outside the domain of stability. In the beginning, the predators' mean induction frequency ν is high, and the proportion of predators expressing the inducible offense is very small (< 0.025). The system is in a nearly steady state where predator-prey cycles drive corresponding cycles in the prey's mean induction threshold μ and in the frequency q of the offense allele C^+ . In the course of the simulation, ν decreases, and more and more predators express the inducible offense. Simultaneously, the frequency of the C^+ allele decreases steadily to zero. In the end, the inducible offense has completely replaced the constitutive one. Model 2a. Parameters: $a_{00} = 0.4$, $a_{10} = 0.06$, $a_{01} = 0.4$, $a_{11} = 0.24$, $b = 0.4$, $c_d = 0.4$, $c_o = 0.4$, $h_n^2 = 1$, $h_p^2 = 1$, $\lambda = 2$, $\sigma_n^2 = 12.25$, $\sigma_p^2 = 1$.

3.3.5 Summary of model results

3.3.5.1 Ecological dynamics ($h_n^2 = h_p^2 = 0$)

Model 1: Addition of an inducible defense to the inherently unstable Nicholson-Bailey model stabilizes the ecological dynamics by providing a negative feedback between predator density and predation efficiency. Predator and prey may coexist indefinitely either in a stable equilibrium or via non-equilibrium dynamics. The latter may range from stable limit cycles to chaos and show a variety of non-linear effects.

A stable equilibrium requires that the defense is strong enough and that the mean induction threshold μ is neither too low nor too high. The latter condition assures that, at equilibrium, both prey types are present at sufficiently high frequencies. Stability may be lost due to overcompensation if the population-level reaction norm of the prey becomes too steep. If the prey's fecundity is high or the costs of the defense are low (i.e. if the mean growth rate of the prey is high), stability is only possible if μ is within narrow boundaries. If the realized plasticity in the prey population (i.e. the slope of prey's population-level reaction norm) is low or absent, stability remains possible, but only if the defense is strong.

If the defense is highly effective and the variance of the induction threshold is low, the model may have multiple ecological equilibria: At the low equilibrium, predator density is low and few prey are defended, whereas at the high equilibrium, predator density is high and many prey are defended. Both equilibria may be stable simultaneously. The additional intermediate equilibrium is always unstable and, therefore, has no biological relevance.

Model 2: An inducible counter-offense in the predator may affect stability in two different ways. On the one hand, it tends to destabilize the interaction by reducing the stabilizing effect of the prey's defense. On the other hand, the costs of the offense have a stabilizing impact because they are imposed on the predators in a density-dependent manner. Which of the two effects prevails depends on the relative magnitude of costs and benefits of the offense.

3.3.5.2 Evolutionary dynamics ($h_n^2 > 0, h_p^2 > 0$)

Model 1: If only the prey is phenotypically plastic, an evolutionary equilibrium exists only in a special case, and this equilibrium can be at best neutrally stable. However, the system may persist by performing non-equilibrium dynamics, with predator-prey cycles driving corresponding cycles in the mean induction threshold μ . In consequence, μ remains at intermediate values and both prey phenotypes are expressed in the population.

Model 2: If the predators possess an inducible counter-offense to the prey's defense, an evolutionary equilibrium exists under a wide range of conditions. At the equilibrium, both phenotypes in both species coexist.

Stability of the evolutionary equilibrium is low if the induction frequency of the predators is intermediate *and* σ_p^2 , variance of the predators' induction threshold, is low. If σ_p^2 is sufficiently large, stability is highest if the equilibrium induction frequency of the prey is high but not too high, which is the case if neither the defense nor the counter-offense are too strong. Under these conditions, the mean fecundity of the prey is low, because many prey have to pay the cost for the defense.

Stability of the evolutionary equilibrium is lost if the variance of the prey's induction threshold is either too low or too high. Furthermore, the domain of evolutionary stability is small if the prey's fecundity is high or the costs of both the defense and the offense are low. Finally, evolution of the prey seems to destabilize the dynamics, as the domain of evolutionary stability is largest if the heritability h_n^2 is low. In contrast, evolution of the predator has only a small impact on stability.

If the equilibrium is not stable, coexistence of predator and prey is possible via non-equilibrium dynamics. Simulations show three types of dynamics: Predator-prey cycles accompanied by cycles in the mean induction thresholds of both species, large-scale evolutionary cycles of the mean induction thresholds that drive "pulsed" oscillations in the population densities, and run-away selection in the predator leading to the loss of one phenotype.

Model 2a: Preliminary results suggest that a major-locus allele coding for constitutive expression of the offense by overriding the induction mechanism is selected against if

the population dynamics are cyclic. In contrast, no selection pressure is exerted at the evolutionary equilibrium.

3.4 Discussion

In the following, I will discuss the effects of phenotypic plasticity on the ecological and evolutionary dynamics of model 1 and 2, and I will provide an outlook on the evolution of inducible defenses and counter-offenses in dynamic predator-prey systems. I will not, however, systematically discuss the effects of individual model parameters, as this has already been dealt with in the Results section.

3.4.1 Ecological dynamics

The inducible defense of the prey is the main stabilizing factor for the ecological dynamics. Whereas, in the basic Nicholson-Bailey model, extinction of one or both populations is inevitable, addition of the defense enables indefinite persistence of predator and prey, either in a stable equilibrium or via non-equilibrium dynamics. The inducible defense produces a negative feedback between predator density and predation efficiency, which enhances the density-dependent regulation of the predator population.

Note, however, that also a non-plastic defense can stabilize the dynamics, provided that both prey phenotypes are present at sufficiently high frequencies. This case arises if the variance of the prey's induction threshold, σ_n^2 , tends towards infinity, that is if the realized plasticity in the population (see section 3.3.2) decreases to zero. The model then converges to the "constant proportion refuge model" analyzed by Hassel and May (1973). These authors have shown that stability is possible if a constant proportion of the prey is in a "refuge" that provides protection from predation. Of course, the refuge may be substituted by any kind of defense. Hassel and May assumed that the protection is complete (i.e. $a_1 = 0$) and has no costs (i.e. $c_d = 0$), but my own results show that these are not necessary conditions for stability. However, stability is increased if expres-

sion of the defense is plastic at the population-level. The transition from model 1 to the constant proportion refuge model should be studied in greater detail.

Phenotypic plasticity in the prey has been found to be stabilizing in other models, too (e.g. Ives and Dobson 1987, Ruxton and Lima 1997; but see McNair 1986, Houston and McNamara 1997, Luttbeg and Schmitz 2000). In the context of Nicholson-Bailey models, inducible defenses are a new entry in a long list of stabilizing mechanisms (reviewed by Hassell 1978). These include density-dependent prey growth (Beddington et al. 1975, 1976), predator aggregation (Hassell and May 1973), prey refuges (Hassell and May 1973) and genetic variation in prey characteristics (Doebeli 1997). Multiple equilibria like those found in model 1 are frequently observed in theory (May 1977) and sometimes in practice (McCauley et al. 1999, Nelson et al. 2001). The complex non-equilibrium dynamics shown in Fig. 31-33 are typical for discrete-time ecological models (e.g. May 1974, Beddington et al. 1975, May 1976, Neubert and Kot 1991). Similarly, the loss of stability associated with high prey fecundity is in accordance with results from other Nicholson-Bailey type models (see Hassell 1978).

For model 2, a detailed analysis of ecological stability was beyond the scope of this thesis. However, my results are sufficient to reveal two basic motifs: On the one hand, the inducible counter-offense reduces the stabilizing effect of the inducible defense, but on the other hand, the offense has a stabilizing impact itself, because it leads to a density-dependent reduction in predator fecundity. The relative importance of these conflicting mechanisms needs to be clarified in future studies. Results from models of patch selection games suggest that flexible behavior in predator and prey may be either stabilizing or destabilizing, depending on details of the model assumptions (van Baalen and Sabelis 1993, Brown et al. 1999, van Baalen and Sabelis 1999).

3.4.2 Evolutionary dynamics and the coexistence of alternative phenotypes

The evolutionary dynamics of models 1 and 2 can be discussed by asking the following questions: What are the conditions and mechanisms leading to the coexistence of alternative phenotypes in predator and prey, and what is the role of (realized) phenotypic

plasticity therein? Note that, in this study, coexistence of alternative phenotypes is equivalent to the maintenance of intermediate induction thresholds.

Most basically, coexistence of alternative phenotypes requires some sort of environmental heterogeneity (Hazel et al. 1990, Moran 1992). In my model, this heterogeneity can be provided by two different mechanisms: Predator-prey cycles and phenotypic diversity. The former operates in model 1 and the latter in model 2.

In model 1, for most parameter combinations, there is no evolutionary equilibrium between defended and undefended prey. This is a general property of the environmental threshold model in spatially homogeneous environments (Hazel et al. 1990) when there is no frequency-dependent selection. Nevertheless, the system can persist by performing predator-prey cycles that drive associated oscillations in the mean induction threshold of the prey. In consequence, alternative prey phenotypes coexist due to temporal heterogeneity created by the *internal* dynamics of the system.

Notably, the above argument may be reversed. The non-existence of an equilibrium between the two prey phenotypes also prevents the existence of a stable equilibrium between the prey and predator populations – even if such an equilibrium exists in the model without evolution. In this sense, evolution of the induction threshold may be a cause for population cycles. Population cycles driven by natural selection have long been hypothesized (Chitty 1960, Abrams and Matsuda 1997b) and have recently been described in an empirical study (Sinervo et al. 2000).

In model 2, an evolutionary equilibrium exists because phenotypic diversity – that is the presence of alternative phenotypes – in the prey provides the heterogeneity necessary for the coexistence of alternative phenotypes in the predator, and vice versa. The alternative phenotypes coexist if the equilibrium is stable or if it is unstable but surrounded by some circular attractor (e.g. a stable limit cycle). In the latter case, the system displays Red Queen dynamics (evolutionary cycling) similar to those found in other models of predator-prey coevolution (e.g. Dieckmann et al. 1995, Gavrillets 1997). Again, evolution in the prey may cause cycles in cases where the system would otherwise be stable.

It is essential to recognize that the evolutionary equilibrium specifies only the proportions of the alternative phenotypes (see eq. 44), but is independent of the genetic mechanism that creates these alternative phenotypes in the first place. In particular, the evolutionary equilibrium does not rely on phenotypic plasticity. However, phenotypic plasticity – or, more precisely, the realized plasticity at the population-level – plays an important role in determining whether the evolutionary equilibrium can be reached and is stable.

As shown in Fig. 43, the realized plasticity in the prey is essential for the stability of the evolutionary equilibrium. The equilibrium cannot be stable if the realized plasticity in the prey becomes too weak (i.e. if the variance of the prey's induction threshold, σ_n^2 , exceeds a maximum). This result differs markedly from the results obtained for the ecological equilibrium (in model 1), which can be stable even in the absence of plasticity. Note, however, that stability of the ecological equilibrium requires the proportion of defended prey, \bar{d} , to be within a certain range (Hassell and May 1973) but that \bar{d} is not free to vary if evolution occurs.

In contrast, the realized plasticity in the predator (which is inversely related to σ_p^2 , the variance of the predators' induction threshold) has a negative impact on the stability of the evolutionary equilibrium. This result is surprising for at least two reasons. First, stability of the evolutionary equilibrium increases with increasing offense costs c_o . However, the mechanism suggested by the analysis of the ecological equilibrium can only operate if there is realized plasticity in the predator population. Second, the inducible offense is bound to cause negative frequency-dependent selection in the prey – when more prey are defended, the benefit of the defense is reduced by an increase in the proportion of induced predators –, and this should be expected to stabilize the dynamics of the induction thresholds. Indeed, the evolutionary equilibrium seems to be destabilized by an increase in σ_p^2 if the population densities in model 2 are kept constant (data not shown). However, in the presence of population dynamics, this effect is exactly reversed. It is difficult to suggest an intuitive explanation for these findings. Obviously, the interaction between the dynamics of the population densities on the one hand and the evolving traits on the other hand is highly complex, and giving a mechanistic, “step-by-step” explanation for the results seems almost impossible.

3.4.3 Outlook regarding the evolution of phenotypic plasticity

Phenotypic plasticity in both model 1 and model 2 is assumed to be present *a priori*. Therefore, the models cannot predict when and how plasticity evolves in the first place. All they can show is adaptive adjustment of the induction thresholds and, as a limiting case, the practical loss of plasticity that occurs if the alternative phenotypes cannot co-exist.

In the predator, coexistence of alternative phenotypes is not possible if the defense or the offense are very weak. In these cases, either the evolutionary equilibrium does not exist or it is evolutionarily unstable (i.e. minor deviations from equilibrium lead to runaway selection of the mean induction threshold; see Fig. 52). It is not possible to observe a similar process in the prey, because the model populations would go extinct beforehand.

If the alternative phenotypes cannot coexist, the individual induction thresholds will evolve towards extremely low or high values, until they are either always or never exceeded by the inducing cue. Plasticity is then practically lost (i.e. the “realized” plasticity, as defined in section 3.3.2, is lost). Furthermore, it is to be expected that selection will no longer maintain the induction mechanism in the individuals, either. Therefore, the loss of plasticity by this mechanism is inseparably linked to the loss of one phenotype.

Model 2a has been designed as a preliminary attempt to investigate the evolution of phenotypic plasticity independent of the coexistence of alternative phenotypes. For that purpose, I have introduced an additional genetic basis for the predator offense: a major locus allele that codes for constitutive expression of the offense by overriding the induction mechanism. Again, this sort of analysis was only possible for the predator.

Preliminary results from model 2a suggest that the major locus allele is selected against if and only if the system performs cyclic population dynamics. This suggests an interesting hypothesis: Inducible defenses as well as inducible counter-offenses might evolve as an adaptation to temporal heterogeneity created by the internal dynamics of predator-prey systems. Given the inherent tendency for cycling found in almost all predator-prey models (and in some natural communities, too), this mechanism might prove to be im-

portant. However, to my knowledge, it has not been proposed before, as models of phenotypic plasticity typically assume some kind of externally imposed heterogeneity (e.g., two-patch models).

On the other hand, once a stable equilibrium of model 2a is reached, selection has no influence on the frequency of the offense allele anymore. This illustrates that, although the evolutionary equilibrium provides a mechanism for the coexistence of alternative phenotypes and, thus, for the *maintenance* of phenotypic plasticity, it does not favor the *evolution* of plasticity. Plasticity is selected for only if the optimal phenotype for an individual varies in space or time.

3.4.4 Future directions

For the future, I suggest to further pursue the approach outlined in model 2a – that is to focus on the evolution of phenotypic plasticity in dynamic predator-prey systems. The key idea is to study the competition between one plastic and two coexisting non-plastic strategies under various dynamic regimes. A similar game-theoretic approach has been applied by Lively (1986a, 1999). Possibly, the plastic strategy might be “penalized” with a cost (van Tienderen 1997, DeWitt et al. 1998). As the preliminary results from model 2a suggest that plasticity might evolve in response to population oscillations, it will be necessary to analyze the non-equilibrium dynamics in a systematic way.

Furthermore, a mechanism should be built into the model that prevents extinction of the model populations but is independent of phenotypic plasticity. This will make it possible to investigate all potential evolutionary outcomes. So far, stability depends critically on (realized) phenotypic plasticity in the prey. Although this facilitates the analysis of population dynamics – because the effects of plasticity can be studied without interference from other mechanism – it restricts the analysis of the evolutionary dynamics. In the present study, it was not possible to investigate cases where the two prey phenotypes cannot coexist. Furthermore, potentially interesting coevolutionary dynamics are likely to be “masked” by the population dynamics if these are too easily destabilized. Therefore, future models should include some alternative stabilizing mechanism, for example a (weak) density-dependence in the prey.

Conclusions

Previous research on phenotypic plasticity in predator-prey interactions has largely focused on inducible prey defenses. However, a full understanding of predator-prey interactions requires knowledge about phenotypic plasticity in both species. In this thesis, therefore, I have looked at plasticity from a predator perspective. I have shown that the inducible offense of *Lembadion bullinum* can be understood within a cost-benefit framework similar to that for inducible defenses. I have then moved on to investigate reciprocal phenotypic plasticity, that is the interaction between the inducible offense of *Lembadion* and an inducible prey defense. Although, in this situation, the offense did not yield a significant fitness benefit for the predator, my results point out that predators, like prey, can adjust their phenotype to the prevailing environmental conditions, and that they should not be expected to remain passive and inflexible while their prey devise sophisticated defense mechanisms. The results of my theoretical model show that reciprocal phenotypic plasticity is bound to influence the predicted reaction norms of predator and prey, as well as predator-prey dynamics and coevolution. Therefore, the combination of inducible defenses and inducible offenses offers fascinating new questions for empirical and theoretical research.

Acknowledgements

Prof. Wilfried Gabriel supervised my work and provided advise with the development and analysis of the model. Somehow, he always managed to have time for me.

Ralph Tollrian advised me with the experimental work and gave me many useful hints.

Prof. Winfried Lampert gave me the opportunity to do my work at the Max-Planck-Institute for Limnology in Plön. He enabled me to attend several external conferences and courses. The Max-Planck-Society provided financial support.

Hans-Werner Kuhlmann introduced me to the handling and cultivation of ciliates. He and Krzysztof Wiackowski provided the algae and ciliates.

Yvonne Funck and Kirsten Kessler repeatedly looked after my cultures.

Sebastian Diehl, Wilfried Gabriel, Johnathan Grey, Colleen Jamieson, Jonathan Jeschke, Klaus Jürgens, Kirsten Kessler, Winfried Lampert and Ralph Tollrian commented on various parts of the manuscript.

The staff of the Max-Planck-Institute for Limnology provided every-day assistance and created a friendly environment, not only during working hours.

Kirsten Kessler and my parents provided all kinds of scientific and non-scientific support.

Thank you!

Danksagungen

Mein Doktorvater Prof. Wilfried Gabriel betreute die vorliegende Arbeit und unterstützte mich bei der Entwicklung und Analyse des Modells. Trotz eines vollen Terminkalenders hat er sich immer die nötige Zeit für mich genommen.

Ralph Tollrian übernahm die Betreuung des experimentellen Teils und stand mir bei vielen Problemen als Ideenquelle und Ratgeber zur Seite.

Prof. Winfried Lampert gab mir die Gelegenheit, meine Arbeit am Max-Planck-Institut für Limnologie in Plön anzufertigen. Er ermöglichte mir auch die Teilnahme an mehreren auswärtigen Tagungen und Kursen. Die Max-Planck-Gesellschaft unterstützte mich mit einem Stipendium.

Hans-Werner Kuhlmann führte mich in das Arbeiten mit Ciliaten ein und stellte mir, ebenso wie Krzysztof Wiackowski, Kulturen der Versuchsorganismen zur Verfügung.

Yvonne Funck und Kirsten Kessler kümmerten sich zeitweise um meine Kulturen.

Sebastian Diehl, Wilfried Gabriel, Johnathan Grey, Colleen Jamieson, Jonathan Jeschke, Klaus Jürgens, Kirsten Kessler, Winfried Lampert und Ralph Tollrian haben verschiedene Teile der vorliegenden Arbeit kritisch gelesen und kommentiert.

Die Mitarbeiter des Max-Planck-Instituts für Limnologie halfen mir bei tagtäglichen Arbeiten und schufen eine freundliche Umgebung, auch außerhalb der Arbeitszeiten.

Kirsten Kessler und meine Eltern unterstützten mich in jeglicher Hinsicht.

Vielen Dank!

Literature cited

- Abrams, P. A. 1986. Adaptive responses of predators to prey and prey to predators: the failure of the arms-race analogy. *Evolution* **40**: 1229-1247.
- Abrams, P. A. 1990. The evolution of anti-predator traits in prey in response to evolutionary change in predators. *Oikos* **59**: 147-156.
- Abrams, P. A. 1997. Evolutionary responses of foraging-related traits in unstable predator-prey systems. *Evolutionary Ecology* **11**: 673-686.
- Abrams, P. A. 1999. The adaptive dynamics of consumer choice. *American Naturalist* **153**: 83-97.
- Abrams, P. A. 2000. The evolution of predator-prey interactions: theory and evidence. *Annual Review of Ecology and Systematics* **31**: 79-105.
- Abrams, P. A., and H. Matsuda. 1997a. Fitness minimization and dynamic instability as a consequence of predator-prey coevolution (Corrected and reprinted from Volume 10, Issue 2, pages 167-186, 1996). *Evolutionary Ecology* **11**: 1-20.
- Abrams, P. A., and H. Matsuda. 1997b. Prey adaptation as a cause of predator-prey cycles. *Evolution* **51**: 1742-1750.
- Abrusán, G. 2003. Morphological variation of the predatory cladoceran *Leptodora kindtii* in relation to prey characteristics. *Oecologia* **134**: 278-283.
- Adler, F. R., and D. Grünbaum. 1999. Evolution of forager responses to inducible defenses. Pages 259-285 *in* R. Tollrian and C. D. Harvell, editors. *The Evolution of Inducible Defenses*. Princeton University Press, Princeton.
- Adler, F. R., and R. Karban. 1994. Defended fortresses or moving targets? Another model of inducible defenses inspired by military metaphors. *American Naturalist* **144**: 813-832.
- Agrawal, A. A. 2001. Phenotypic plasticity in the interaction and evolution of species. *Science* **294**: 321-326.
- Alonzo, S. H. 2002. State-dependent habitat selection games between predators and prey: the importance of behavioural interactions and expected lifetime reproductive success. *Evolutionary Ecology Research* **4**: 759-778.
- Bakker, R. T. 1983. The deer flees, the wolf pursues: incongruencies in predator-prey coevolution. Pages 350-382 *in* D. Futuyma and M. Slatkin, editors. *Coevolution*. Sinauer, Sunderland.

- Beddington, J. R., C. A. Free, and J. H. Lawton. 1975. Dynamic complexity in predator-prey models framed in difference equations. *Nature* **255**: 58-59.
- Beddington, J. R., C. A. Free, and J. H. Lawton. 1976. Concepts of stability and resilience in predator-prey models. *Journal of Animal Ecology* **45**: 791-816.
- Bernays, E. A. 1986. Diet-induced head allometry among foliage-chewing insects and its importance of graminivores. *Science* **231**: 495-497.
- Bernays, E. A., and R. F. Chapman. 2000. Plant secondary compounds and grasshoppers: beyond plant defenses. *Journal of Chemical Ecology* **26**: 1773-1794.
- Bernot, R. J., and A. M. Turner. 2001. Predator identity and trait-mediated indirect effects in a littoral food web. *Oecologia* **129**: 139-146.
- Bertram, B. C. R. 1978. Living in groups: predators and prey. Pages 64-96 in J. R. Krebs and N. B. Davies, editors. *Behavioural Ecology: an evolutionary approach*. Blackwell, Oxford.
- Bolter, C. J., and M. A. Jongsma. 1995. Colorado potato beetles (*Leptinotarsa decemlineata*) adapt to proteinase inhibitors induced in potato leaves by methyl jasmonate. *Journal of Insect Physiology* **41**: 1071-1078.
- Brodie, E. D., III, and E. D. Brodie, Jr. 1990. Tetrodotoxin resistance in garter snakes: an evolutionary response of predators to dangerous prey. *Evolution* **44**: 651-659.
- Brodie, E. D., III, and E. D. Brodie, Jr. 1999. Predator-prey arms races: asymmetrical selection on predators and prey may be reduced when prey are dangerous. *BioScience* **49**: 557-568.
- Brown, J. S., J. W. Laundre, and M. Gurung. 1999. The ecology of fear: optimal foraging, game theory, and trophic interactions. *Journal of Mammalogy* **80**: 385-399.
- Buhse, H. E. J. 1967. Microstome-macrostome transformation in *Tetrahymena vorax* strain V₂ Type S induced by a transforming principle, Stomatin. *Journal of Protozoology* **14**: 608-613.
- Carnahan, B., H. A. Luther, and J. O. Wilkes. 1969. *Applied numerical methods*. John Wiley & Sons, New York.
- Chitty, D. 1960. Population processes in the vole and their relevance to general theory. *Canadian Journal of Zoology* **38**: 99-113.
- Chivers, D. P., E. L. Wildy, and A. R. Blaustein. 1997. Eastern long-toed salamander (*Ambystoma macrodactylum columbianum*) larvae recognize cannibalistic conspecifics. *Ethology* **103**: 187-197.
- Clark, C. W., and C. D. Harvell. 1992. Inducible defenses and the allocation of resources: a minimal model. *American Naturalist* **139**: 521-539.

- Collins, J., and J. Cheek. 1983. Effect of food and density on development of typical and cannibalistic salamander larvae in *Ambystoma tigrinum nebulosum*. *American Zoologist* **23**: 77-84.
- de Jong, G., and N. Behera. 2002. The influence of life-history differences on the evolution of reaction norms. *Evolutionary Ecology Research* **4**: 1-25.
- de Jong, G., and P. Bijma. 2002. Selection and phenotypic plasticity in evolutionary biology and animal breeding. *Livestock Production Science* **78**: 195-214.
- de Jong, G., and S. Gavrillets. 2000. Maintenance of genetic variation in phenotypic plasticity: the role of environmental variation. *Genetical Research* **76**: 295-304.
- De Puytorac, P. 1984. Le polymorphisme. Pages 581-620 in *Traité de Zoologie*. Masson, Paris.
- DeWitt, T. J., A. Sih, and D. S. Wilson. 1998. Costs and limits of phenotypic plasticity. *Trends in Ecology and Evolution* **13**: 77-81.
- Dieckmann, U., P. Marrow, and R. Law. 1995. Evolutionary cycling in predator-prey interactions - population dynamics and the red queen. *Journal of Theoretical Biology* **176**: 91-102.
- Doebeli, M. 1997. Genetic variation and the persistence of predator-prey interactions in the Nicholson-Bailey model. *Journal of Theoretical Biology* **188**: 109-120.
- Edelstein-Keshet, L., and M. D. Rausher. 1989. The effects of inducible plant defenses on herbivore populations. 1. Mobile herbivores in continuous time. *American Naturalist* **133**: 787-810.
- Ehlinger, T. J. 1990. Habitat choice and phenotype-limited feeding efficiency in bluegill: individual differences and trophic polymorphism. *Ecology* **71**: 886-896.
- Ehlinger, T. J., and D. S. Wilson. 1988. Complex foraging polymorphism in bluegill sunfish. *Proceedings of the National Academy of Sciences of the United States of America* **85**: 1878-1882.
- Falconer, D. S., and T. F. C. Mackay. 1996. *An introduction to quantitative genetics*, 4th edition. Pearson Education Limited, Harlow.
- Fenchel, T. 1982. Ecology of heterotrophic microflagellates. III. Adaptations to heterogeneous environments. *Marine Ecology Progress Series* **9**: 25-33.
- Finlay, B. J., and T. Fenchel. 1996. Ecology: role of ciliates in the natural environment. Pages 417-440 in K. Hausmann and P. C. Bradbury, editors. *Ciliates: cells as organisms*. Gustav Fischer Verlag, Stuttgart.
- Foissner, W., H. Berger, and F. Kohmann. 1994. Taxonomische und ökologische Revision der Ciliaten des Saprobiensystems - Band III: Hymenostomata, Prostomatida, Nassulida. Bayerisches Landesamt für Wasserwirtschaft, München.

- Frank, S. A. 1993. A model of inducible defense. *Evolution* **47**: 325-327.
- Gabriel, W. 1999. Evolution of reversible plastic responses: inducible defenses and environmental tolerance. Pages 286-305 in R. Tollrian and C. D. Harvell, editors. *The ecology and evolution of inducible defenses*. Princeton University Press, Princeton.
- Gabriel, W., and M. Lynch. 1992. The selective advantage of reaction norms for environmental tolerance. *Journal of Evolutionary Biology* **5**: 41-60.
- Gabriel, W., and B. Thomas. 1988. Vertical migration of zooplankton as an evolutionarily stable strategy. *American Naturalist* **132**: 199-216.
- Gardner, S. N., and A. A. Agrawal. 2002. Induced plant defence and the evolution of counter-defences in herbivores. *Evolutionary Ecology Research* **4**: 1131-1151.
- Gavrilets, S. 1997. Coevolutionary chase in exploiter-victim systems with polygenic characters. *Journal of Theoretical Biology* **186**: 527-534.
- Gavrilets, S., and S. M. Scheiner. 1993. The genetics of phenotypic plasticity. V. Evolution of reaction norm shape. *Journal of Evolutionary Biology* **6**: 31-48.
- Giese, A. C. 1973. *Blepharisma: the biology of a light-sensitive protozoan*. Stanford University Press, Stanford.
- Giese, A. C., and R. H. Alden. 1938. Cannibalism and giant formation in *Stylonychia*. *Journal of Experimental Zoology* **78**: 117-134.
- Gilbert, J. J. 1980. Female polymorphism and sexual reproduction in the rotifer *Asplanchna*: evolution of their relationship and control by dietary tocopherol. *American Naturalist* **116**: 409-431.
- Gilbert, J. J., and R. S. Stemberger. 1985. The costs and benefits of gigantism in polymorphic species of the rotifer *Asplanchna*. *Ergebnisse der Limnologie (Archiv für Hydrobiologie Beiheft)* **21**: 185-192.
- Goldman, J. C., and M. R. Dennett. 1990. Dynamics of prey selection by an omnivorous flagellate. *Marine Ecology Progress Series* **59**: 183-194.
- Gomez-Saladin, E., and E. B. Small. 1993. Prey-induced transformation of *Miamiensis avidus* strain Ma/2 by a soluble factor. *Journal of Eukaryotic Microbiology* **40**: 550-556.
- Gomulkiewicz, R., and M. Kirkpatrick. 1992. Quantitative genetics and the evolution of reaction norms. *Evolution* **46**: 390-411.
- Greene, E. 1989. A diet-induced developmental polymorphism in a caterpillar. *Science* **243**: 643-646.
- Gurney, W. S. C., and R. M. Nisbet. 1998. *Ecological Dynamics*, 1st edition. Oxford University Press, New York.

- Hampton, S. E., and P. L. Starkweather. 1998. Differences in predation among morphotypes of the rotifer *Asplanchna silvestrii*. *Freshwater Biology* **40**: 595-605.
- Hartl, D. L., and A. G. Clark. 1997. Principles of population genetics, 3rd edition. Sinauer Associates, Inc., Sunderland.
- Hassell, M. P. 1978. The dynamics of arthropod predator-prey systems. Princeton University Press, Princeton, New Jersey.
- Hassell, M. P., and R. M. May. 1973. Stability in insect host-parasite models. *Journal of Animal Ecology* **42**: 693-736.
- Hazel, W. N., and R. Smock. 1993. Modeling selection on conditional strategies in stochastic environments. Pages 147-154 in J. Yoshimura and C. W. Clark, editors. *Lecture notes in biomathematics: adaptation in stochastic environments*. Springer, Berlin.
- Hazel, W. N., R. Smock, and M. D. Johnson. 1990. A polygenic model for the evolution and maintenance of conditional strategies. *Proceedings of the Royal Society of London - Series B: Biological Sciences* **242**: 181-188.
- Hewett, S. W. 1980. Prey-dependent cell size in a protozoan predator. *Journal of Protozoology* **27**: 311-313.
- Hewett, S. W. 1988. Predation by *Didinium nasutum*: effects of predator and prey size. *Ecology* **69**: 135-145.
- Houston, A. I., and J. M. McNamara. 1997. Patch choice and population size. *Evolutionary Ecology* **11**: 703-722.
- Ives, A. R., and A. P. Dobson. 1987. Antipredator behavior and the population dynamics of simple predator-prey systems. *American Naturalist* **130**: 431-447.
- Janzen, D. H. 1980. When is it coevolution? *Evolution* **34**: 611-612.
- Jeschke, J. M., M. Kopp, and R. Tollrian. 2002. Predator functional responses: discriminating between handling and digesting prey. *Ecological Monographs* **72**: 95-112.
- Jongsma, M. A., and C. Bolter. 1997. The adaptation of insects to plant protease inhibitors. *Journal of Insect Physiology* **43**: 885-895.
- Kamra, K., and G. R. Sapsa. 1994. Quantitative regulation of ciliary structures in polymorphic states of the hypotrichous ciliate *Onychodromus indica*, Kamra and Sapsa 1993. *European Journal of Protistology* **30**: 379-393.
- Karban, R., and A. A. Agrawal. 2002. Herbivore offense. *Annual Review of Ecology & Systematics* **33**: 641-664.
- Karban, R., and I. T. Baldwin. 1997. *Induced responses to herbivory*. University of Chicago Press, Chicago.

- Kopp, M., and R. Tollrian. 2003. Trophic size polyphenism in *Lembadion bullinum*: costs and benefits of an inducible offense. *Ecology* **84**: 641-651.
- Kot, M. 2001. *Elements of mathematical ecology*. Cambridge University Press, Cambridge.
- Krebs, J. R., and R. Dawkins. 1979. Arms races between and within species. *Proceedings of the Royal Society of London B* **205**: 489-511.
- Kuhlmann, H. 1993. Giants in *Lembadion bullinum* (Ciliophora, Hymenostomata) - general morphology and inducing conditions. *Archiv für Protistenkunde* **143**: 325-336.
- Kuhlmann, H., and K. Heckmann. 1985. Interspecific morphogens regulating prey-predator relationships in protozoa. *Science* **227**: 1347-1349.
- Kuhlmann, H., and K. Heckmann. 1994. Predation risk of typical ovoid and 'winged' morphs of *Euplotes* (Protozoa, Ciliophora). *Hydrobiologia* **284**: 219-227.
- Kuhlmann, H.-W., J. Kusch, and K. Heckmann. 1999. Predator-induced defenses in ciliated protozoa. Pages 142-159 in R. Tollrian and C. D. Harvell, editors. *The Evolution of Inducible Defenses*. Princeton Press, Princeton.
- Kusch, J. 1993a. Behavioural and morphological changes in ciliates induced by the predator *Amoeba proteus*. *Oecologia* **96**: 354-359.
- Kusch, J. 1993b. Predator-induced morphological changes in *Euplotes* (Ciliata): Isolation of the inducing substance released from *Stenostomum sphagnetorum* (Turbellaria). *Journal of Experimental Zoology* **265**: 613-618.
- Kusch, J. 1999. Self-recognition as the original function of an amoeban defense-inducing kairomone. *Ecology* **80**: 715-720.
- Kusch, J., and H. Kuhlmann. 1994. Cost of *Stenostomum*-induced morphological defence in the ciliate *Euplotes octocarinatus*. *Archiv für Hydrobiologie* **130**: 257-267.
- Lennartz, D. C. 1986. A preliminary study of induction of macrostomal development in *Tetrahymena vorax* V-2s treated with dextro-alpha tocopheryl succinate. *Acta Protozoologica* **25**: 147-152.
- Lennartz, D. C., and E. C. Bovee. 1980. Induction of macrostome formation in *Blepharisma americanum* (Suzuki, 1954) by alpha-tocopheryl succinate. *Transactions of the American Microscopical Society* **99**: 310-317.
- Lessard, E. J., M. P. Martin, and D. J. S. Montagnes. 1996. A new method for live-staining protists with DAPI and its application as a tracer of ingestion by walleye pollock (*Theragra chalcogramma* Pallas) larvae. *Journal of Experimental Marine Biology and Ecology* **204**: 43-57.

- Lima, S. L. 1998. Nonlethal effects in the ecology of predator-prey interactions. *BioScience* **48**: 25-34.
- Lima, S. L. 2002. Putting predators back into behavioral predator-prey interactions. *Trends in Ecology & Evolution* **17**: 70-75.
- Lively, C. M. 1986a. Canalization versus developmental conversion in a spatially variable environment. *American Naturalist* **128**: 561-572.
- Lively, C. M. 1986b. Predator-induced shell dimorphism in the acorn barnacle *Chthamalus anisopoma*. *Evolution* **40**: 232-242.
- Lively, C. M. 1999. Developmental strategies in spatially variable environments: barnacle shell dimorphism and strategic models of selection. Pages 306-321 in R. Tollrian and C. D. Harvell, editors. *The ecology and evolution of inducible defenses*. Princeton University Press, Princeton.
- Lundberg, S., J. Järemo, and P. Nilsson. 1994. Herbivory, inducible defence and population oscillations: a preliminary theoretical analysis. *Oikos* **71**: 537-540.
- Luttbeg, B., and O. J. Schmitz. 2000. Predator and prey models with flexible individual behavior and imperfect information. *American Naturalist* **155**: 669-683.
- Lynch, M., and W. Gabriel. 1987. Environmental tolerance. *American Naturalist* **129**: 283-303.
- Lynn, D. H., D. J. S. Montagnes, and W. Riggs. 1987. Divider size and the cell cycle after prolonged starvation of *Tetrahymena corlissi*. *Microbial Ecology* **13**: 115-128.
- Mangel, M., and B. D. Roitberg. 1992. Behavioral stabilization of host-parasite population dynamics. *Theoretical Population Biology* **42**: 308-320.
- May, R. M. 1974. Biological populations with non-overlapping generations: stable points, stable cycles, and chaos. *Science* **186**: 645-647.
- May, R. M. 1976. Some mathematical models with very complicated dynamics. *Nature* **269**: 471-477.
- May, R. M. 1977. Thresholds and breakpoints in ecosystems with a multiplicity of stable states. *Nature* **269**: 471-477.
- McCauley, E., R. M. Nisbet, W. W. Murdoch, A. M. de Roos, and W. S. C. Gurney. 1999. Large-amplitude cycles of *Daphnia* and its algal prey in enriched environments. *Nature* **402**: 653-656.
- McNair, J. N. 1986. The effects of refuges on predator-prey interactions: a reconsideration. *Theoretical Population Biology* **29**: 38-63.
- Meyer, A. 1987. Phenotypic plasticity and heterochrony in *Cichlasoma managuense* (Pisces, Cichlidae) and their implications for speciation in cichlid fishes. *Evolution* **41**: 1357-1369.

- Meyer, A. 1989. Cost of morphological specialization: feeding performance of the two morphs in the trophically polymorphic cichlid fish *Cichlasoma citrinellum*. *Oecologia* (Heidelberg) **80**: 431-436.
- Mittelbach, G. C., C. W. Osenberg, and P. C. Wainwright. 1999. Variation in feeding morphology between pumpkinseed populations: phenotypic plasticity or evolution? *Evolutionary Ecology Research* **1**: 111-128.
- Miyake, A. 1981. Physiology and biochemistry of conjugation in ciliates. Pages 125-198 in M. Levandowsky and S. H. Hutner, editors. *Biochemistry and physiology of protozoa*. Academic Press, New York.
- Moran, N. A. 1992. The evolutionary maintenance of alternative phenotypes. *American Naturalist* **139**: 971-989.
- Nelsen, E. M., and L. E. Debault. 1978. Transformation in *Tetrahymena pyriformis*: description of an inducible phenotype. *Journal of Protozoology* **25**: 113-119.
- Nelson, W. A., E. McCauley, and F. J. Wrona. 2001. Multiple dynamics in a single predator-prey system: Experimental effects of food quality. *Proceedings of the Royal Society of London - Series B: Biological Sciences* **268**: 1223-1230.
- Neubert, M. G., and M. Kot. 1991. The subcritical collapse of predator populations in discrete-time predator-prey models. *Mathematical Biosciences* **110**: 45-66.
- Nicholson, A. J. 1933. The balance of animal populations. *Journal of Animal Ecology* **2**: 132-178.
- Nicholson, A. J., and V. A. Bailey. 1935. The balance of animal populations. *Proceedings of the Zoological Society of London, Part 1* **1935**: 551-598.
- Padilla, D. K. 2001. Food and environmental cues trigger an inducible offence. *Evolutionary Ecology Research* **3**: 15-25.
- Padilla, D. K., and S. Adolph, C. 1996. Plastic inducible morphologies are not always adaptive: the importance of time delays in a stochastic environment. *Evolutionary Ecology*. **10**: 105-117.
- Peacor, S. D., and E. E. Werner. 1997. Trait-mediated indirect interactions in a simple aquatic food web. *Ecology* **78**: 1146-1156.
- Peters-Regehr, T., J. Kusch, and K. Heckmann. 1997. Primary structure and origin of a predator released protein that induces defensive morphological changes in *Euplotes*. *European Journal of Protistology* **33**: 389-395.
- Pfister, G., and H. Arndt. 1998. Food selectivity and feeding behaviour in omnivorous filter-feeding ciliates: a case study for *Stylonychia*. *European Journal of Protistology* **34**: 446-457.
- Pigliucci, M. 2001. *Phenotypic plasticity: beyond nature and nurture*. Johns Hopkins University Press, Baltimore.

- Press, W. H., S. A. Teukolsky, W. T. Vetterling, and B. P. Flannery. 2001. Numerical recipes in FORTRAN 77: the art of scientific computing, 2nd edition. Cambridge University Press.
- Relyea, R. 2000. Trait-mediated indirect effects in larval anurans: reversing competition with the threat of predation. *Ecology* **81**: 2278-2289.
- Ricci, N., and R. Banchetti. 1993. The peculiar case of the giants of *Oxytricha bifaria* (Ciliata, Hypotrichida): a paradigmatic example of cell differentiation and adaptive strategy. *Zoological Science* **10**: 393-410.
- Ricci, N., G. Grandini, A. Bravi, and R. Banchetti. 1991. The giant of *Oxytricha bifaria*: a peculiar cell differentiation triggered and controlled by cell to cell contacts. *European Journal of Protistology* **27**: 127-133.
- Robinson, B. W., D. S. Wilson, and G. O. Shea. 1996. Trade-offs of ecological specialization: an intraspecific comparison of pumpkinseed sunfish phenotypes. *Ecology* **77**: 170-178.
- Roff, D. A. 1994. Evolution of dimorphic traits - effect of directional selection on heritability. *Heredity* **72**: 36-41.
- Roff, D. A. 1996. The evolution of threshold traits in animals. *The Quarterly Review of Biology* **71**: 3-35.
- Roff, D. A. 1997. Evolutionary quantitative genetics. Chapman & Hall, New York.
- Ruxton, G. D., and S. L. Lima. 1997. Predator-induced breeding suppression and its consequences for predator-prey population dynamics. *Proceedings of the Royal Society of London B* **264**: 409-415.
- Saloniemi, I. 1993. A coevolutionary predator-prey model with quantitative characters. *American Naturalist* **141**: 880-896.
- Salt, G. W. 1979. Density, starvation and swimming rate in *Didinium* populations. *American Naturalist* **113**: 135-143.
- Scheiner, S. M. 1993. Genetics and evolution of phenotypic plasticity. *Annual Review of Ecology & Systematics* **24**: 35-68.
- Sherr, B. F., E. B. Sherr, and A. C. Pedros. 1989. Simultaneous measurement of bacterioplankton production and protozoan bacterivory in estuarine water. *Marine Ecology-Progress Series* **54**: 209-219.
- Sinervo, B., E. Svensson, and T. Comendant. 2000. Density cycles and an offspring quantity and quality game driven by natural selection. *Nature* **406**: 985-988.
- Smith, L. D., and A. R. Palmer. 1994. Effects of manipulated diet on size and performance of Brachyuran crab claws. *Science* **264**: 710-712.
- Smith-Somerville, H. E., J. K. Hardman, R. Timkovich, W. J. Ray, K. E. Rose, P. E. Ryals, S. H. Gibbons, and H. E. J. Buhse. 2000. A complex of iron and nucleic

- acid catabolites is a signal that triggers differentiation in a freshwater protozoan. *Proceedings of the National Academy of Sciences of the United States of America* **97**: 7325-7330.
- Snyder, M. J., and J. I. Glendinning. 1996. Causal connection between detoxification enzyme activity and consumption of a toxic plant compound. *Journal of Comparative Physiology A-Sensory Neural & Behavioral Physiology* **179**: 255-261.
- Sokal, R. R., and F. J. Rohlf. 1995. *Biometrie*, 3rd edition. Freeman & Co., San Francisco.
- Stearns, S. C. 1989. The evolutionary significance of phenotypic plasticity. *BioScience* **39**: 436-445.
- Sultan, S. E., and H. G. Spencer. 2002. Metapopulation structure favors plasticity over local adaptation. *American Naturalist* **160**: 271-283.
- Taylor, W. D., and J. Berger. 1980. Microspatial heterogeneity in the distribution of ciliates in a small pond. *Microbial Ecology* **6**: 27-34.
- Thompson, D. B. 1992. Consumption rates and the evolution of diet-induced plasticity in the head morphology of *Melanoplus femurrubrum* (Orthoptera: Acrididae). *Oecologia* **89**: 204-213.
- Tollrian, R., and C. D. Harvell, editors. 1999a. *The ecology and evolution of inducible defenses*. Princeton University Press, Princeton.
- Tollrian, R., and C. D. Harvell. 1999b. The evolution of inducible defenses: current ideas. Pages 306-321 in R. Tollrian and C. D. Harvell, editors. *The ecology and evolution of inducible defenses*. Princeton University Press, Princeton.
- Trowbridge, C. D. 1991. Diet specialization limits herbivorous sea slug's capacity to switch among food species. *Ecology* **72**: 1880-1888.
- Tufto, J. 2000. The evolution of plasticity and nonplastic spatial and temporal adaptations in the presence of imperfect environmental cues. *American Naturalist* **156**: 121-130.
- Underwood, N. 1999. The influence of plant and herbivore characteristics on the interaction between induced resistance and herbivore population dynamics. *American Naturalist* **153**: 282-294.
- Underwood, N., and M. Rausher. 2002. Comparing the consequences of induced and constitutive plant resistance for herbivore population dynamics. *American Naturalist* **160**: 20-30.
- van Baalen, M., and M. W. Sabelis. 1993. Coevolution of patch selection strategies of predator and prey and the consequences for ecological stability. *American Naturalist* **142**: 646-670.

- van Baalen, M., and M. W. Sabelis. 1999. Nonequilibrium population dynamics of "ideal and free" prey and predators. *American Naturalist* **154**: 69-88.
- van den Bosch, F., de Roos, A. M., and Gabriel, W. 1988. Cannibalism as a life-boat mechanism. *Journal of Mathematical Biology* **26**: 619-633.
- van Dooren, T. J. M. 2001. Reaction norms with bifurcations shaped by evolution. *Proceedings of the Royal Society of London - Series B: Biological Sciences* **268**: 279-287.
- van Tienderen, P. H. 1997. Generalists, specialists, and the evolution of phenotypic plasticity in sympatric populations of distinct species. *Evolution* **51**: 1372-1380.
- Vermeij, G. J. 1994. The evolutionary interaction among species: selection, escalation, and coevolution. *Annual Review of Ecology & Systematics* **25**: 219-236.
- Via, S., R. Gomulkiewicz, G. De Jong, S. M. Scheiner, C. D. Schlichting, and P. H. van Tienderen. 1995. Adaptive phenotypic plasticity: consensus and controversy. *Trends in Ecology and Evolution* **10**: 212-217.
- Via, S., and R. Lande. 1985. Genotype-environment interaction and the evolution of phenotypic plasticity. *Evolution* **39**: 505-522.
- Vos, M., B. J. G. Flik, J. Vijverberg, J. Ringelberg, and W. M. Mooij. 2002. From inducible defences to population dynamics: modelling refuge use and life history changes in *Daphnia*. *Oikos* **99**: 386-396.
- Waddell, D. R. 1992. Cannibalism in lower eukaryotes. *in* M. A. Elgar and B. J. Crespi, editors. *Cannibalism - ecology and evolution among diverse taxa*. Oxford University Press, New York.
- West, K., A. Cohen, and M. Baron. 1991. Morphology and behavior of crabs and gastropods from Lake Tanganyika (Africa): implications for lacustrine predator-prey coevolution. *Evolution* **45**: 589-607.
- Wicklow, B. J. 1988. Developmental polymorphism induced by intraspecific predation in the ciliated protozoan *Onychodromus quadricornutus*. *Journal of Protozoology* **35**: 137-141.
- Wicklow, B. J. 1997. Signal-induced defensive phenotypic changes in ciliated protists: morphological and ecological implications for predator and prey. *Journal of Eukaryotic Microbiology* **44**: 176-188.
- Williams, N. E. 1961. Polymorphism in *Tetrahymena vorax*. *Journal of Protozoology* **8**: 403-410.
- Zalkinder, V. 1979. Correlation between cell nutrition, cell size and division control. Part I. *BioSystems* **11**: 295-307.

Curriculum vitae

MICHAEL KOPP

Born on 17th of September 1973, German citizenship

- 08/1998 – 02/2003 PhD-student at the Max-Planck-Institute for Limnology
(inscribed at the University of Munich until summer 2001)
- 08/1997 – 04/1998 Diploma thesis on *Phenotypic plasticity in ciliates and its influence on predator-prey interactions*
- 11/1992 – 04/1998 Study of *Biology* at the Ludwig-Maximilian-University Munich
major: zoology, minors: ecology, statistics and informatics
- 07/1992 Abitur (school leaving exam) at the Gymnasium (high school)
Dorfen

Lebenslauf

MICHAEL KOPP

Geboren am 17. September 1973, deutsche Staatsangehörigkeit

08/1998 – 02/2003 Doktorarbeit am Max-Planck-Institute für Limnologie
(als Promotionsstudent eingeschrieben an der LMU München bis
SS 2001)

08/1997 – 04/1998 Diplomarbeit an der Ludwig-Maximilian-Universität
München über *Phänotypische Plastizität bei Ciliaten und ihr Ein-
fluß auf Räuber-Beute-Interaktionen*

11/1992 – 04/1998 Studium der Biologie an der Ludwig-Maximilian-Universität
München mit den Fächern Zoologie (Hauptfach), Ökologie, Sta-
tistik und Informatik

07/1992 Abitur am Gymnasium Dorfen